ECOLOGY AND PHYSIOLOGICAL POTENTIAL OF TUNDRA SOIL BACTERIA

By

PRESHITA GADKARI

A dissertation submitted to the

School of Graduate Studies

Rutgers, The State University of New Jersey

In partial fulfillment of the requirements

For the degree of

Doctor of Philosophy

Graduate Program in Microbial Biology

Written under the direction of

Max Häggblom

And approved by

_____

_____

_____

_____

New Brunswick, New Jersey

January 2019

ABSTRACT OF THE DISSERTATION

ECOLOGY AND PHYSIOLOGICAL POTENTIAL OF TUNDRA SOIL BACTERIA

By

PRESHITA GADKARI

Dissertation Director:

Max Häggblom

Arctic tundra soils cover a vast portion of the planet, store massive amounts of carbon, and harbor microbial life throughout all seasons. Bacteria in Arctic tundra soils impact global carbon cycling, and their capabilities are becoming more consequential with climate change. This research aimed to understand metabolic capabilities of tundra bacteria and identify metabolically-active bacteria in frozen tundra soil. The Arctic tundra site of Kilpisjärvi, Finland served as a model landscape to explore the ecology and physiological potential of bacteria using bacterial isolates and soil incubations.

The effect of thaw on tundra soil bacteria is starting to be better understood, but very little is known about the impact of subzero temperature changes, when the ground is frozen. Soil respiration continues in the winter, though at slower rates. Identifying cryo-active bacterial communities is important since soil respiration is largely determined by microbial C mineralization through

decomposition of complex soil organic matter. Although previous studies have examined the microbiomes of frozen soils, most have failed to detect which members of the bacterial communities are metabolically active. This detection is important as cold temperatures preserve commonly measured biomolecules such as DNA, RNA, etc., and may provide misleading information. To ascertain metabolically-active bacteria, stable-isotope probing of tundra soil incubations with ^{13}C-cellobiose at subzero temperatures of 0, -4, and -16°C was carried out, and numerous active bacterial phyla including the *Ignavibacteria*, Candidatus Saccharibacteria, *Verrucomicrobia* were detected. Temperature was shown to impact which members of the bacterial community assimilated cellobiose, even within subzero ranges. Phylogenies of members of cryo-active bacterial phyla were further explored, and added new insights to known physiological capabilities of these groups. Implications of different bacterial communities active within subzero temperatures may suggest that nutrient cycling may be impacted by temperature shifts within frozen soils.

Another gap in tundra bacteriology is understanding the physiological abilities of tundra soil isolates. Arctic tundra soil isolates such as *Mucilaginibacter mallensis*, along with other members of the *Mucilaginibacter* genus are hypothesized to play an important role in processing carbon, but their genomic capabilities remain unexplored. Genomic analysis revealed that *M. mallensis* strain MP1X4 was adapted to process complex carbon, and had an abundance of loci associated with polysaccharide utilization and Carbohydrate-Active EnZYmes (CAZymes) compared to other members of the genus. Other Arctic

tundra isolates such as the *Acidobacteria* were found to have unusual membrane-bound isoprenoid structures such as hopanoids and carotenoids. These carotenoids and hopanoids are hypothesized to aid maintaining membrane fluidity. Arctic *Acidobacteria* such as *Granulicella mallensis* MP5ACTX8, *Granulicella tundricola* MP5ACTX9, *Terriglobus saanensis* SP1PR4, and new isolates A2288, M8UP23, M8UP39, MP8S11, MP8S7, and MP8S9 had their genomes sequenced, from which isoprenoid pathways were investigated. From genomic analysis of these *Acidobacteria*, biosynthetic pathways of carotenoids, such as phytoene, zeta-carotene, neurosporene, lycopene, and hopanoids, such such as diploptene, adenosylhopane, ribosylhopane, bacteriohopanetetrol (BHT), BHT acetylglucosamine, BHT glucosamine, and BHT cyclitol ether, were detected for some species.

Investigation into the ecology and genomes of Arctic bacteria provided insights into the bacterial communities assimilating carbon in subzero temperatures, and the possible genomic adaptations that allow these bacteria to live in the Arctic tundra soils.

TABLE OF CONTENTS

	Page
Abstract	ii
Table of Contents	v
Chapter 1. Introduction	1
1.1 Soil Respiration in Frozen Arctic Tundra Soils	1
1.2 Microbial Ecology of Arctic Tundra Soils	4
1.3 Insights from Genomes and Isolates	10
1.4 Research Questions and Goals	15
Chapter 2: Effect of Temperature On Cryo-Active Bacteria	19
2.1 Introduction	20
2.2 Methodology of Subzero-SIP	22
2.3 Results	29
2.4 Discussion	47
Chapter 3: Hopanoids and Carotenoids of Arctic *Acidobacteria*	53
3.1 *Acidobacteria*	53
3.2 Introduction to Isoprenoids	56
3.3 Methodology	62
3.4 Results and Discussion	64
3.5 Supplemental Information	85
Chapter 4: The Complete Genome Sequence of the Arctic Tundra Soil Bacterium *Mucilaginibacter mallensis*	93
4.1 Introduction	93

4.2 Organism Information 95

4.3 Genome Sequencing 101

4.4 Genomic Insights 105

4.5 Conclusions 112

Chapter 5: Discussion 113

5.1 Overall Dissertation Goals 113

5.2 Key Aims and Findings 113

5.3 Conclusions 117

References 118

CHAPTER 1: INTRODUCTION

Bacteria are metabolically diverse and found in almost every biome (Nealson and Conrad 1999; Gibbons and Gilbert 2015). The Earth and her microbes have pre-dated humankind, co-evolved for billions of years, and will likely outlast other organisms on this planet (Barghoorn and Schopf 1966). This includes microorganisms that have adapted, and impacted Arctic tundra soils to develop a subzero-active niche (Nikrad et al. 2016). These subzero-active microorganisms impact soil respiration and biogeochemical cycling, but their ecology and impact on soil organic matter cycling is poorly understood. This dissertation digs deeper into understanding both microbial ecology of frozen tundra soils, and the genomic capabilities of the bacteria that are found in this ecosystem.

1.1. SOIL RESPIRATION IN FROZEN ARCTIC TUNDRA SOILS

Soil respiration is a key process by which fixed carbon (C) is cycled back into the Earth's atmosphere (Schlesinger and Andrews 2000). The important sources of organic matter (OM) in soil respiration are microorganisms, mycorrhizal networks, and below ground plant matter such as roots (Högberg and Högberg 2002; Schimel and Schaeffer 2012). Soil respiration is largely determined by microbial C mineralization through decomposition of complex soil organic matter (SOM) (Schimel and Schaeffer 2012). This biogeochemical cycling by microorganisms is important since Arctic tundra and permafrost soils are responsible for the vast amounts of greenhouse gas (GHG) emissions in the

form of N_2O, CH_4 and CO_2, and are part of the global C and nitrogen (N) cycles (Michaelson and Ping 2003; Wagner et al. 2003; Natali et al. 2015; Voigt et al. 2017). Tundra and permafrost soils are important especially since they hold the world's vast C stores. Northern Arctic soils are estimated to hold about 25% of the world's organic C stock even though they occupy only 16% of the global land area (Tarnocai et al. 2009). Several abiotic factors impact Arctic tundra bacteria and their activities of SOM decomposition, mineralization, and overall nutrient cycling. Consequences of the abiotic factors temperature and precipitation may include freeze-thaws, snow-cover, and temperature.

Arctic tundra soils freeze during the winter and thaw in the summer season, unlike permafrost soils that remain frozen all year (by definition, for at least two consecutive years). As a result, freeze-thaws can impact tundra soil microbial respiration, and have been shown to produce a burst of respired carbon following thaw (Schimel and Clein 1996). Similarly, freeze-thaws have also been shown to affect microbial substrate use, and are thought for increased uptake of N-rich microbial products (Schimel and Mikan 2005). Other studies have shown bursts of N_2O and CO_2 by the disturbance and release of tundra soil aggregate carbon, and the death of microorganisms, which provides a new spike in available organic carbon (Bullock et al. 1988; Christensen and Tiedje 1990; Edwards and Cresser 1992; Sharma et al. 2006). Diurnal freeze-thaw repetitions in high- and low-altitude Arctic soils have shown to have decreased microbial biomass C and soil inorganic N, but no loss of microbial biomass N, despite having varying vegetation composition (Larsen et al. 2002). Thus, it can be

argued that tundra seasonal freeze-thaws produce microbial “seasons” where soil processes may vary depending on the bloom of substrate and change in microbial activities (Schimel and Clein 2005). Freeze-thaws appear to have mild effects on microbial community structure of the Arctic tundra soils (Männistö et al. 2009). Similarly, freeze-thaw cycles and warming of Antarctic soils showed that bacterial community structure was impacted, though the effect was more pronounced by warming (Yergeau and Kowalchuk 2008).

Similar to the variations in respiration brought on by freeze-thaws, another abiotic effect that impacts soil microbial respiration and community structure is snow-cover (Schimel et al. 2004; Männistö et al. 2009; Yi et al. 2015; Gavazov et al. 2017; Lupascu et al. 2018). Snow-cover creates an insulation effect by keeping the ground temperature more constant, and thus likely ameliorates effects of seasonal temperature fluctuations (Zhang et al. 2005; Gouttevin et al. 2012; Gavazov et al. 2017). Furthermore, this insulation effect is relevant to microbial activities and overall ecosystem function since increased snow-cover can promote winter net N mineralization, which can in turn affect bioavailable N to tundra vegetation (Schimel et al. 2004). The same observation has been made regarding CO_2 emissions due to increased soil respiration with deeper snow, with fewer freeze-thaws, and more stable winter-temperatures, that can even place Arctic C flux previously regarded as a C sink into a C source (Nobrega and Grogan 2007).

One overlapping abiotic factor that is impacts freeze-thaws, snow-cover, and seasons is temperature. Polar regions were thought to be C sinks since

there is a large store of C with relatively lower soil respiration rates due to low temperatures (Oechel et al. 1993). Though temperature is shown to impact soil respiration rates, subzero temperatures slow but do not prevent soil microbial respiration (Mikan et al. 2002). Despite having overall lower rates of soil respiration due to colder temperatures, cold season emissions of the Arctic tundra soils may account for more than 50% of their critical GHG emissions (Zona et al. 2016). Though poorly understood, biological activities are well known to occur below 0 °C, as long as liquid water is available, and cell membrane fluidity is maintained (Arthur and Watson 1976; Bakermans et al. 2003; Mykytczuk et al. 2013; Schaefer and Jafarov 2016). Winter-time emissions have even been postulated to affect the tundra vegetation over time (Sturm et al. 2005).

The key question remains how subzero temperature shapes the composition of the bacterial communities that are metabolically active when the ground is frozen. Further, as many organisms survive seasonal freezing and thawing in the tundra, it is interesting to understand how bacteria take part in the carbon cycling process at subzero temperatures, and what adaptations or capabilities they possess to grow in tundra soils.

1.2 MICROBIAL ECOLOGY OF ARCTIC TUNDRA SOILS

Ecological knowledge of microorganisms is useful since presence or absence of a particular species can be interpreted as an indirect metric of activity, function, outcome, health, etc. of an ecosystem, and is often measured

by the presence/identification of nucleic acids (Schwartz et al. 2000; Graham et al. 2016). Nucleic acid sequencing often provides copious data, and requires robust statistical and computational tools to get meaningful information. Moreover, the presence of DNA does not necessarily dictate that an organism is metabolically active, and thus may not be ecologically relevant (Radajewski et al. 2000; Singer et al. 2017).

Ideally, it would be optimal if one could culture every single species, describe its metabolism, and understand its community function. Hence, nucleic acid sequencing can help provide more information on microbial communities as most members are not able to be cultured yet. It still useful to ascertain which bacterial species are present by methods including 16S rRNA gene surveys, but it does not directly answer what microorganisms are doing metabolically.

Methods for examining the composition of bacterial communities of Arctic tundra soils have been carried out using both DNA (16S rRNA gene) and mRNA surveys. For example, using these methods, members of the *Acidobacteria*, *Actinobacteria*, and *Alphaproteobacteria* were detected as dominant phyla in the summer in the in Arctic tundra soils of Kilpisjärvi, Finland (Männistö et al. 2013). Along with the members of the *Bacteroidetes*, members of the *Acidobacteria*, *Actinobacteria*, and *Alphaproteobacteria* have been identified as the main bacterial phyla in other cold soils (Chu et al. 2010; Yergeau et al. 2010; Kim et al. 2014; Koyama et al. 2014; Shi et al. 2015; Taş et al. 2018). For a summary of DNA and RNA surveys of Arctic tundra soil bacterial community composition, see Table 1.1

The presence of DNA, RNA, or another biomolecule, may be misleading in cold environments, since subzero temperatures can often prolong or preserve biomolecules. Thus, the use of such a marker may not always indicate metabolically active bacterial communities, and may result in misleading information if these biomolecules are used as a sole measure of metabolically activity. To overcome this challenge, methodologies using the incorporation of isotopically labeled substrates can be effective in discerning the cryo-active bacterial community composition since isotopes have to be metabolized to further tag or label microorganisms (Radajewski et al. 2000; Dumont and Murrell 2005; Tuorto et al. 2014; Singer et al. 2017). Therefore, stray biomolecules in the ecosystem from dead or dormant bacteria will not be measured since the isotopic label will not be assimilated. This robust approach to study the microbial composition of an ecosystem by detecting and identifying metabolically active organisms is stable isotope probing (SIP).

SIP is an excellent methodology to determine active tundra soil bacteria. Briefly, the isotopically labeled substrate that the organism can assimilate is administered either *in situ* or in soil incubations. To distinguish which organisms are metabolically active, isotopically labelled biomolecules such as nucleic acids are then physically separated by ultracentrifugation. Analysis of the heavy (isotope assimilated, “active” microbial representative) and light (non-assimilated) nucleic acids are then analyzed to distinguish metabolically active organisms. For a summary of the newest stable isotope probing (SIP) methodologies to understand Arctic bacterial ecology, refer to Table 1.2.

Even though several studies have used stable isotope probing (SIP) to elucidate microbes active in C cycling in tundra soils, there is a large gap in our knowledge of metabolically active bacteria at subzero temperatures. From Table 1.2, it is apparent that most of these SIP studies are focused on the effect of thaw, and thus are not carried out at environmentally relevant subzero-temperatures of frozen soils.

Soil sample	Location	Methodology	Top 3 Dominant Phyla	Publication
Arctic tundra	Kilpisjärvi, Finland	DNA, RNA	*Acidobacteria, Bacteroidetes, Alphaproteobacteria*	Männistö et al 2013
Arctic Permafrost	Toolik Lake-Alaska, USA	DNA	*Alphaproteobacteria, Acidobacteria, Actinobacteria*	Koyama et al. 2014
Arctic Permafrost	Barrow-Alaska, USA	DNA	*Actinobacteria, Alphaproteobacteria, Acidobacteria*	Taş et al. 2018
Arctic peat	Svalbard, Norway	DNA	*Alphaproteobacteria, Deltaproteobacteria, Acidobacteria*	Tevit et al. 2014
Arctic tundra heath	USA, Canada, Europe	DNA	*Acidobacteria, Alphaproteobacteria, Actinobacteria,*	Chu et al. 2010
Arctic permafrost	Eureka, Canada	DNA	*Actinobacteria, Betaproteobacteria, Bacteroidetes*	Yergeau et al. 2010
Subarctic tundra	Alaska, USA	DNA	*Alphaproteobacteria, Acidobacteria, Actinobacteria*	Kim et al. 2014
Subarctic tundra	Yellowknife, Canada	DNA	*Acidobacteria, Alphaproteobacteria, Actinobacteria*	Shi et al. 2015
Arctic permafrost/bog	Alaska, USA	DNA, RNA	*Proteobacteria, Actinobacteria, Chloroflexi*	Hultman et al. 2015

Table 1.1: Analysis of bacterial communities of Arctic soils using mostly DNA and some RNA. Bacterial phyla of are listed in the order of relative abundance in the soil bacterial community.

Soil sample	SIP Amendment	Methodology	Location	Top 3 Active Phyla	Publication
Antarctic desert	$^{18}O\ H_2O$	DNA	McMurdoDry Valley, Antarctica	*Alphaproteobacteria, Gammaproetobacteria, Actinobacteria*	Schwartz et al. 2015
Arctic permafrost	^{13}C Acetate	DNA	Alaska, USA	*Chloroflexi, Actinobacteria, Proteobacteria*	Tuorto et al. 2014
Rice field	$^{13}CH_4$	DNA, PLFA, RNA	Hangzhou, China	*Proteobacteria(Delta,Gamma, Beta), Thermomicrobia, Acidobacteria*	Qiu et al. 2008
Rhizosphere of *Arabidopsis thaliana*	$^{13}CO_2$	DNA, RNA	Saint-Paul-lez-Durance, France	*Proteobacteria (Alpha, Beta, Gamma), Firmicutes*	Haichar et al. 2012
Rhizosphere of wild oats (*Avena fatua*	$^{13}CO_2$, DNA	DNA	Berkeley, USA	construction of Candidatus Teamsevenus rhizospherense genome	Starr et al. 2018
Rhizosphere of oilseed rape	$^{13}CO_2$, RNA	RNA	Ultuna, Sweden	*Proteobacteria, Actinobacteria, Planctomycetes*	Gkarmiri et al. 2017
Agricultural	^{13}C-glucose, cellulose, senescent maize leaves/roots	RNA	Göttingen, Germany	*Proteobacteria, Actinobacteria, Bacteroidetes*	Kramer et al. 2016
Arctic tundra	^{13}C-cellulose, glucose	DNA	Resolute Bay, Canada	*Proteobacteria, Bacteroidetes, and Chloroflexi*	Pinnell et al. 2014
Clay	$^{18}O\ H_2O$	DNA and RNA	South Dakota, USA	*Acidobacteria, Actinobacteria, Alphaproteobacteria*	Rettedal and Brözel 2015
Garden	^{13}C isoprene	DNA	Coventry, UK	*Rhodococcus, Commamonas, Variovorax*	Khawand et al. 2016
Beech forest	$^{15}N_2$	DNA	Klausen–Leopoldsdorf, Austria	*Firmicutes, Planctomycetes, Proteobacteria*	Angel et al. 2018
Wheat rhizosphere	$^{13}CO_2$	DNA	Hebei, China	*Proteobacteria, Actinobacteria,*	Ai et al. 2015
Tall grass prairie	^{13}C-shoot biomass	DNA	Oklahoma, USA	*Proteobacteria, Actinobacteria, Acidobacteria*	Cheng et al. 2017
Rice field	^{13}C-glucose	DNA	Jiangsu, China	*Firmicutes, Proteobacteria,* Candidatus Saccharibacteria	Kong et al. 2018
Deciduous forest	^{13}C-methanol	DNA	Steigerwald, Germany	*Beijerinckiaceae, Microbacteriaceae, Chitinophagaceae*	Morawe et al. 2017
Arctic tundra	^{13}C-glucose, cellobiose, xylose, arabinose, cellulose	DNA	Daring Lake, Camada	*Actinobacteria, Proteobacteria (Alpha, Beta, Delta, Gamma)*	Verastegui et al. 2014
Temperate rainforest sandy loam	^{13}C-glucose, cellobiose, xylose, arabinose, cellulose	DNA	Vancouver Island, Canada	*Proteobacteria (Alpha, Beta), Actinobacteria, Verrucomicrobia*	Verastegui et al. 2014
Agricultural silt loam	^{13}C-glucose, cellobiose, xylose, arabinose, cellulose	DNA	Elora Research Station, Canada	*Proteobacteria (Alpha, Beta,Gamma), Actinobacteria, Firmicutes*	Verastegui et al. 2014
Arctic tundra	$^{13}CH_4$	DNA	Eureka, Canada	*Proteobacteria (Beta, Delta, Gamma), Bacteroidetes*	Martineau et al. 2010

Table 1.2: Examples of studies of SIP at subzero temperatures are highlighted in grey. Detected bacterial phyla are listed in the order of relative abundance.

1.3 INSIGHTS FROM GENOMES AND ISOLATES

Genomes provide insights into the bacterial adaptations that have allowed for growth in frigid tundra soils. Overall, the mechanisms that allow a bacterial cell to survive and be metabolically active at subzero temperatures ensure that the internal environment of the cell is kept at homeostasis, and that membrane fluidity is maintained. Examples of cryo-bacterial adaptations that have been experimentally verified are listed in Table 1.3.

One of the most important features for survival, persistence, or optimal growth of the organism is the maintenance of membrane fluidity (Russell 2008). Membrane fluidity can be sustained by a variety of strategies such as increasing the ratio of branched fatty acids to saturated fatty acids in the lipid membrane (Russell 1984). When *Listeria monocytogenes* grows at low temperatures, there is an increase in branched fatty acids such as anteiso-C15:0 (Annous et al. 1998). However, some bacteria react differently to the cold, and can increase their saturated fatty acid ratios by increasing C18:0 specifically, as demonstrated in the growth of *Planococcus halocryophilus* (Mykytczuk et al. 2013).Another strategy of maintaining membrane fluidity is by producing more unsaturated fatty acids, as demonstrated by psychrophilic, mesophilic, and even thermophilic *Flavobacterium* spp. grown at lower temperatures compared to *Flavobacterium* spp. grown under mesophilic conditions (Králová et al. 2017). Maintaining membrane fluidity, and thus homeostasis, can also be achieved by producing accessory pigments such as carotenoids. Examples of carotenoids leading to cold temperature tolerance have been described in *Arthrobacter agilis* in the form

of C-50 carotenoids, and glycosylated derivatives (Fong et al. 2001). Similarly, the production of carotenoids such as zeaxanthins is increased upon cold exposure in *Sphingobacterium antarcticus* (Jagannadham et al. 2000). Carotenoids, are hypothesized to stabilize the bacterial membrane, depending on their polarity and branching. Further, it has even been revealed that carotenoid producing heterotrophic Antarctic bacteria are able to endure frequent bursts of freezing compared to non-carotenoid producers (Dieser et al. 2010). In addition, carotenoid pigmentation, along with glycine betaine and inositol, has been shown to ameliorate stress from solar radiation in cold environments (Pérez et al. 2017). C-30 isoprenoid molecules similar to carotenoids such as hopanoids, are also hypothesized to play a role in thermal stress adaptations in some bacteria by modifying cell-membrane dynamics (Damsté et al. 2017).

It is also vital for microorganisms to maintain protein flexibility in cold environments (Raymond-Bouchard et al. 2018). This adaptation can be accomplished by having a higher specific activity at lower temperatures, thus reducing the activation energy needed (Feller and Gerday 2003; De Maayer et al 2014). In some cases, critical enzymes such as DNA ligases have a decrease in residues such as arginine and proline, as demonstrated in the cryo-active *Pseudoalteromonas haloplanktis* (Georlette et al. 2003). Likewise, proteomic profiles from *Psychrobacter arcticus* have shown a decrease in amino acids residues such as proline and arginine when the bacterium was grown at -10°C, by which protein flexibility was likely improved (Ayala-del-Río et al 2010).

Other protein adaptations include Cold Inducible Proteins (CIPs), Cold Adaptation Proteins (CAPs), and Cold Shock Proteins (Csps), which have similar functions but are differentially expressed under varying environmental and growth conditions (Phadtare et al. 1999). CAPs are expressed continuously during bacterial growth, with constant exposure of the organism to the cooler temperatures during growth (Beckering et al. 2002). Examples of CAPs include trigger factors that interact with newly manufactured polyketides, as demonstrated in the Antarctic isolate *Pseudoalteromonas haloplanktis* (Piette et al. 2012). Csps belong to a specific family of proteins, which are highly expressed following bacterial exposure to a temperature downshift, and provide stability to vulnerable, critical cellular machinery, such as secondary RNA structures and protein folds, and are part of the umbrella term “CIPs” (Phadtare et al. 1999, 2008; Barria et al. 2013). Other CIPs include proteins such as trehalose synthases encoded by the *otsAB* pathway, which are induced upon temperature downshifts to increase trehalose production (Kandror et al. 2002). Trehalose has been shown to protect cells during the increased osmotic stress, which is prevalent from the increase of solutes in unfrozen, subzero temperature water (Reina-Bueno et al. 2012).

Some adaptations of Arctic bacteria are multifunctional such as exopolysaccharide (EPS) production. This is widely leveraged by microorganisms to persist through freeze-thaws, and survive the osmotic stress of saline, subzero temperature liquid water (Liu et al. 2012). Other overlapping strategies also include anti-freeze proteins and carotenoid pigmentation to

overcome such low-temperature challenges (Dieser et al. 2010: Singh et al 2014).

Adaptation	Feature	Organism	Temperature (°C)	Publication
Membrane Fluidity	Increase ratio of branched to saturated fatty acids	*Planococcus halocryophilus*	-15	Mykytczuk et al. 2013
	Increase unsaturated fatty acids	Antarctic *Flavobacterium* spp	10	Králová et al. 2017
	Increase anteiso-branched fatty acids	Antarctic *Flavobacterium* spp	10	Králová et al. 2017
	Increased polar C-50 carotenoid production	*Arthrobacter agilis*	5	Fong et al. 2001
	Increased polar carotenoid zeaxanthin	*Sphingobacterium antarcticus*	5	Jagannadham et al. 2000
	Decreased apolar carotenoid beta-carotene	*Sphingobacterium antarcticus*	5	Jagannadham et al. 2000
Protein Flexibility	Decreased use of proline and arginine	*Psychrobacter arcticus*	-10	Ayala-del-Río et al 2010
	DNA liagase's decrease in arginine, proline residues	*Pseudoalteromonas haloplanktis*	18	Georlette et al. 2003
Cold Inducible Proteins (CIPs)	AtpF, EF-Ts, TolC, Pcryo_1988, FecA	*Psychrobacter cryohalolentis* K5	-4	Bakermans et al. 2007
	Cold Shock Protein (Csp) family	*Escherichia coli*	8	Ivancic et al. 2013
Cold Acclimation Proteins (CAPs)	Trigger factor (tig)	*Pseudoalteromonas haloplanktis*	4	Piette et al. 2012
	CAPs of <30 kDas during continous growth	*Enterococcus faecalis*	8	Panoff et al. 1997
	trehalose synthases, *otsAB* pathway	*Escherichia coli*	4	Kandror et al. 2002
Solar Radiation [ROS protection]	Carotenoid pigmentation	Carotenoid pigmentation	4	Dieser et al. 2010
	Increase in glycine betaine, inositol	*Rhodobacter* spp.	28	Pérez et al. 2017
Osmotic Tolerance	Exopolysaccharides (EPS), 2-α-, 6-α-mannosyl	*Pseudoalteromonas* strain SM20310	15	Liu et al. 2012
	Increase in glycine betaine, inositol	*Rhodobacter* spp.	28	Pérez et al. 2017
Freeze-thaw Survival	Anti-freeze proteins, high thermal hysteresis	*Pseudomonas ficuserectae*	-1, 4, 15	Singh et al. 2014
	Carotenoid pigmentation	Carotenoid pigmentation	4	Dieser et al. 2010
	Exopolysaccharides (EPS), 2-α-, 6-α-mannosyl	*Pseudoalteromonas* strain SM20310	4,-80, 25	Liu et al. 2012

Table 1.3: Examples of cold adaptation in bacteria

1.4 RESEARCH QUESTIONS AND GOALS

The overall goals of this dissertation are to understand bacterial life in Arctic tundra soils, using analyses at the community and genome levels. It has been established that soil respiration by bacteria occurs at subzero temperatures, but a major gap remains in our understanding of which bacteria are active at subzero temperature ranges in Arctic tundra soils. Another disparity is understanding how some of the tundra soil isolates are able to thrive in these environments. Using Arctic tundra soil incubation from Kilpisjärvi, Finland, along with several tundra soil isolates from the same site, the bacterial biology was explored with the following aims:

SPECIFIC AIM 1

Identification of subzero-active bacterial communities

The goal was to determine the subzero-active bacterial community of the Arctic tundra soils of Kilpisjärvi, Finland using Stable Isotope Probing (SIP) and 16S rRNA gene sequencing. By testing a range of subzero temperatures of 0°C, -4°C, and -16 °C, the aim was to determine if temperature within subzero ranges has an impact on active bacterial community composition. Implications of different active bacterial communities may suggest that subzero nutrient cycling may be impacted by temperature shifts in frozen soils.

Hypothesis: Because of the stark temperature differences between summer and winter temperatures of Arctic tundra soils, it is unlikely that the same bacterial communities that were reported to be dominant during warmer temperatures are

equally dominant at subzero temperatures. Therefore, other phyla whose members are not abundant or below detection in the summer, may be dominant in the winter. There may also be a stark difference in organisms that are active at 0°C vs. -16 °C.

SPECIFIC AIM 2

Analysis of isoprenoid biosynthetic pathways of hopanoids and carotenoids in the genomes of ubiquitous Arctic tundra soil *Acidobacteria*

The genomes of three established *Acidobacteria* species and six newly sequenced undescribed *Acidobacteria* isolates from the Kilpisjärvi tundra region were examined. *Acidobacteria* are well-adapted to the tundra soil environment and represent a large portion of the bacterial community. The analysis focused on genes involved in the synthesis of isoprenoid structures of hopanoids and carotenoids. These are postulated to play a role in bacterial adaptation and survival, and are relatively unexplored. Though little is known about their general role, some members of *Acidobacteria* have been found to synthesize varietals of either C_{30} isoprenoids (hopanoids) or the C_{40} isoprenoids (carotenoids) (Garcia Costas et al. 2012; Damsté et al. 2017). *Granulicella mallensis* strain MP5ACTX8, *Granulicella tundricola* strain MP5ACTX9, and *Terriglobus saanensis* strain SP1PR4 along with six new *Acidobacteria* strains (A2288, M8UP23, M8UP39, MP8S11, MP8S7, and MP8S9) were analyzed using their genomes. This pangenomic analysis will be coupled with the other biochemical characterization in the laboratory of Dr. Männistö in Finland for the potential announcement of new species.

SPECIFIC AIM 3

Genome analysis of the tundra soil bacterium, *Mucilaginibacter mallensis*

The Arctic tundra site of Kilpisjärvi, Finland, serves as a model landscape to explore the ecology and biology of tundra soil bacteria. Here, *Mucilaginibacter mallensis* strain MP1X4 isolated from the same Kilpisjärvi tundra soil as used in the SIP study was explored by analyzing genomic capabilities and carbon cycling.

Mucilaginibacter spp., members of the phylum *Bacteroidetes,* are poorly understood soil, plant, and gut bacteria that are found globally in carbon-rich environments. *Mucilaginibacter* isolates have been obtained from cold Arctic tundra soils, volcanic forest soils and agricultural rhizospheres, rotten wood, plant matter, and from lichens (Madhaiyan et al. 2009; Männistö et al. 2010; Jiang et al. 2011; Khan et al. 2013; Kämpfer et al. 2014; Baek et al. 2015; Oh et al. 2016). Three *Mucilaginibacter* species, namely *M. lappiensis*, *M. mallensis*, and *M. frigotolerans* have been isolated from soils and lichen mostly from the Kilpisjärvi tundra site (Männistö et al. 2010). These bacteria grow between 0 and 33°C as aerobic chemo-heterotrophs and form slimy, mucoid colonies (Männistö et al. 2010). Notably, in characterization of *Mucilaginibacter* isolates, they were also shown to produce copious amounts of extracellular polysaccharides. This observation, along with the note that they are isolated from carbon-rich environments, may suggest that they are well-adapted to process complex organic molecules. Hence, a genome analysis of *M. mallensis* may provide

insights into the specifics of these capabilities and will set the stage for future, targeted experiments.

CHAPTER 2: EFFECT OF TEMPERATURE ON CYRO-ACTIVE BACTERIA IN TUNDRA SOILS

ABSTRACT

Arctic soils cover large areas of Earth, store vast amounts of carbon, and are subject to intense climate change. As temperatures shift, the Arctic tundra soils may also undergo changes in the composition of their microbial communities. While numerous studies have examined effects of thaw on the composition and activities of soil microorganisms, little is known about the consequences of warming within subzero temperatures in frozen soils. This study identifies tundra soil bacteria active at subzero temperatures using a stable isotope probing (SIP) approach. Incubations with tundra soil from Kilpisjärvi, Finland were amended with ^{13}C-cellobiose and held at 0, -4, and -16°C for 5-40 weeks. 16S rRNA gene sequence analysis of ^{13}C-labelled DNA revealed distinct subzero-active bacterial taxa. Our SIP experiments demonstrated that members of Candidatus Saccharibacteria, *Melioribacteraceae*, *Verrucomicrobiaceae*, *Burkholderiaceae*, *Acetobacteraceae*, *Armatimonadaceae*, and *Planctomycetaceae* were capable of synthesizing ^{13}C-DNA at subzero temperatures. Members of *Oxalobacteraceae,* and *Rhizobiaceae* were found to be more active at 0°C than at -4°C or -16°C, whereas *Melioribacteriaceae* were active at all subzero temperatures tested. Phylogenetic analyses of ^{13}C-labelled 16S rRNA genes from the *Melioribacteriaceae*, *Verrucomicrobiaceae*, and Candidatus Saccharibacteria suggested that these bacterial taxa formed subzero-active clusters closely related to members from other cryo-

environments. This study demonstrates that subzero temperatures impact active bacterial community composition and may influence global biogeochemical cycles.

2.1 INTRODUCTION

The Arctic is among the most vulnerable regions with respect to climate change, and is currently exhibiting dramatic ecosystem changes. Many of these changes will have widespread implications, including alterations in Earth's carbon budget and climate. Primarily, this is because Arctic soil environments harbor vast stores of organic carbon (C), and decomposition of these C stores is expected to be a significant contributor to atmospheric chemistry and climate (Tarnocai et al. 2009; Natali et al. 2011; Biasi 2014; Schuur 2015; Jansson and Tas 2014). As a consequence of a changing climate, these vulnerable polar environments are shifting from historic carbon sinks to contemporary carbon sources (Oechel et al. 1993; Belshe 2013; Natali et al. 2015). These changes are largely due to microbial responses to temperature shifts in the tundra (Biasi et al. 2014; McCalley et al. 2014; Voigt et al. 2016). While there has been extensive research on tundra soil microbial communities active at temperatures above 0°C (e.g., Sjögersten et al. 2003; Rinnan et al. 2006; Natali et al. 2010; Graham et al. 2012; Stark et al. 2015; Schuur et al. 2015; Stackhouse et al. 2016), little is known about effects of temperature changes within subzero ranges on active microbial communities. Though understudied, biological activities are well established to occur below 0 °C, as long as cellular membrane fluidity is

maintained (Arthur and Watson 1976; Clein and Schimel 1995; Bakermans et al. 2003; McMahon et al. 2009; Öquist et al. 2009; Mykytczuk et al. 2013; Mykytczuk et al. 2016; Goordial et al. 2016; Schaefer and Jafarov 2016).

Approaches to study life at subzero temperatures have included transcriptomics, metagenomics, RNA studies, respirometry, enzymatic capabilities, microbial biomass measurements, and (meta)genome analyses (for reviews see Jansson and Tas 2014; Nikrad et al. 2016). These provide evidence that microbes are active at subzero temperatures and that their interactions are complex. However, ascertaining identities of active microorganisms is difficult with these methods because of the caveat of frozen environments—DNA or RNA may remain preserved, despite the lack of metabolic activity, while respirometry demonstrates activity but does not identify the responsible organism. To overcome this challenge, methods such as stable isotope probing (SIP) have been employed to identify and track active community members relevant to understanding overall subzero microbial activities (Tuorto et al. 2014; Nikrad et al. 2016).

In this study, we used SIP methodology to identify the active subzero bacterial community in Arctic tundra soils. Here, we carried out SIP and 16S rRNA gene bacterial sequencing of seasonally frozen Arctic tundra soils using ^{13}C-cellobiose as the carbon substrate at subzero temperatures of -16, -4, and 0°C. Cellobiose is representative of the plant-derived C in the tundra, an important C source in the global C cycle. Active microorganisms at subzero temperatures will assimilate the ^{13}C into their DNA when replicating their

genomes, allowing for separation and sequencing of the newly synthesized ^{13}C-DNA. This study not only identifies bacterial members that were active in processing cellobiose at subzero temperatures but also answers whether subzero temperature ranges affect bacterial community composition.

2.2 METHODOLOGY OF SUBZERO-SIP

Study site and tundra soil collection

Tundra soils for the laboratory incubations were collected from Malla Nature Preserve, Kilpisjärvi, in northwestern Finland in July, 2012. The sampling site is located at 69° 3’ 48.229” N, 20° 44' 38.791" E, within the subalpine Scandinavian mountain range, with vegetation consisting of shrubs, lichens, and grasses, and the soil is primarily at a pH of ~7 (Männistö et al. 2007; Männistö et al. 2013; Männistö et. al., 2009; Männistö et al. 2011). The mean annual air temperature is -2.2°C, with the soil temperature fluctuating from 0°C to -25°C in the winter (Männistö et al. 2007; Kumar et al. 2017; Männistö et al. 2013). The growing season is only 100 days long and the soils are subject to subzero temperatures for the majority of the year (Männistö et al. 2013). For this study, the soils were collected by coring to approximately 5 cm depth in the organic layer. After sampling, soils were sieved and stored in the laboratory at 4°C for 22 months to deplete them of labile carbon prior to initiating SIP experiments.

Subzero SIP Incubation Setup

A set of replicate tundra soil incubations (0.3 g) were established in 2 mL microcentrifuge tubes with cellobiose as the carbon source to represent plant-derived organic matter. Individual incubations were amended with either ^{13}C- or ^{12}C-cellobiose (1 mg C/per gram soil C added in a total volume of 100 µL water per replicate) and held at temperatures of 0°C, -4°C, and -16°C. All incubations were monitored with an internal thermometer, where daily temperature logs were maintained. The incubation temperatures varied briefly, maintaining averages of -15.8, -4, and -0.4°C over the course of 40 weeks. After 5 and 40 weeks of incubation, triplicate incubations from each set were sacrificed for DNA extraction and downstream analysis. For an illustration of this methodology, please see Figure 2.1.

Soil incubation processing

DNA was extracted using a hexadecyltrimethylammonium bromide (CTAB) — phenol-chloroform extraction method similar to Männistö et al. (2009). Briefly, soils were extracted with equal volumes of 5% CTAB and phenol-chloroform isoamyl alcohol (25:24:1) by bead-beating with two 3 mm glass beads on a bench-top vortex for 3 minutes. The soil was pelleted by centrifugation and the top phase was mixed with an equal part chloroform isoamyl alcohol (24:1). After centrifugation, the upper phase was transferred to a new microfuge tube, to which 2X volume of 30% w/v polyethylene glycol 8000 (PEG) was added, and allowed to stand at 4°C for 45 minutes before centrifugation. The supernatant

was removed and DNA was precipitated. DNA was then washed and centrifuged with cold 100% ethanol at 4°C. The supernatant was removed and followed by a 70% ethanol wash/centrifugation. The DNA pellets were then dried at room temperature and resuspended in DNAse-free water. The extracted DNA suspension was quantified on a 2% gel to verify for sufficient DNA (greater than 300 ng) and prepared for ultracentrifugation.

Prior to ultracentrifugation, 100 ng of archaeal ^{13}C-labeled carrier DNA from *Halobacterium salinarium* was added to ~100 ng of sample DNA and amended with ethidium bromide to allow for distinct separation and visualization of light and heavy DNA bands under UV light (Gallagher et al. 2005; Tuorto et al. 2014). A total of 200-250 ng of DNA was applied in cesium chloride (CsCl) to each column for isopycnal ultracentrifugation at 225,000 x g for 48 hours. Light (^{12}C) and heavy (^{13}C) DNA bands were then visualized under UV light and collected by pipette from the CsCl gradient.

Screening for bacterial activity using community fingering:

DNA from the ^{13}C-bands were amplified using bacterial 16S rRNA gene 27F(5'-AGAGTTTGATCCTGGC TCAG-3') - R1100 (5'-AGGGTTGCGCTCGTTG-3') primers using the following parameters: 2 minutes at 94 °C; followed by cycles of 27 of 30 seconds at 94 °C, 40 seconds at 53 °C, and 1 minute at 72 °C; and elongation for 5 minutes at 72 °C. Unambiguous ^{13}C-DNA synthesis was assessed by verifying that there was no amplification in the ^{13}C carrier bands of ^{12}C-cellobiose amended incubations, while there was positive amplification in the

^{13}C-cellobiose carrier bands in ^{13}C amended incubations. 16S rRNA gene amplicons from the ^{13}C carrier bands were digested with MspI and screened by terminal restriction fragment length polymorphism (TRFLP) community analysis, per methods of Tuorto et al. (2014). The TRFLP community profile analysis allowed for the pre-screening of samples that were subsequently selected for Illumina MiSeq sequencing of the bacterial 16S rRNA gene.

Amplicon DNA Sequencing

Analysis of heavy DNA bands was carried out by MRDNA (Shallowater, Texas, USA) using the 16S rRNA MiSeq Illumina amplicon sequencing platform. DNA primers were chosen to selectively amplify only bacterial sequences DNA was amplified using 2-step PCR with 27F(5'-AGAGTTTGATCCTGGCTCAG-3')-R1100 (5'-AGGGTTGCGCTCGTTG-3') followed by F341 (5'-CCTACGGGNGGCWGCAG-3') -R785 (5'-GACTACHVGGGTATCTAATCC-3') primers (Klindworth et al. 2012), with a barcode on the forward primer for 30 cycles using the following conditions: 3 minutes at 94°C; followed by cycles of 28 of 30 seconds at 94°C C, 40 seconds at 53°C, and 1 minute at 72°C; and elongation for 5 minutes at 72°C. PCR products were checked by 2% agarose gel electrophoresis. Samples were further purified using Ampure XP beads to prepare for DNA libraries. DNA libraries were prepared according to the Illumina TrueSeq protocol and sequencing was carried out by MRDNA via a MiSeq Illumina Sequencer using manufacturer's protocols and data were processed using MRDNA's pipeline (MRDNA, Shallowater, Texas, USA).

Bioinformatic Pipeline and Analyses

DNA sequences were trimmed of barcodes, and sequences less than 150 bp were discarded, along with ambiguous base calls. Chimeric sequences were removed and operational taxonomic units (OTUs) were defined by clustering at 97% similarity (3% divergence). OTUs were taxonomically classified using BLASTn, using GreenGenes, RDPII, and NCBI 16S rRNA gene databases. Similarity criteria for classification at different phylogenetic levels were as follows: >97% species, 95-97% Genus, 90-95% Family, 80-85% Class, and 77-80% Phylum.

Data were imported into ClustVis using R packages including pcaMethods (R package version 0.7.7) for Principal Component Analysis (PCA) with unit variance scaling, Singular Value Decomposition (SVD), and imputation to calculate principal components (Metsalu and Vilo 2015). Heat maps to compare relative abundances of bacterial populations were also generated with ClustVis using ggplot2 heatmap (R package version 0.7.7), unit variance scaling, hierarchical clustering, correlation distance, and average linkage (Metsalu and Vilo 2015).

Phylogenetic Analysis

Alignments for the ^{13}C-labeled 16S rRNA genes were built using Molecular Evolutionary Genetics Analysis version 7.0 (MEGA 7; Kumar et al. 2016) with representative closest matches identified by Blast and with 16S rRNA genes from similar polar environments (e.g., Arctic soil, lake water, etc.). Sequences were

aligned by ClustalW with manual verification, and trimmed to the length of the shortest OTUs within bacterial taxa. Molecular phylogenetic analysis was carried out using the maximum likelihood methods based on the Tamura-Nei substitution model (Tamura and Nei 1993). The bootstrap consensus tree inferred from 500 replicates represents the evolutionary history of the taxa analyzed, and branches corresponding to partitions reproduced in greater than 50% bootstrap replicates are listed (Felsenstein 1985; Kumar et al. 2016). The fraction of replicate trees in which the associated taxa clustered together in the bootstrap test (500 replicates) are shown next to the branches. Phylogenetic trees were edited in iTOL (Letunic and Bork 2016) for visualization and labeling.

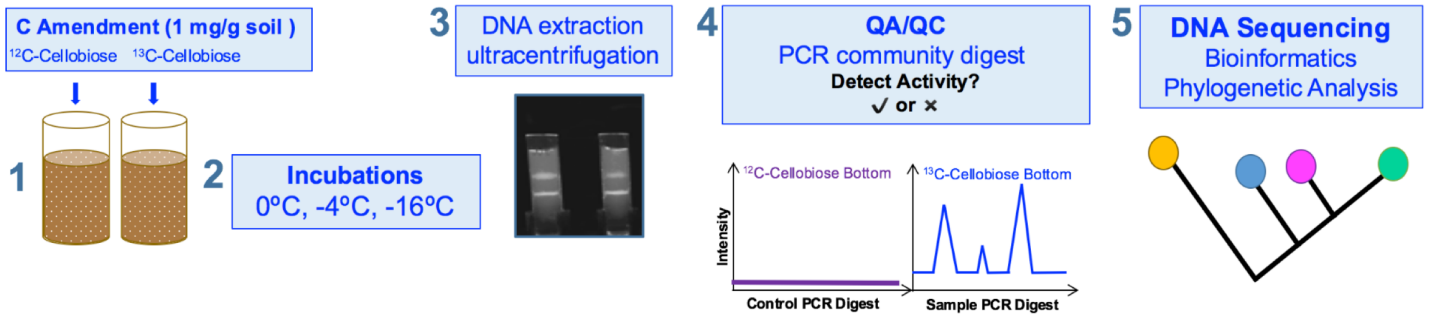

Figure 2.1: Methodology of SIP using tundra soil incubations with ^{12}C, ^{13}C-cellobiose amendments,1. The incubations up to 40 weeks, 2. After incubations, DNA was extracted; DNA screened for isotopic assimilation in 3,4. After detection of activity, 16S rRNA gene amplicon sequencing was carried out, along with data analysis, 5.

2.3 RESULTS

This study aimed to identify metabolically active bacteria at subzero temperatures in Arctic tundra soils using SIP with cellobiose amendments. Metabolically active bacteria will have assimilated the isotopic label and will allow for physical separation of their DNA. Prior to DNA sequencing and bacterial identification, soil incubations were screened for detectable metabolic activity.

Soil Incubation Screening

The subzero active members of the bacterial community were delineated from triplicate independent tundra soil incubations destructively sampled and analyzed for incorporation of ^{13}C-cellobiose into DNA. 16S rRNA gene terminal restriction fragment length polymorphisms (TRFLP) of the top and bottom bands of the ^{13}C- and ^{12}C-cellobiose amended incubations were used to screen for metabolic activity and unambiguously determine subzero activity. A key quality assurance step involved examining the bottom, heavy band of the ^{12}C-cellobiose amended incubations. A flat line in the TRFLP profile indicated that there was no contamination or shearing from the top band (^{12}C-DNA), and was also representative of this technique's replication and quality when handling the ^{13}C-cellobiose amended samples. A signal in the ^{13}C-cellobiose amended bottom band was used to detect subzero bacterial activity. The earliest time points for detection of subzero activity and incorporation of ^{13}C into DNA was after a 5-week incubation at 0 and -4˚C and 40 weeks at -16˚C (no assimilation was detected at previous timepoints of 5 and 8 weeks). The evidence of subzero

bacterial activity at -16, -4, and 0˚C by TRFLP screening is shown in Figures 2.2, 2.3, and 2.4, respectively.

DNA Sequencing

The heavy, bottom DNA bands ^{13}C-cellobiose amended 0, -4, and -16°C incubations were then sequenced by Illumina MiSeq. Amplicons of >200 bp were assigned OTUs after bioinformatic quality checks, and normalized to relative abundance. Table 2.1 shows the number of reads detected per temperature condition.

	Replicates		
Condition	**1**	**2**	**3**
Initial	43573	76652	64492
0 ºC	75298	68850	80424
-4ºC	108998	90727	107615
-16ºC	62872	91558	84513

Table 2.1: Number of reads detected per biological replicate of initial resident community and subzero incubations (^{13}C-amended Bottom Bands).

Resident and Subzero-Active Bacteria of Tundra Soils

The resident tundra bacterial community (determined from initial, time zero, incubation samples) was comprised largely of members of the phyla (in order of abundance) *Proteobacteria, Actinobacteria, Acidobacteria, Verrucomicrobia, Bacteroidetes,* and *Planctomycetes* (Figure 2.5). Members of *Chloroflexi, Fusobacteria, Firmicutes, Cyanobacteria, Chlamydia, Ignavibacteria, Candidatus Saccharibacteria,* and *Armatimonadetes* were also detected at lower

abundance (Figure 2.5). The dominant resident bacterial family members in initial (time zero) incubations were mostly (in order of abundance) comprised of *Nitrosomonadaceae, Acidobacteriaceae, Thermomonosporaceae, Sinobacteraceae, Acidimicrobiaceae, Hyphomicrobiaceae, Holophagaceae,* and *Chitinophagaceae* (Figures 2.6). The bacterial community members active at the different subzero temperatures were distinctly different from that of the resident community. Bacteria active at subzero temperatures included members of the phyla *Ignavibacteriae*, *Proteobacteria*, *Armatimonadetes*, *Actinobacteria*, *Verrucomicrobia*, Candidatus Saccharibacteria, *Chloroflexi*, *Cyanobacteria*, *Firmicutes*, *Deinoccocus Thermus*, Candidatus Brocadiaceae, and *Planctomycetes* (Figure 2.5). In contrast, members of the *Bacteroidetes*, *Chlamydia*, and *Fusobacteria* that we detected in the resident community were not detected in the subzero SIP incubations and determined to be inactive. Relative abundances of members of the *Actinobacteria*, *Acidobacteria*, *Bacteroidetes*, *Chloroflexi*, and *Proteobacteria* decreased from the initial untreated soil incubations, while relative abundances of members of the *Ignavibacteriae*, Candidatus Saccharibacteria, *Deinococcus Thermus*, *Planctomycetes*, *Armatimonadetes*, and *Verrucomicrobia* increased (Figure 2.5).

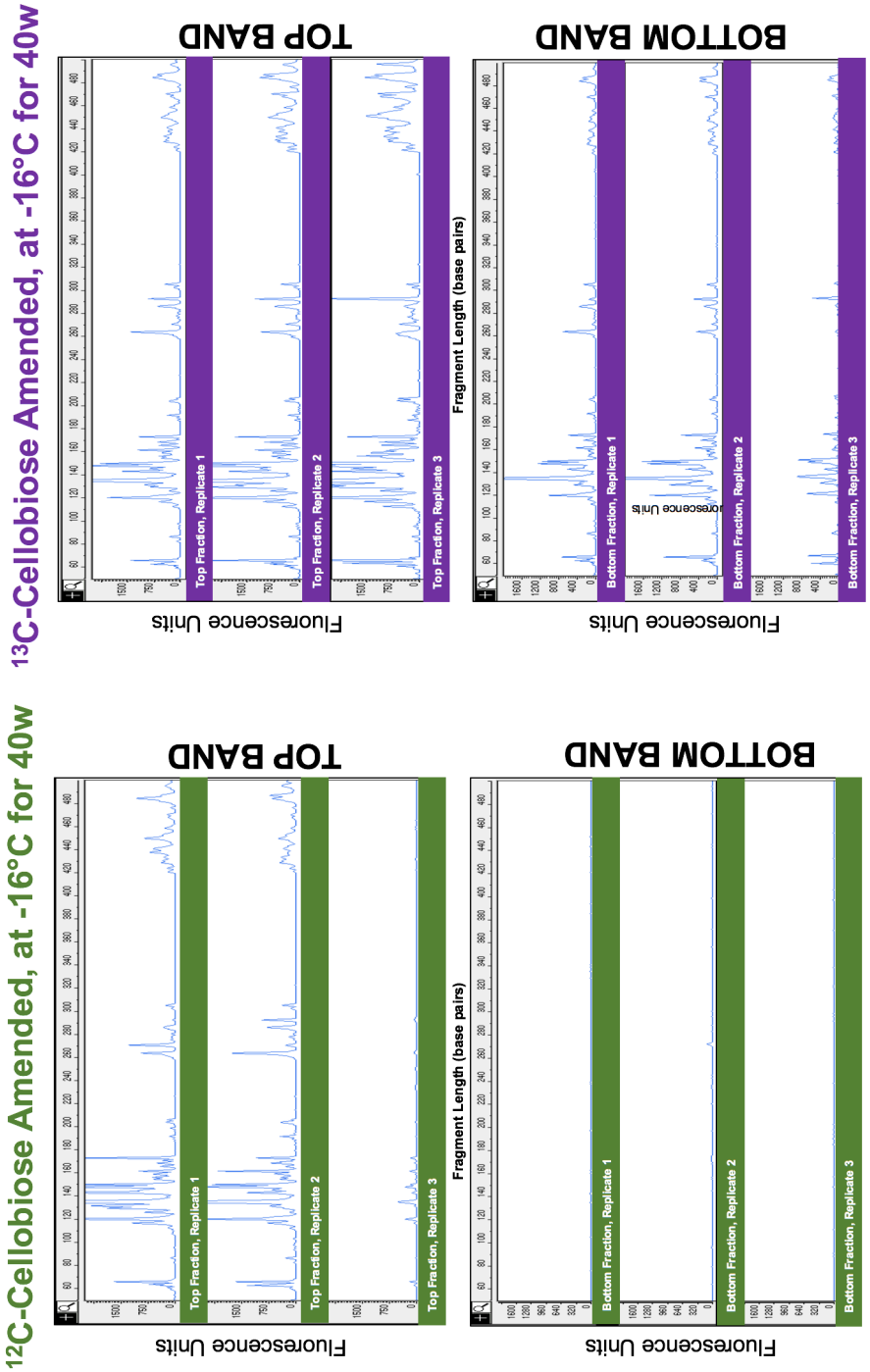

Figure 2.2: TRFLP Control and Experimental 16S rRNA gene Stable Isotope Probing of incubations at -16°C

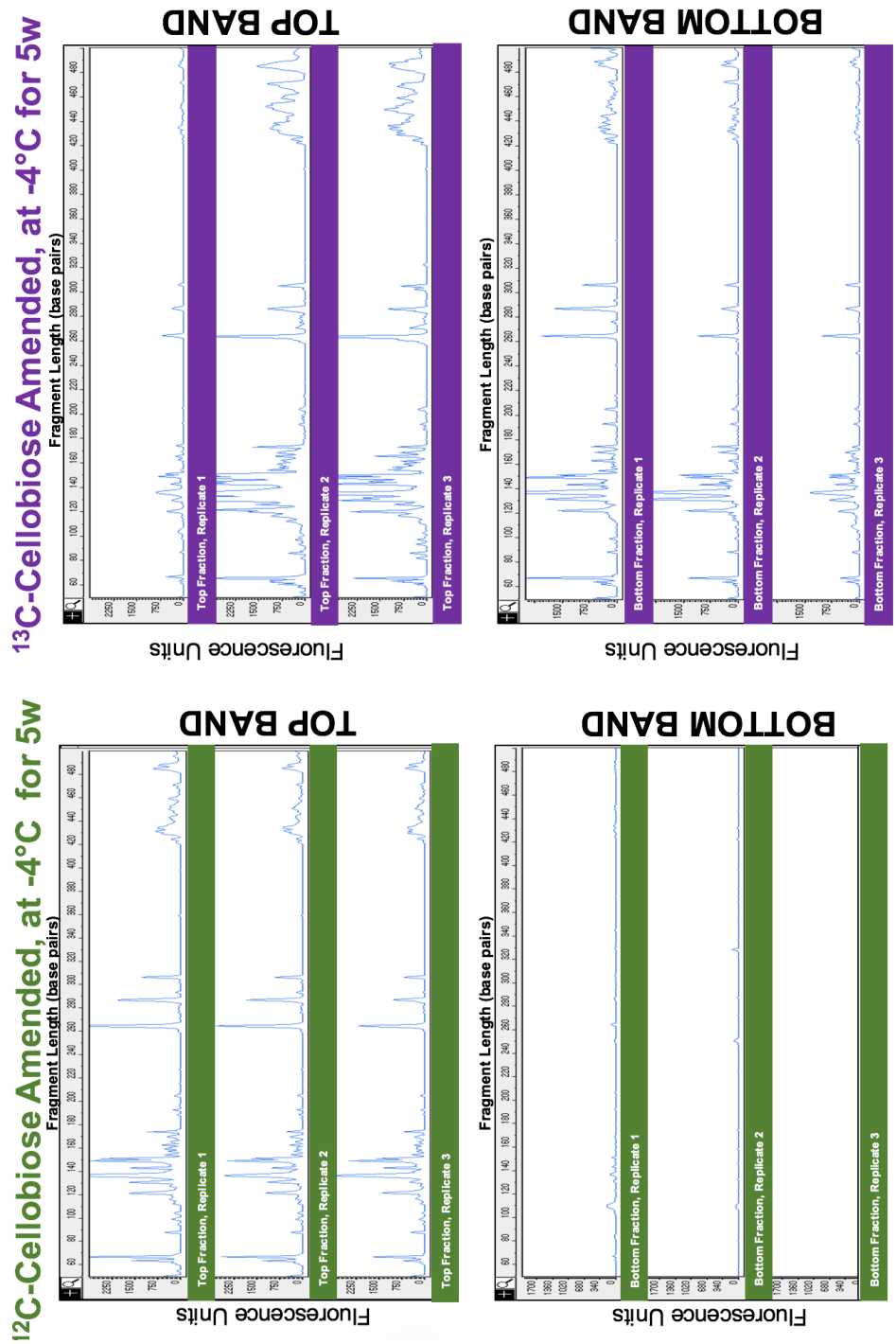

Figure 2.3: TRFLP Control and Experimental 16S rRNA gene Stable Isotope Probing of incubations at at -4 ˚C.

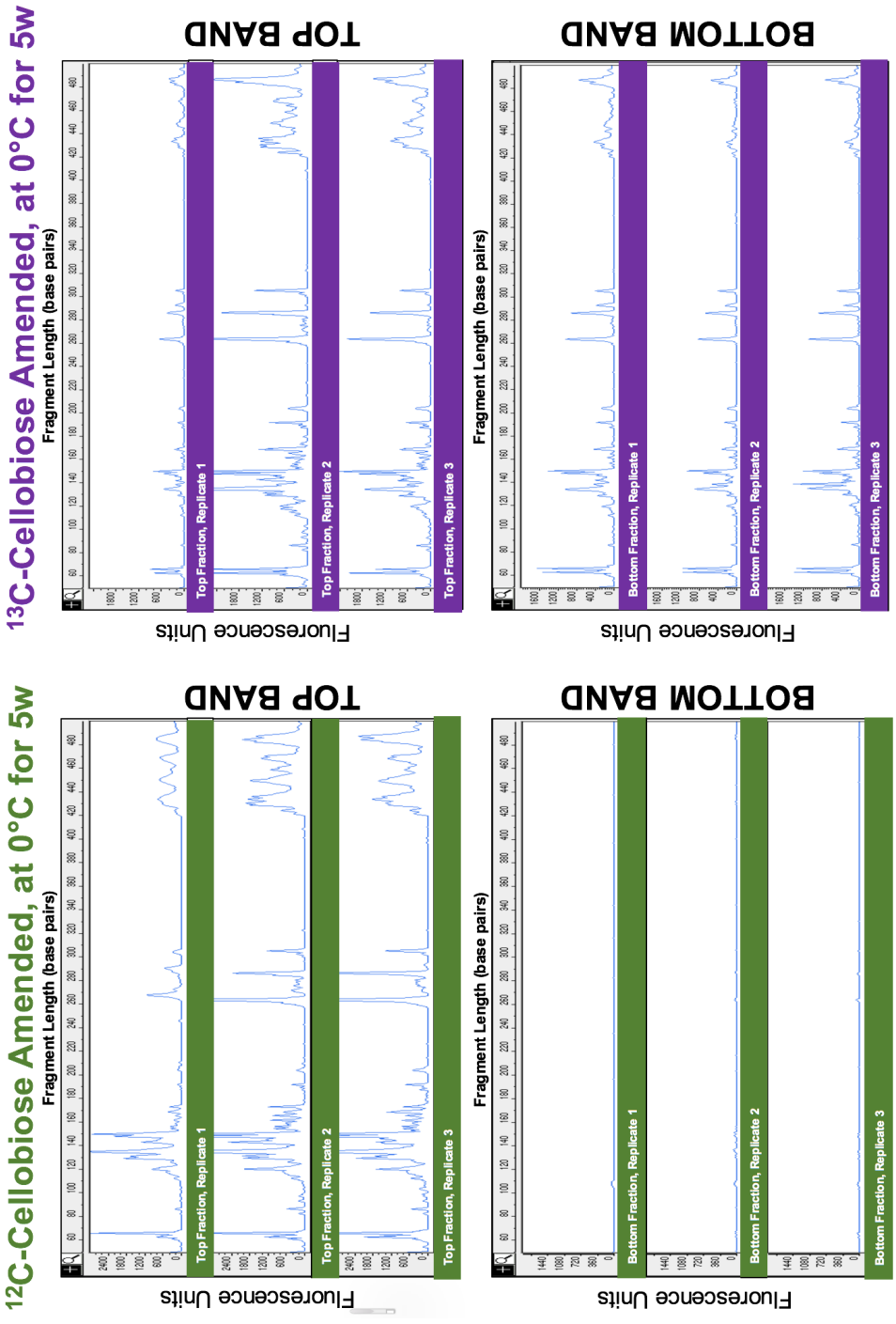

Figure 2.4: TRFLP Control and Experimental 16S rRNA gene Stable Isotope Probing of incubations at at 0˚C.

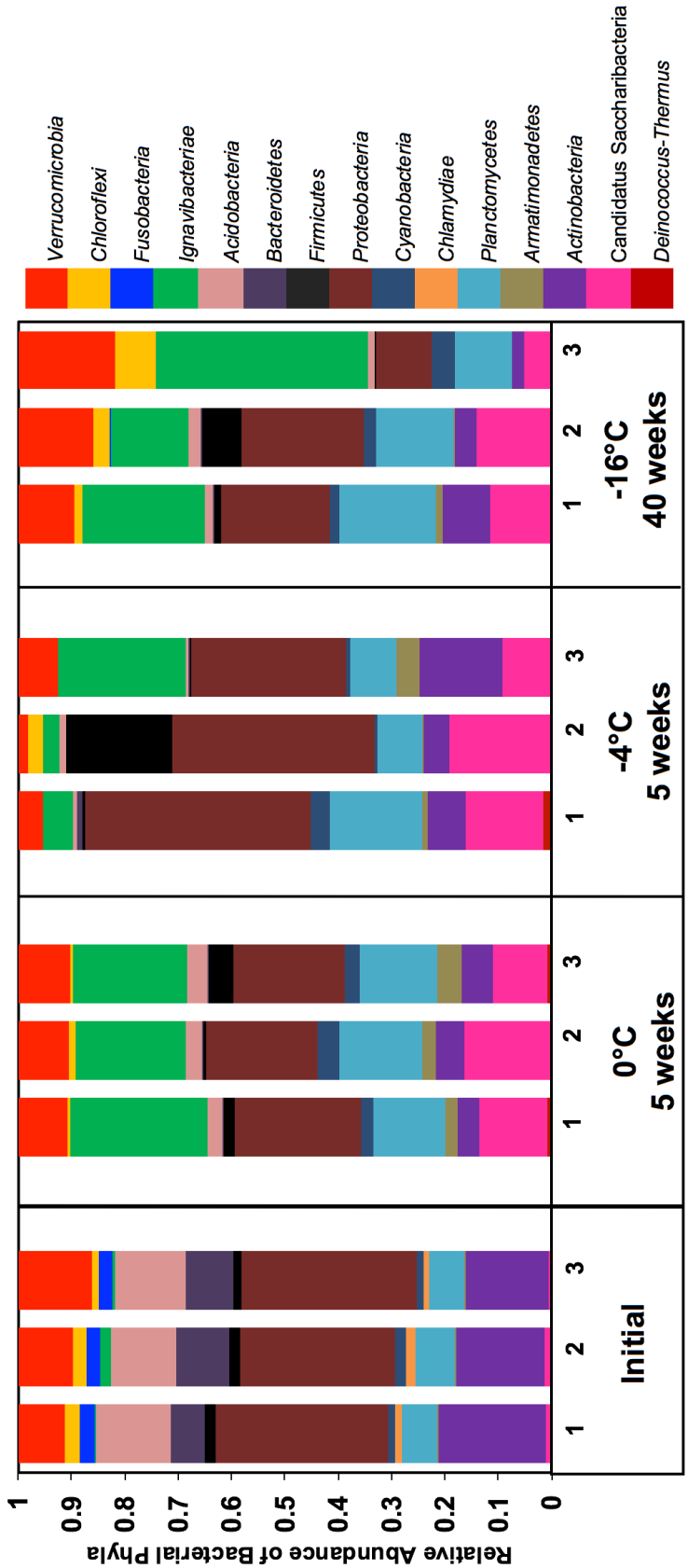

Figure 2.5: Relative abundance of bacterial phyla in triplicate tundra soil Incubations at initial and subzero incubations. The time of incubation here represents the earliest detection of ^{13}C-assimilation signal.

Active Members of Bacterial Families Detected at Subzero Temperatures

The cellobiose assimilating bacteria varied across the different subzero temperatures. (Figure 2.6). Bacteria active at 0°C included members of Candidatus Saccharibacteria, *Melioribacteriaceae*, *Armatimonadaceae, Thermacae*, *Desulfobacteraceae*, *Nocardiaeae*, *Oxalobacteraceae*, and *Prochlorococcceae*. Bacteria active at -4°C included members of the *Rubrobacteraceae*, Candidatus Saccharibacteria, and *Oxalobacteraceae*. Of particular interest was the detection of bacteria active at -16°C, including members of the Candidatus Saccharibacteria, *Melioribacteriaceae*, Candidatus Brocadiaceae, *Pelobacteraaceae*, *Acetobacteraceae*, *Armatimonadaceae*, *Desulfobacteraceae*, *Anaerolineae*, *Verrucomicrobiaceae*, and *Planctomycetaceae.* PCA demonstrated clustering of the bacterial communities based on temperature, with the soil communities incubated at 0 and -4°C clustering closer to each other than those incubated at -16°C (Figure 2.7), and all clearly separate from the initial community.

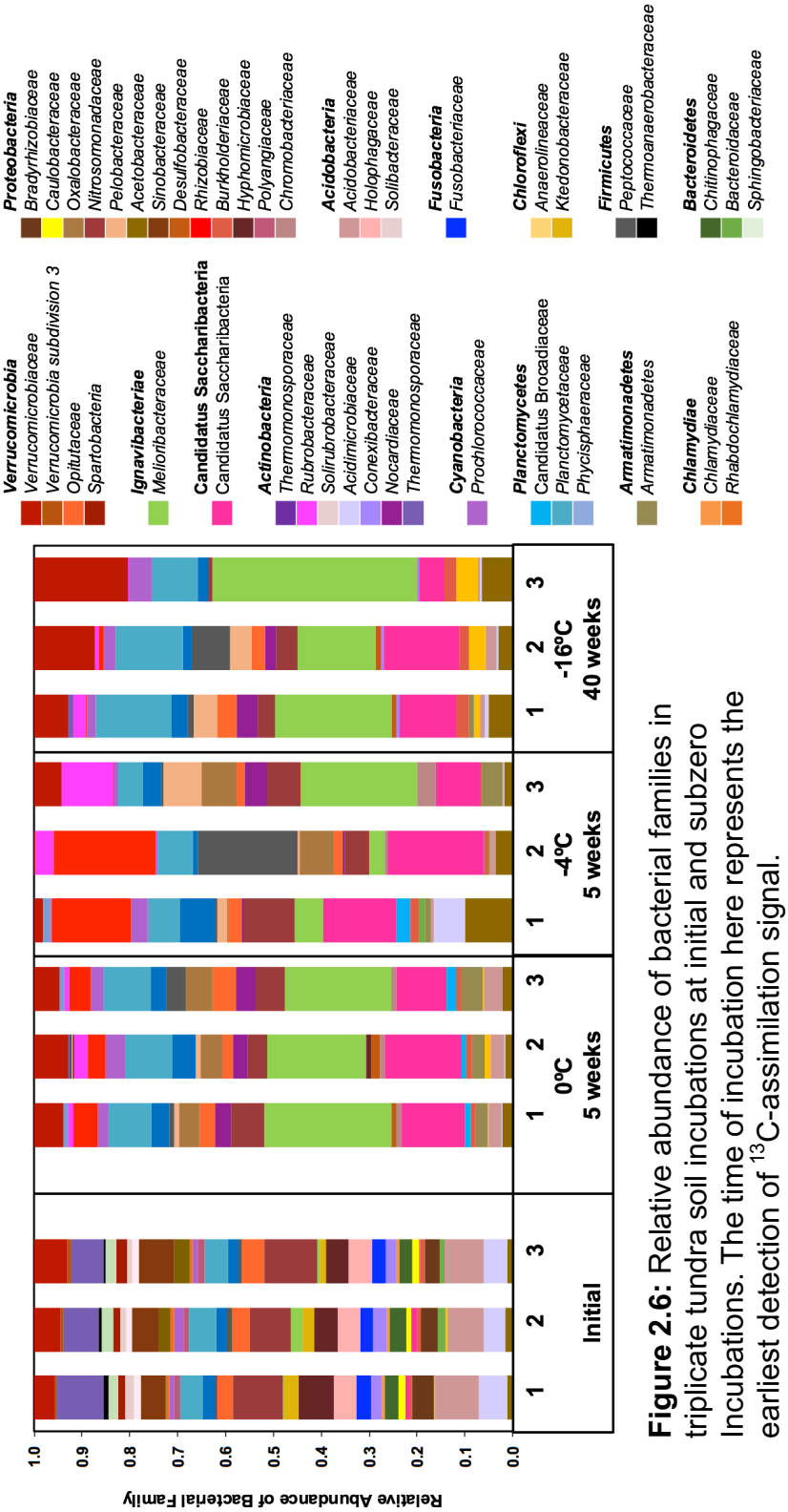

Figure 2.6: Relative abundance of bacterial families in triplicate tundra soil incubations at initial and subzero Incubations. The time of incubation here represents the earliest detection of ^{13}C-assimilation signal.

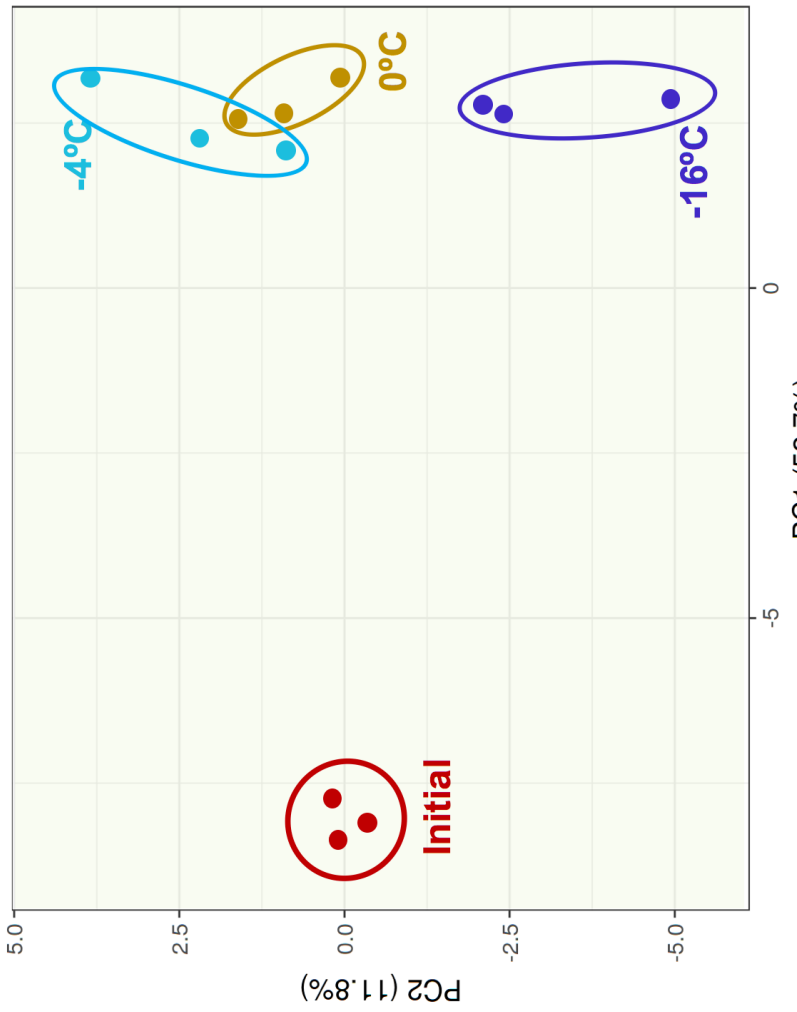

Fig 2.7: Principal component analysis of subzero-SIP families in each temperature condition. Principal component analysis was carried out using unit variance scaling is applied to rows; singular value decomposition with imputation is used to calculate principal components.

Several members of the resident bacterial families that were detected in the initial soil sample were apparently unable to assimilate and unable to utilize cellobiose at subzero temperatures. These included members of the *Holophagaceae, Acidobacteriaceae, Chitinophagaceae, Polyangiaceae, Thermoanaerobacteraecae, Bradyrhizobiaceae, Fusobacteriaceae, Connexibacteriaceae, Ktedonobacteraceae, Hyphomicrobiaceae, Thermomonosporaceae, Solirubrobacteraceae, Sphingobacteraceae, Spartobacteria, Sinobacteraceae, Rhabdochlamydiaceae, Chlamydiaceae, Verrucomicrobia* subdivison 3*, Bacteroidaceae,* and *Burkholderiaceae* (Figure 2.6).

A heat map (Figure 2.8) displays the relative the abundance of each bacterial family member within the biological replicates of each incubation to each those from every incubation and initial community. From this analysis, it can be discerned that there is a striking high abundance of bacterial members detected in the initial community that were not detected to be cryo-active. In the -16°C incubations, members of *Verrucomicrobiacaeae*, *Acetobacteraceae*, Candidatus Saccharibacteria, *Melioribacteraceae*, *Planctomycetaceae*, and *Burkholderiaceae* were in higher abundances. In the -4°C and 0°C incubations, Candidatus Saccharibacteria were also detected at high relative abundances. Similarly, members of *Phycisphaeraceae***,** were more prevalent in these -4°C and 0°C incubations.

At -4°C, members of *Rhizobiaceae*, were more abundant than at any other subzero temperature. At 0°C, members of Candidatus Saccharibacteria were

again active, along with members of *Armatimonadetes*, *Oxalobacteraceae*, *Chromobacteraceae*, *Melioribacteraceae*, *Planctomycetaceae*, and *Verrucomicrobiaceae*. Interestingly, Candidatus Brocadiaceae were most abundantly active at 0°C. Interestingly, members of the *Planctomycetaceae* were abundant at 0°C and -16°C, but not as abundant at -4°C.

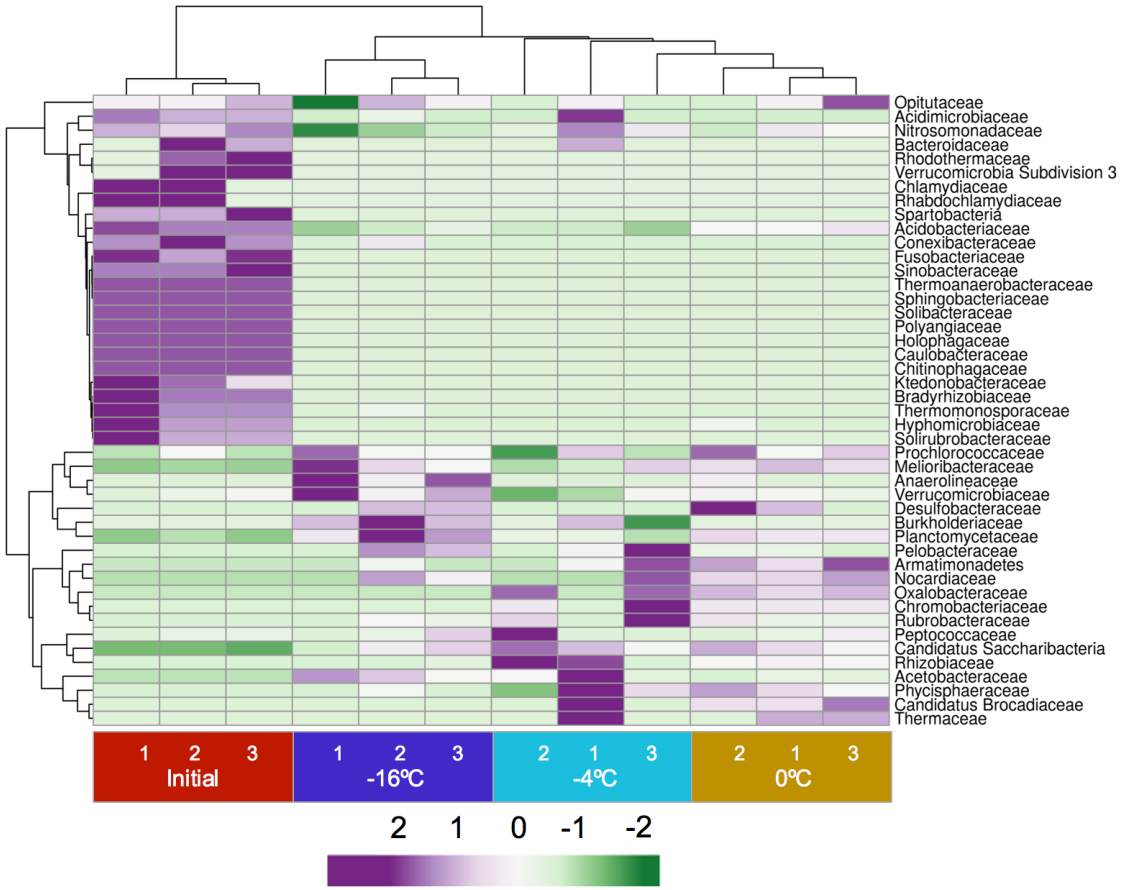

Figure 2.8: Relative abundances of tundra soil bacterial family members compared across incubationsVisualization of active tundra bacterial families from SIP treatment shown in heatmap. Rows and columns clustered using correlation distance and average linkage.

To further compare ecological patterns of bacterial families that were detected to be metabolically active in frozen soils, the diversity and species evenness was calculated for all soil cold incubations and SIP amendments, and compared to that of the initial soil bacterial community in Figure 2.9. It was observed that both diversity and evenness of bacterial communities that were able to assimilate cellobiose in subzero temperatures was lower than that of the initial soil bacterial community. The initial bacterial community is comparable to those from Greenland permafrost soils (Ganzert et al. 2014).

	Initial-1	Initial-2	Initial-3	0°C-1	0°C-2	0°C-3	-4°C-1	-4°C-2	-4°C-3	-16°C-1	-16°C-2	-16°C-3
H'	3.09	3.30	3.16	2.56	2.65	2.67	2.56	2.15	2.45	2.53	2.53	1.75
E	0.81	0.87	0.83	0.67	0.70	0.70	0.67	0.57	0.64	0.66	0.66	0.46

Figure 2.9: Shannon diversity index (H) and evenness (E) for OTUs assigned on a family level, consistent with PCA of bacterial families (Figure 2.7) and heatmap of bacterial families (Figure 2.8) for all initial and SIP amended cold incubations.

Novel Cryo-active Bacterial Clades

Phylogenetic analysis of subzero active community members, especially those of the phyla Candidatus Saccharibacteria, *Verrucomicrobia* and *Ignavibacteria* were carried out to investigate the relationships of the cryo-active OTUs of these phyla with those of isolates and uncultured bacterial phylotypes (Figures 2.10, 2.11. 2.12). Within the Candidatus Saccharibacteria, three subzero-active OTUs were detected. These OTUs were most closely related to relatives detected in other polar or cold environments, including Svalbard ice cores, Antarctic soils, Arctic soils, thawing Canadian permafrost soils, and

Chilean desert soils (Figure 2.11). While representatives of Candidatus Saccharibacteria have been detected in diverse environments, ranging from human oral cavities to sponges, the OTUs representing subzero active members of Candidatus Saccharibacteria were most closely related to representatives from cold environments.

Within the *Verrucomicrobia*, four OTUs representing subzero active members were detected (Figure 2.12). Three of the OTUs clustered closely together and were most closely related to *Opitutus* clones from limnopolar and meromictic lakes in Antarctica and France, respectively. The more divergent OTU of the subzero active *Verrucomicrobia* was shown to be more closely related to OTUs from Arctic and paddy soils, as well as from a nematode host (*Xiphimema americanum*). All subzero active OTUs clustered uniquely and represent newly distinguished cryo-active tundra soil bacteria members.

An unexpected observation was the detection of subzero-active *Ignavibacteria*. Members of the *Ignavibacteria* have mainly been found in thermophilic environments, such as hot springs, volcanic lakes, wastewater or deep aquatic sediments. However, here we detected six subzero active OTUs within the *Ignavibacteria* that formed a distinct group divergent from the known isolates and curated sequences of the phylum. The closest known relative to these active members was from a rhizosphere soil from India (Figure 2.10).

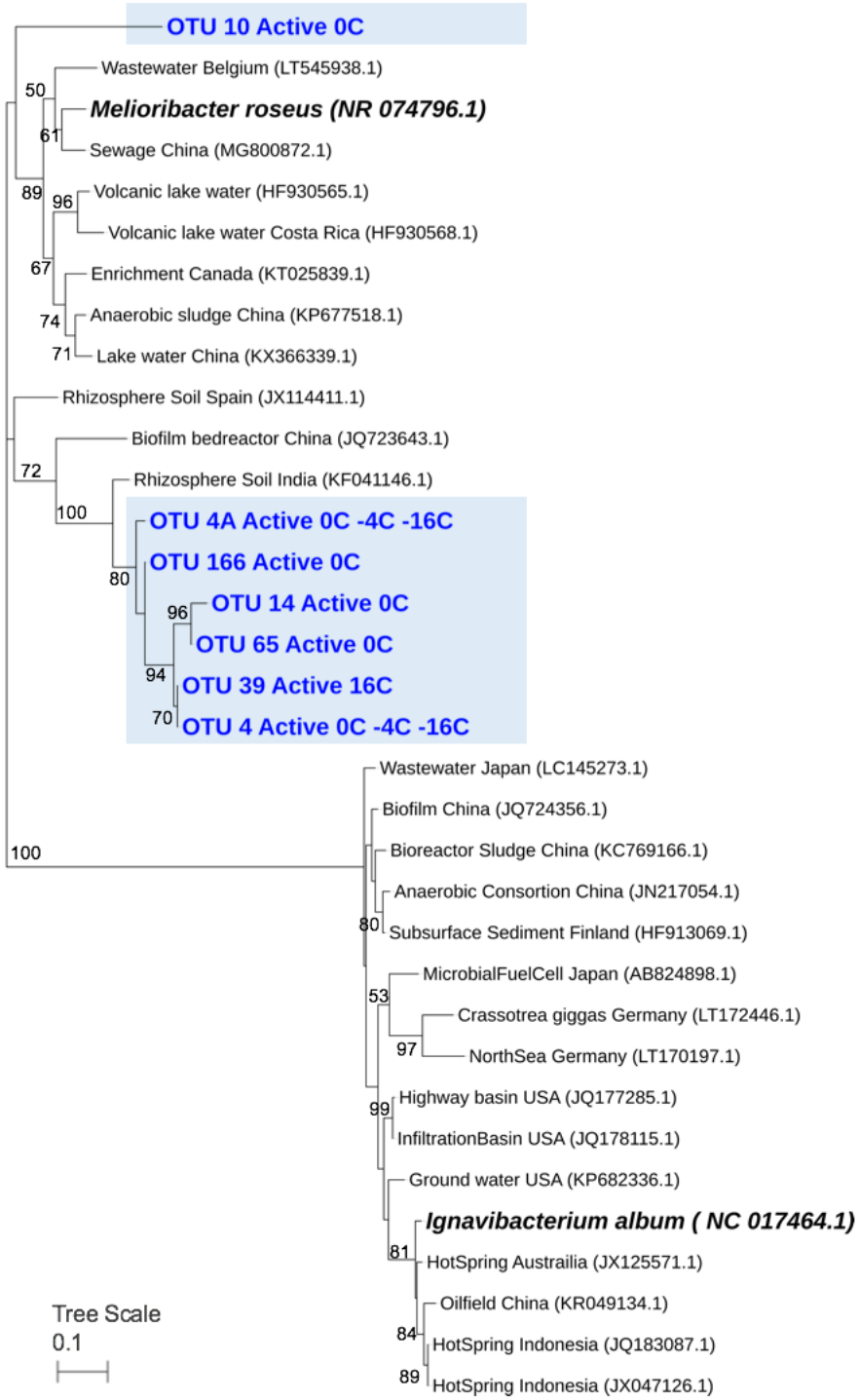

Figure 2.10:16S rRNA gene phylogeny of *Ignavibacteria* was constructed using the ML methodology using 457 bp. OTUs from this study are in blue font, taxa from cold environments are in blue background. The only 2 isolates in the phylum are in bold. Bootstrap values of 500 replicate iterations are listed. All other taxa are listed with sample source.

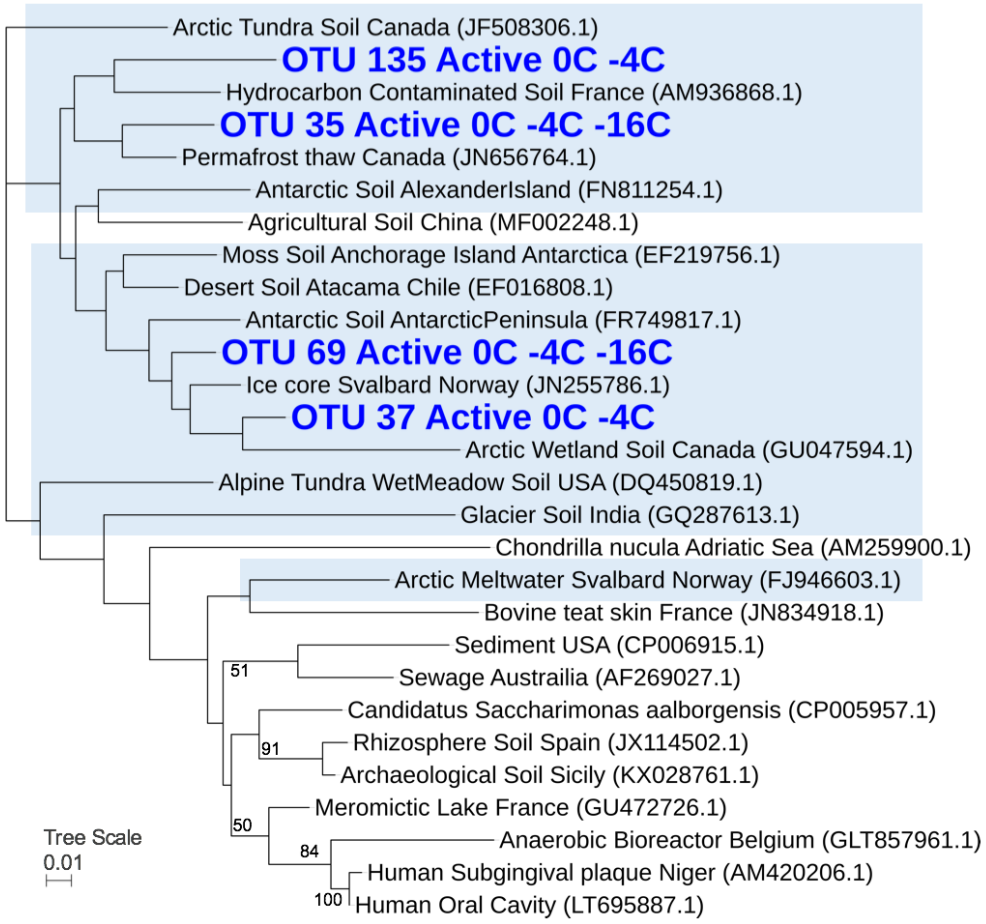

Figure 2.11: 16S rRNA gene phylogeny of the Candidatus Saccharibacteria was constructed using the ML methodology using 429 bp with 500 bootstraps replicates. OTUs from this study are in blue font, taxa from cold environments are in blue background. Bootstrap values of 500 replicate iterations are listed. All other taxa are listed with sample source.

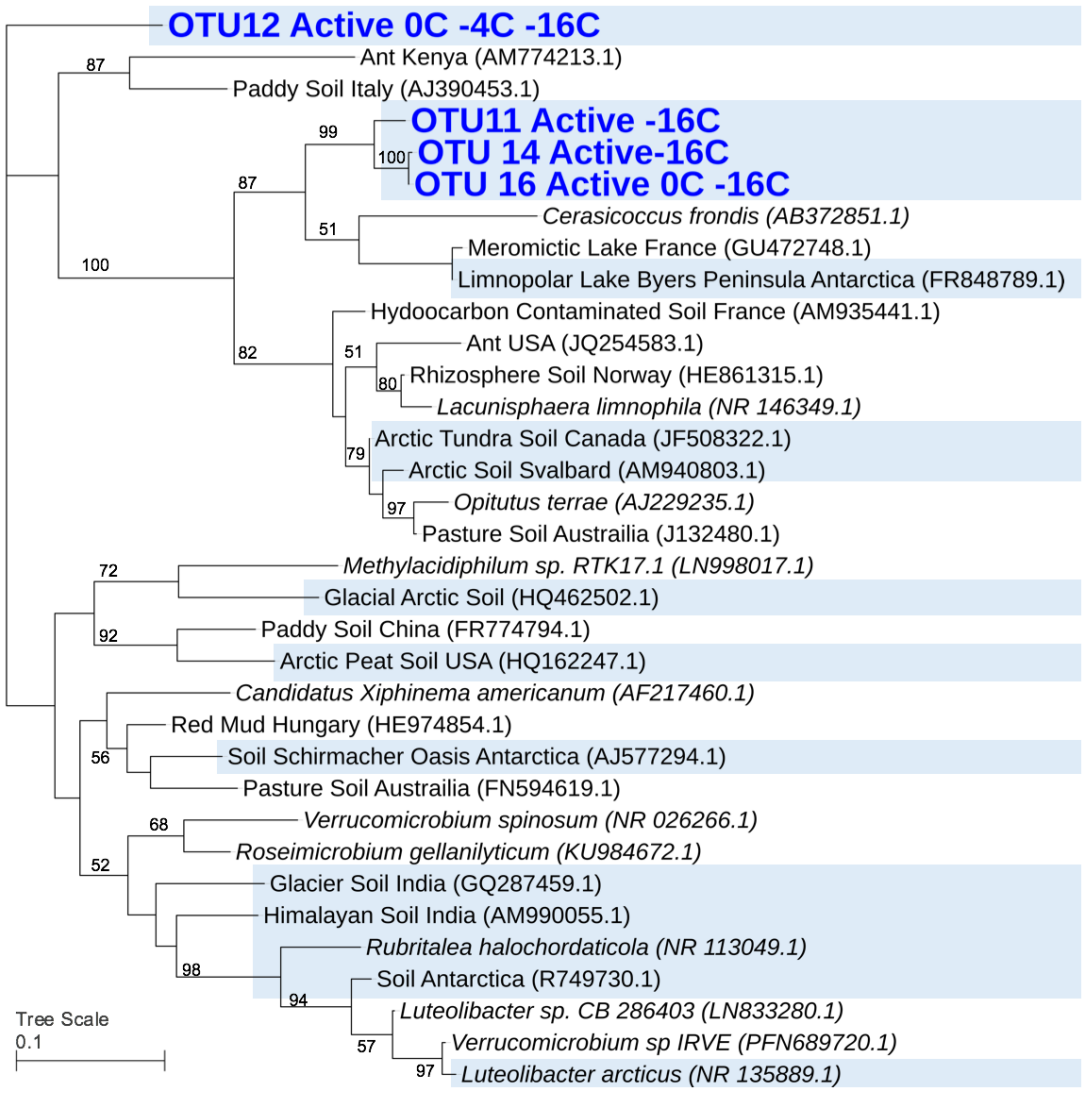

Figure 2.12: 16S rRNA gene phylogeny of the *Verrucomicrobia* was constructed using the ML methodology using 455 bp with 500 bootstraps replicates. OTUs from this study are in blue font, taxa from cold environments are in blue background. Taxa representing species in cultures are italicized. Bootstrap values of 500 replicate iterations are listed. All other taxa are listed with sample source.

2.4 DISCUSSION

Subzero metabolism in frozen soils has been detected by production of gases such as CO_2, and CH_4 (Flanagan and Veum 1974; Fahnestock et al. 1999; Panikov and Dedysh 2000; Mikan et al. 2002; Monson et al. 2005; Panikov et al. 2006; Schuur et al. 2009; Öquist et al. 2009; Drotz et al. 2010; Sistla et al. 2013), but not much has been done to distinguish specific members that are metabolically active in frozen tundra soils and can assimilate cellobiose. When contrasting to SIP studies of soils using cellobiose as an amendment, there was no particular bacterial indicator species across tundra, temperate forest, and agricultural soils, suggesting that cellobiose assimilation is ubiquitous to most bacterial communities (Verastegui et al. 2014). This study set out to investigate how different subzero temperatures impact and shape the active bacterial community composition in Arctic tundra soils.

One the most stunning discoveries from this study was the identification of a new group of cryo-active *Ignavibacteria*. The *Ignavibacteria* have been characterized as mesophiles to thermophiles, they have been detected in hot springs and lakes, and the two known isolates of this phylum are thermophiles (Lino et al. 2010; Podosokorskaya et al. 2013; Juottonen et al. 2017). Two cultured *Ignavibacteria* isolates have the ability to degrade cellobiose (Lino et al. 2010; Podosokorskaya et al. 2013). The cryo-active *Ignavibacteria* OTUs from a distinct cluster separate from the previously described phylotypes (Figure 2.9). This result suggests that subzero cellobiose degradation and C cycling in the cold tundra soil is part of the lifestyle of some *Ignavibacteria*. This finding is

consistent with the characterization of the phylum, as it supports that *Ignavibacteria* are able to use cellobiose as a carbon source (Lino et al. 2010; Podosokorskaya et al. 2013). Other tundra studies using metagenomics suggest that tundra soil *Ignavibacteria* are likely active in fermentative pathways, anaerobic methanotrophy, or sulfur reduction by matching to a bin representing Coenzyme B-Coenzyme M heterodisulfide reductase genes (Johnston et al. 2016). It may be possible that the microcosms were eventually depleted of oxygen, hence giving rise to anaerobic bacteria as *Desulfobacteraceae*, *Anaerolinaceae*, and *Pelobacteraceae*.

OTUs belonging to members of Candidatus Saccharibacteria were detected in this study, and generally clustered with other representative phylotypes from cold soils, e.g. polar and desert environments (Figure 2.10). While phylotypes from colds soils and the OTUs from this study clustered together, taxa from cold-environments appear dispersed within the phylum. This finding suggests that cold and temperate representatives of Candidatus Saccharibacteria can adapt to a wide range of temperate-cold environments. However, it is difficult to ascertain additional features about these phylotypes as there is yet no cultivated representative of Candidatus Saccharibacteria.

The cryo-active *Verrucomicrobia* members identified in this study formed a relatively tight cluster, and were not closely related to other representatives from cryo-environments (Figure 2.12). Furthermore, members from cold environments were dispersed widely throughout the phylum, suggesting that cold tolerance or cryo-activity is a ubiquitous adaptation across the *Verrucomicrobia*. One of the

closest relatives to a cluster of *Verrucomicrobia* OTUs is reported to utilize C in leaves, similar to cellobiose incorporation demonstrated in this study. The other close relatives are from an Arctic peat soil and paddy soils, as well as soil-nematode associated members. Being an endosymbiont or part of the associated microbiota of nematode can infer advantages for both the nematode (access to C, as cellobiose is degraded) as well the microbe (protection from predators, microbial competitors, abiotic stress etc.) as demonstrated in previous studies (Vandekerckhove et al. 2000; Murfin et al. 2012).

The remaining OTUs representing *Verrucomicrobia* were spread throughout the phylum (Figure 2.12), and have relatives to lakes and other soils, reminding that members of *Verrucomicrobia* are ubiquitous to the planet's soil environments (Bergmann et al. 2011; Navarrete et al. 2015). Overall, many members of the *Verrucomicrobia* have been found in polar environments using both culture-dependent and -independent techniques (Neufeld and Mohn 2005; Fierer et al. 2012; Deng et al. 2015; Kim et al. 2015).

Interestingly, known cellobiose degraders and prevalent members in the resident community of these tundra soils such as the *Acidobacteriaceae* (Pankratov et al. 2011; Pankratov 2012; Rawat et al. 2012; Eichorst et al. 2018) were not detected in the ^{13}C-DNA band of the subzero incubations (Figures 2.6, 2.8). This suggests a seasonal dynamic in the community members active in C-degradation, and may imply that the *Acidobacteria* are seasonally active in processing carbon (Rawat et al. 2012). The members of the *Ignavibacteriae*, Candidatus Saccharibacteria, and *Verrucomicrobiaceae* that were active at

subzero temperatures were, unsurprisingly, related to families in these phyla known to degrade cellulose, cellobiose, or are suggested to have saccharolytic activities (Lino et al. 2010; Dai et al. 2016; Juottonen et al. 2017).

Several members of the *Melioribacteraceae*, *Desulfobacteraceae*, *Anaerolinaceae* and *Pelobacteraceae* that are thought to be cold-adapted or have been detected in polar regions (Gittel et al. 2014; Lee et al. 2014; Goordial et al. 2016; Reyes et al. 2016) were shown to be active at various subzero temperatures in this study. In C-usage of cellulose/cellobiose, this study is consistent with ^{13}C-cellulose amended SIP of soils from coastal regions, grasslands, and desert, on reporting that bacterial members of *Burkholderiales*, *Rhizobiales*, and *Sphingobacteriales* were metabolically active (Eichorst and Kuske, 2012). Cellulose degrading bacteria are globally found in soils, and appear to be adapted to the temperature of that habitat (Eichorst and Kuske, 2012). There are also known diazotrophs, such as the *Oxalobacteraceae*, that were active at both -4 and 0 °C, making them likely key players in relatively C-rich, N-limited environments such as the Arctic tundra soils (Yang et al. 2014).

It was hypothesized that the active bacterial community would differ at different subzero temperatures, as has been demonstrated in a permafrost study (Tuorto et al. 2014). This effect of temperature on active bacterial community composition was demonstrated by the clustering of the temperature treated biological replicates by PCA analysis (Figure 2.7). The active bacterial communities clustered distinctly by temperature and separated from the initial

resident tundra soil community. A tighter clustering at temperatures of 0°C and -4°C was observed, while the -16°C incubation cluster was more distinct.

While we aimed to detect the earliest assimilation of the ^{13}C-labeled cellobiose, it is possible to have either cross-feeding or further bacterial succession over time. However, despite the potential for cross-feeding, this study still discerns the active bacterial communities at subzero temperatures. Interestingly, even if there was cross-feeding, the SIP successfully identified bacterial members that assimilate the by-products of the initial food chain. A long incubation time (40 weeks) was required to obtain a detectable signal from the SIP amended incubation at -16°C. This time frame is relevant and appropriate to contrast to the warmer subzero temperatures since respiration occurs at a slower rate at colder temperatures (Llyod and Taylor 1994). Another study that examined bacterial replication at subzero temperatures in Alaska permafrost soil incubations also took a similar time frame (Tuorto et al. 2014).

Finally, the active bacterial community distinguished by this SIP study is different from that detected by rRNA-studies during the growing season in these tundra soils (Männistö et al. 2013). Here, using rRNA as a measure of activity, it was determined that the *Acidobacteria* and *Gammaproteobacteria* dominate at the site (Männistö et al. 2013). Though they were not the most abundant in the resident bacterial community, members of the *Planctomycetes*, *Deinococcus-Thermus*, *Actinobacteria*, and *Bacteroidetes* were active at subzero temperatures and also detected at the summer season temperatures (Männistö et al. 2013). This detection makes sense since the soil is from the same site and would be

expected to bear the same inoculum of microbes—it is simply the activity by various bacterial family members that may shift depending on the temperature and/or season. However, it is also prudent to recognize that here the effect of vegetation and other environmental factors may be not be able to be measured as conducted *in situ*.

Understanding which members of the tundra soil microbial community are active at subzero temperatures is critical in developing a better understanding of soil C cycling as well as for assessing how climate change may impact vulnerable polar environments. Here it was demonstrated that temperature has an impact on cryo-active bacteria through the assimilation of ^{13}C-cellobiose into bacterial DNA. This study suggests that temperature changes even within subzero ranges may impact bacterial community composition, and thereby affect soil microbial activities. This effect is further supported by differential responses in respiration and C turnover in soils at similar subzero ranges, and this study identifies the active bacterial family compositions within subzero ranges (Llyod and Taylor 1994; Mikan et al. 2002; Michaelson and Ping 2003; Bore et al. 2017).

CHAPTER 3: HOPANOIDS AND CAROTENOIDS OF ARCTIC TUNDRA *ACIDOBACTERIA*

3.1 INTRODUCTION TO *ACIDOBACTERIA*

The phylum *Acidobacteria* was first described when *Acidobacterium capsulatum* was isolated from an acidic mine drainage in Japan (Kishimoto et al. 1992). Members of the phylum *Acidobacteria* are among the most ubiquitous soil bacteria (Jones et al. 2009), and a dominant bacterial group in Arctic tundra soils (Pankratov 2012; Männistö et al. 2013). There are currently 26 known subdivisions within the *Acidobacteria*, with most isolates in subdivision 1 (Kielak et al. 2016; Eichorst et al. 2018). Examples of *Acidobacteria* spp. are listed in Table 3.1. As rhizosphere-dwellers, *Acidobacteria* have been shown to have plant-growth stimulating effects, and even make exopolysaccharides in order to attach cells to plant roots (Kielak et al. 2016).

Members of *Acidobacteria* are mostly chemoheterotrophs that can live in acidic-neutral soils, with the exception of the photoheterotrophic *Chloracidobacterium thermophilum*, which grows in mildly acidic-alkaline soils (Tank and Bryant 2015). In particular, the prevalence of subdivision 1 *Acidobacteria* appear to be driven by soil pH (Sait et al. 2006; Jones et al. 2009; Rousk et al. 2010). As a phylum of diverse metabolisms, recent studies have even shown that some species have the potential to scavenge H_2 to persist in these soils (Greening et al. 2015). Others have shown that they are capable of contributing to the global sulfur cycle by exhibiting dissimilatory sulfur metabolism

(Hausmann et al. 2018). Some have argued that the *Acidobacteria* have a similar breadth of diversity as the phylum *Proteobacteria* (Kielak et al. 2016; Eichorst et al. 2018).

For this study, the dominance and survival of *Acidobacteria* in oligotrophic, Arctic tundra soils raises the question of what features they possess that make them so successful. To address this question, tundra *Acidobacteria* genomes from Kilpisjärvi, Finland were explored. These Arctic tundra soil isolates are *Granulicella mallensis* (Männistö et al. 2012), *Granulicella tundricola* (Männistö et al. 2012), *Terriglobus saanensis* (Männistö et al. 2011), along with undescribed new isolates strains of A2288, M8UP23, M8UP39, MP8S11, MP8S7, and MP8S9 from the same Arctic tundra region of Kilpisjärvi, Finland.

Bioinformatic analysis of genomes of soil isolates is important since genomic insights will pave the path for future testable experiments. The current understanding of soil bacterial capabilities is relatively limited, and thus soil bacteria are vastly overlooked for their potential biotechnological value and overall roles in many ecosystems (Crits-Christoph et al. 2016). Here, using described and novel acidobacterial isolates from the Kilpisjärvi tundra site, bioinformatic analysis was conducted focusing on the hopanoid and carotenoid pathways. This study aims to set the groundwork for future targeted lab experiments on the acidobacterial isolates.

Strain	Subdivision	Isolation source	Country	Publication	NCBI:txid
Granulicella pectinivorans	1	sphagnum peat bog	Russia	Pankratov and Dedysh 2010	474950
Granulicella rosea	1	sphagnum peat bog	Russia	Pankratov and Dedysh 2010	474952
Granulicella mallensis	1	tundra soil	Finland	Männistö et al. 2012	682795
Granulicella tundricola	1	tundra soil	Finland	Männistö et al. 2013	1198114
Terriglobus saanensis	1	tundra soil	Finland	Männistö et al. 2014	401053
Terriglobus roseus	1	loamy soil	United States	Eichorst et al. 2007	926566
Acidobacterium capsulatum	1	acid drainage soil	Japan	Kishimoto et al. 1991	240015
Bryocella elongata	1	sphagnum peat	Russia	Dedysh et al. 2012	863522
Bryobacter aggregatus	3	sphagnum peat bog	Russia	Kulichevskaya et al. 2010	1340493
Edaphobacter dinghuensis	1	forest soil	China	Wang et al. 2016	1560005
Edaphobacter aggregans	1	forest soil	Germany	Koch et al. 2008	1121860
Edaphobacter lichenicola	1	lichen	Russia	Belova et al. 2012	2051959
Silvibacterium bohemicum	1	forest soil	Czech Republic	Lladó et al. 2016	1577686
Candidatus Solibacter usitatus Ellin6076	3	pasture soil	Austrailia	Ward et al. 2009	234267
Candidatus Sulfopaludibacter	3	peatland soil	Germany	Hausmann et al. 2018	2043164
Candidatus Koribacter versatilis	1	pasture soil	Austrailia	Ward et al. 2009	204669
Geothrix fermentans	8	petroleum aquifers	United States	Coates et al. 1999	1121920
Terracidiphilus gabretensis	1	forest soil	Czech Republic	García-Fraile et al. 2015	1577687
Chloracidobacterium thermophilum strain B	4	hot spring mat	United States	Tank and Bryant 2015	981222
Acidipila rosea	1	acid drainage soil	Japan	Okamura et al. 2011	768535
Acidicapsa acidisoli	1	forest soil	Japan	Matsui et al. 2017	1615681
Acidicapsa ligni	1	decaying wood	Russia	Kulichevskaya et al. 2012	542300
Chloracidobacterium sp. CP2_5A	4	hot spring mat	Japan	Ward et al. 2017	2012633
Occallatibacter savannae	1	savannah soil	Namibia	Foesel et al 2016	1002691
Luteitalea pratensis	6	grassland	Germany	Vieira et al. 2017	1855912
Candidatus Blastocatellia bacterium AA13	4	meadow soil	United States	n/a	2169413
Candidatus Sulfotelmatobacter kueseliae	1	peatland soil	Germany	Hausmann et al. 2018	2042962
A2288	1	tundra	Finland	This study	N/A
M8UP23	1	tundra	Finland	This study	N/A
M8UP39	1	tundra	Finland	This study	N/A
MP8S11	1	tundra	Finland	This study	N/A
MP8S7	1	tundra	Finland	This study	N/A
MP8S9	1	tundra	Finland	This study	N/A

Table 3.1: Described species of the Phylum *Acidobacteria.* Their source of isolation, source location, and publication is listed.

3.2 INTRODUCTION TO ISOPRENOIDS

In paleobiology, one of the oldest identified lipid biomolecules of bacteria are the isoprenoids, which are based on C_5 units of isoprene. These include the C_{30} isoprenoid such as hopanoids, which are membrane bound, as well pigmented isoprenoid C_{40} molecules, the carotenoids (Lange et al. 2000; Anwar et al. 1977).

Carotenoids, or tetraterisoprenoids, are organic pigments that are made by all domains of life (Hertzberg et. al 1976; Goodwin 1980; Alcaíno 2016). They are split into two classes, xanthophylls with oxygen in the tetraterisoprenoids, and carotenes that are solely hydrocarbon based. Carotenoids are commonly characterized by pigment color, though there are also carotenoids such as phytoene and phytofluene that are colorless (Meléndez-Martínez et al. 2015). Some carotenoids are of high prophylactic value, such as vitamins and anti-oxidants, and have even been observed to have anti-carcinogenic activity (Young et al. 1991; Seddon et al. 1994; Nishino et al. 2002). Carotenoids are central in photosynthesis in cyanobacteria (Paerl 1984), but their presence is also observed in many non-photosynthetic organisms, including tundra bacteria (Thirkell and Strang 1967; Krinsky et al 1978; Kirti et al. 2014; Han et al. 2016). See Table 3.2 for more details and examples.

Non-Photosynthetic Organism	Carotenoid	Condition	Source
Micrococcus roseus	bacterioruberins	decrease in temperature led to increase in pigmentation	Chattopadhyay et al. 1997
Antarctic bacterial isolates	orange, red, yellow	pigmentation boosted survival under solar radiation stress	Dieser et al. 2010
Antarctic bacterial isolates	orange, red, yellow	pigmentation boosted survival under freeze-thaws	Dieser et al. 2010
Janthinobacterium sp. Ant5-2	purple violet	cold tolerance	Mojib et al. 2010
Janthinobacterium sp. Ant5-2	purple violet	UV tolerance	Mojib et al. 2010
Arthrobacter agilis	bacterioruberin	decrease in temperature led to increase in pigmentation	Fong et al. 2001
Exiguobacterium antarcticum B7	orange	cold adaptation, increase expression in transcripts	Dall'Agnol et al. 2014
Pedobacter	red	prevention of oxidative damage	Correa-Llantén et al. 2012
Microbacterium sp. strain PAMC28756	lycopene	UV radiation	Han et al. 2016
Winogradskyella psychrotolerans	yellow	cold tolerance	Begum et al. 2013

Table 3.2: Roles of carotenoids in non-photosynthetic bacteria, and the condition in which they are associated in.

Briefly, carotenoids biosynthesis stems from the terpenoid biosynthesis pathway, where molecules of farnesyl diphosphate or geranyl-geranyl diphosphate are catalyzed into various forms of phytoene by enzymes of CrtB, (15-cis-phytoene synthase) as illustrated in Figure 3.1. Next, CrtI (phytoene desaturase) catalysis ultimately leads to pigmented carotenoids of zeta-carotene, neurosporene, lycopene (Wang et al. 2012; Kanehisa et al. 2016). Examples of carotenoid and bacterial carotenoid producers are listed in Table 3.3.

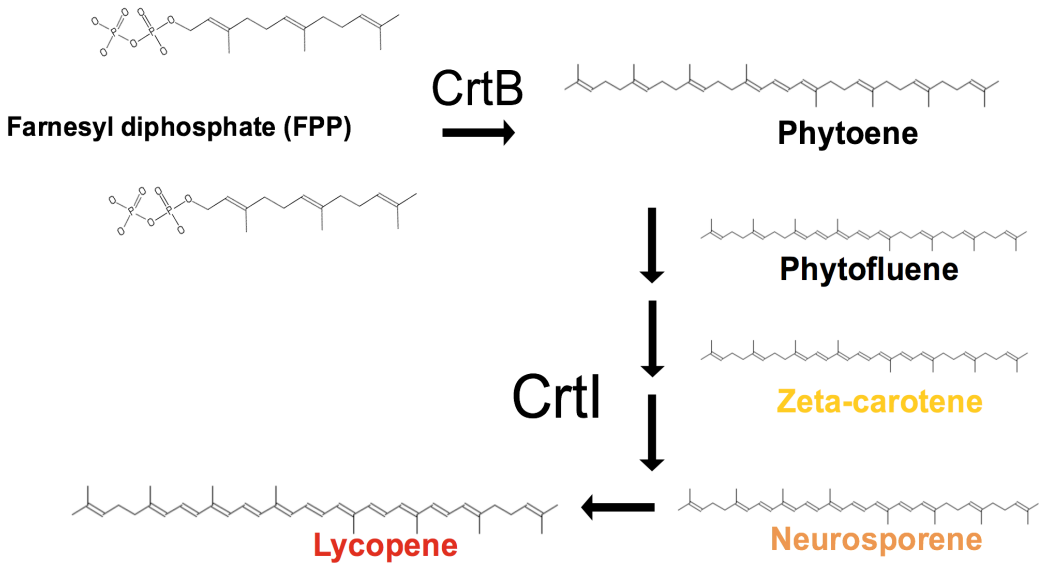

Figure 3.1: Carotenoid biosynthesis pathway described in bacteria. The key enzymes are CrtB and CrtI.

Carotenoid	Enzyme(s) Needed	Bacterial examples
Beta-carotene	CrtI, CrtY	Candidatus Chloracidobacterium thermophilum, *Sphingobacterium antarcticus, Rhodococcus erythropolis*
Zeaxanthin	CrtZ, CrtR	*Flavobacterium frigidarium, Xanthobacter autotrophicus, Acaryochloris marina*
Astaxanthin	CrtW, CrtZ	*Sphingomonas astaxanthinifaciens, Paracoccus carotinifaciens, Altererythrobacter ishigakien*
Lycopene	CarC, CrtH, CrtI, CrtL	*Roseospira mediosalina,* Candidatus Chloracidobacterium thermophilum, *Afifella marina*
Beta-cryptoxanthin	CrtR, CrtZ	*Sphingobacterium antarcticus, Natronocella acetinitrilica, Erythrobacter longus*
Spirilloxanthin	CrtF, CrtC	*Thiocapsa roseopersicina, Acidiphilium facile, Methylobacterium radiotolerans*
Neurosporene	CrtI, carC,	*Acholeplasma laidlawii, Rubribacterium polymorphum, Mycobacterium phlei*
Rhodopin	CrtC, CrtF, CrtI	*Allochromatium warmingii, Ectothiorhodospira salini, Thiorhodovibrio wigradskyi*
Bacterioruberin	CrtY, CrtI	*Micrococcus roseus, Azospirillum brasilense, Rubrobacter radiotolerans*

Table 3.3 Examples of carotenoids, carotenoid biosynthesis enzymes, and carotenoid producing bacteria. This information on carotenoid biosynthesis enzymes and bacterial producers was curated by the Prokaryotic Carotenoid Database, ProCarDB (Nupur et al. 2016).

Sharing a metabolic pathway with the carotenoids are hopanoids. Hopanoids are pentacyclic triterpenes that play a role in maintaining cellular membrane stability in some bacteria (Ourisson et al. 1979). As bacterial analogs of cholesterol, hopanoids are thought to be the bacterial equivalent of sterols, and vital in maintaining membrane fluidity (Welander et al. 2009; Sáenz et al. 2015). Hopanoids with methylation at C-2 or C-3 were long thought as biomarkers of cyanobacteria and methanotrophs, but recent studies have discovered that these membrane-bound lipids are found in the phylum *Acidobacteria* (Rohmer et al. 1984; Summons et al. 1999; Fischer et al. 2005; Damsté et al. 2017).

Hopanoid formation relies on three key steps, elucidated in *E. coli* using gene homologs from *Zymomonas* and *Rhodopseudomonas* (Pan et al. 2015). Briefly, two molecules of farnesyl diphosphate (FPP) are catalyzed into presqualene, and then reduced to the centrally important molecule of squalene. Squalene is then cyclized by the enzyme squalene-hopene cyclase (SHC) to form the simplest hopanoid, diploptene (Figure 3.2).

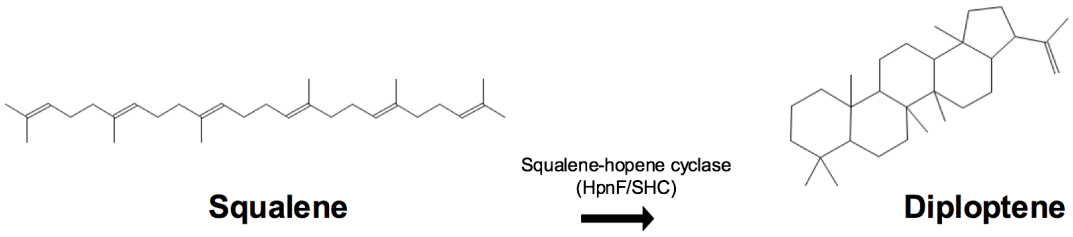

Figure 3.2: Key step in the biosynthesis of the simplest hopanoid catalyzed by the enzyme squalene-hopene cyclase (HpnF/SHC).

Further modifications of diploptene leading to more complex hopanoids are possible by variations of the hopanoid (Hpn) pathway. While the central reaction of hopanoid biosynthesis is catalyzed by squalene-hopene cyclase, or HpnF, modifications to diploptene are found in some bacteria (Schmerk et al. 2015; Damsté et al. 2017; Belin et al. 2018). Further modifications by HpnH (radical SAM protein), HpnG (phosphorylase), HpnA (sugar epimerase), HpnI (glycosyl transferase), HpnK (deacetylase), and HpnJ (radical SAM protein) lead to adensoyl hopane, ribsoyl hopane, bacteriohopanetetrol (BHT), BHT acetylglucosamine, BHT glucosamine, and BHT cyclitol ether, respectively (see Figure 3.3; Pan et al. 2015; Damsté et al. 2017; Belin et al. 2018).

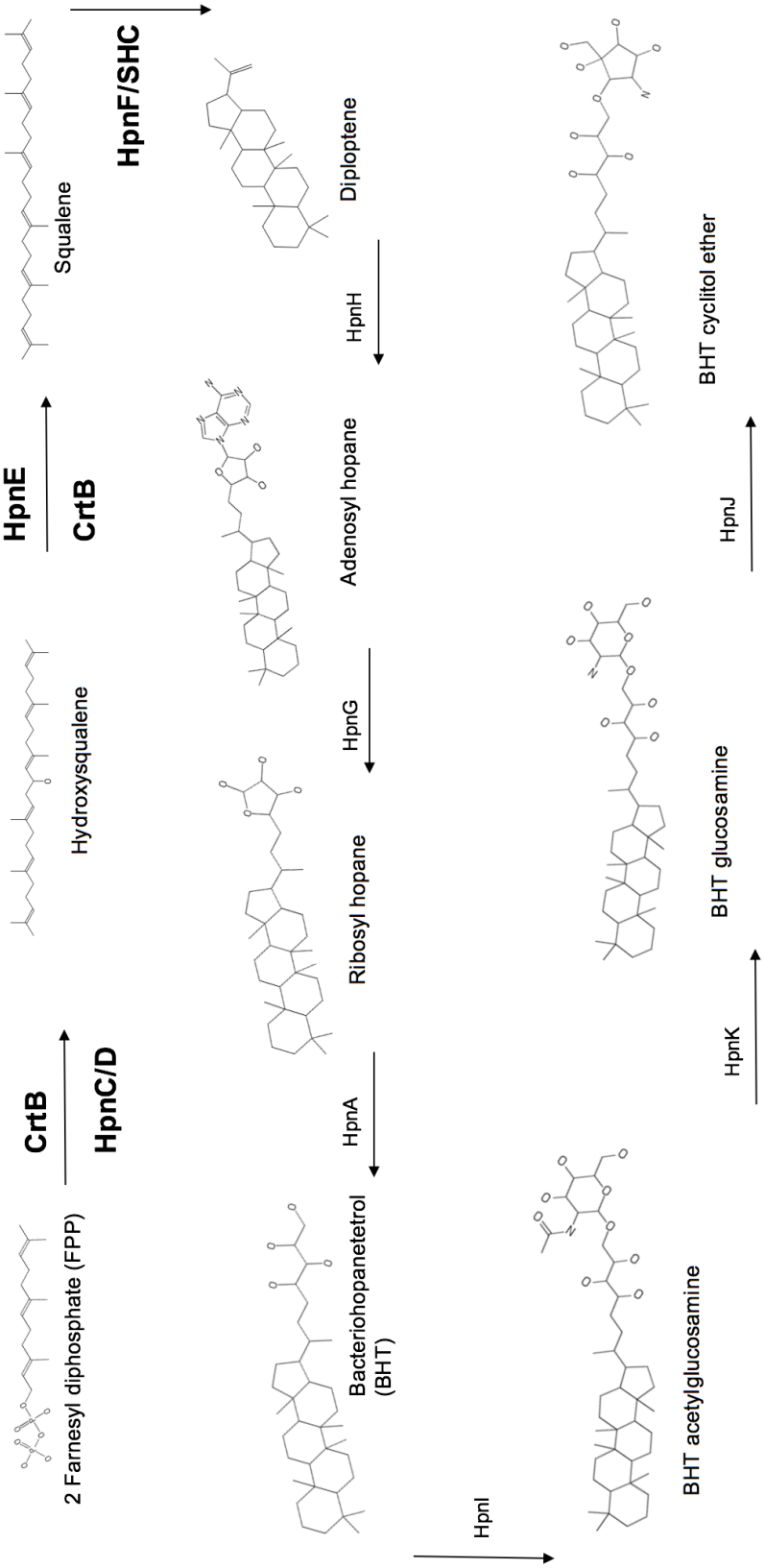

Figure 3.3: Example of biosynthetic pathway of carotenoids in bacteria.

It is intriguing that these isoprenoid molecules, once associated with photosynthesis, are now being identified in non-photosynthetic organisms, and little is known about their function or ecological significance. Hence, bioinformatic analysis of these pathways are especially interesting and necessary. Bioinformatic analysis is required to pave the path for future experiments of tundra isolates of *Acidobacteria* from Kilpisjärvi, Finland. New isolates of *Acidobacteria* have also been cultured from the same tundra region, and thereby one can hypothesize that similar hopanoid and carotenoid production abilities may be present, as the isoprenoids possibly allow for survival benefits in the same tundra ecosystem.

3.3 METHODOLOGY

Species Descriptions and Culturing

Three Arctic tundra acidobacterial isolates, *Granulicella mallensis* strain MP5ACTX8 (Männistö et al. 2012; Rawat et al. 2013), *Granulicella tundricola* strain MP5ACTX9 (Männistö et al. 2012; Rawat et al. 2014), and *Terriglobus saanensis* strain SP1PR5 (Männistö et al. 2011; Rawat et al. 2012) were chosen for genome analysis. These described species can grow aerobically from 4 to 26˚C, at pH 3-7.5 on a range of sugars (Männistö et al. 2011, 2012). Previous genome analyses of *G. mallensis*, *G. tundricola*, and *T. saanensis* have shown that they have carbohydrate active enzymes (CAZymes), but other characteristics such as isoprenoid capabilities remain unexplored (Rawat et al. 2012, 2013, 2014).

New tundra acidobacterial strains A2288, M8UP23, M8UP39, MP8S11, MP8S7, and MP8S9 were also isolated by Dr. Männistö from the Kilpisjarvi tundra site. Polysaccharide utilization and enzymatic capabilities were tested using API Zym strips in the laboratory of Dr. Männistö in Finland on these new isolates. All new *Acidobacteria* with the exception of MP8S7 grew as mucoid colonies initially, and varied slightly by color. A2288 was a creamy beige, strain MP8S11 was slightly yellow, strains M8UP23 and M8UP39 were light yellow when grown on ½ strength R2A media, at room temperature after 72 hours. Strain MP8S7 was unable to be re-cultured in the Rutgers laboratory.

Genome Sequencing and Assembly

Strains for DNA extraction were grown in the laboratory of Dr. Männistö, and DNA was extracted and were sequenced by LGC Genomics. Using Illumina MiSeq 300 bp paired-end sequencing, these six genomes generated 5 million read pairs. Genome assembly and scaffolding was carried out using SPAdes version 3.5.0. SPAdes assemblies of all new genomes were used for a bioinformatic analysis with Roary version 3.11.2, using de novo assembly of pangenomes to analyze further core genome phylogeny (Page et al. 2015). These genomes were graciously annotated by Ms. Allison Hicks, using the computing clusters of Harvard Medical School. Each assembly was then annotated by Prokka (Seemann 2014), with running Prodigal for identification of coding sequences (CDS) (Hyatt et al. 2010). Assemblies of new *Acidobacteria* strains were also analyzed by QUAST, to determine overall contigs, genome

size, CDS, and G+C content % (Gurevich et al. 2013). Following genome annotation, gene sequences of interest were extracted for phylogenetic analysis.

Identification of Hopanoid and Carotenoid Biosynthetic Genes

For both isoprenoid biosynthesis pathways, all relevant genes were exhaustively chosen from the databases of KEGG, InterPro, and JGI's COG database to compare against those of the *Acidobacteria* from this study (Hunter et al. 2009; Markowitz et al. 2015; Kanehisa et al. 2016). Gene sequences of other *Acidobacteria* were gathered from NCBI and JGI databases. Each gene was identified on the scaffold *of G. mallensis, G. tundricola*, and *T. saanensis*, and then used as a reference for extracting genes from new strains A2288, M8UP23, M8UP39, MP8S11, MP8S7, and MP8S9. Genes for 16S rRNA gene phylogeny were extracted from the new acidobacterial strains following the annotation, to be used in generating routine 16S rRNA gene phylogeny.

3.4 RESULTS AND DISCUSSION

Microscopic observations of new Acidobacteria strains

After transport to the Rutgers laboratory, new strains were cultivated on ½ strength R2A media at room temperature at pH 5.5. All isolates with the exception of MP8S7 were grown and then further observed under the microscope (Figure 3.4). Phase-contrast microscopy at 1000X total magnification shows that the isolates are rods in the range of 1-3 μm in length can appear in pairs, and in a chain (Figure 3.4). All isolates appeared to be non-motile.

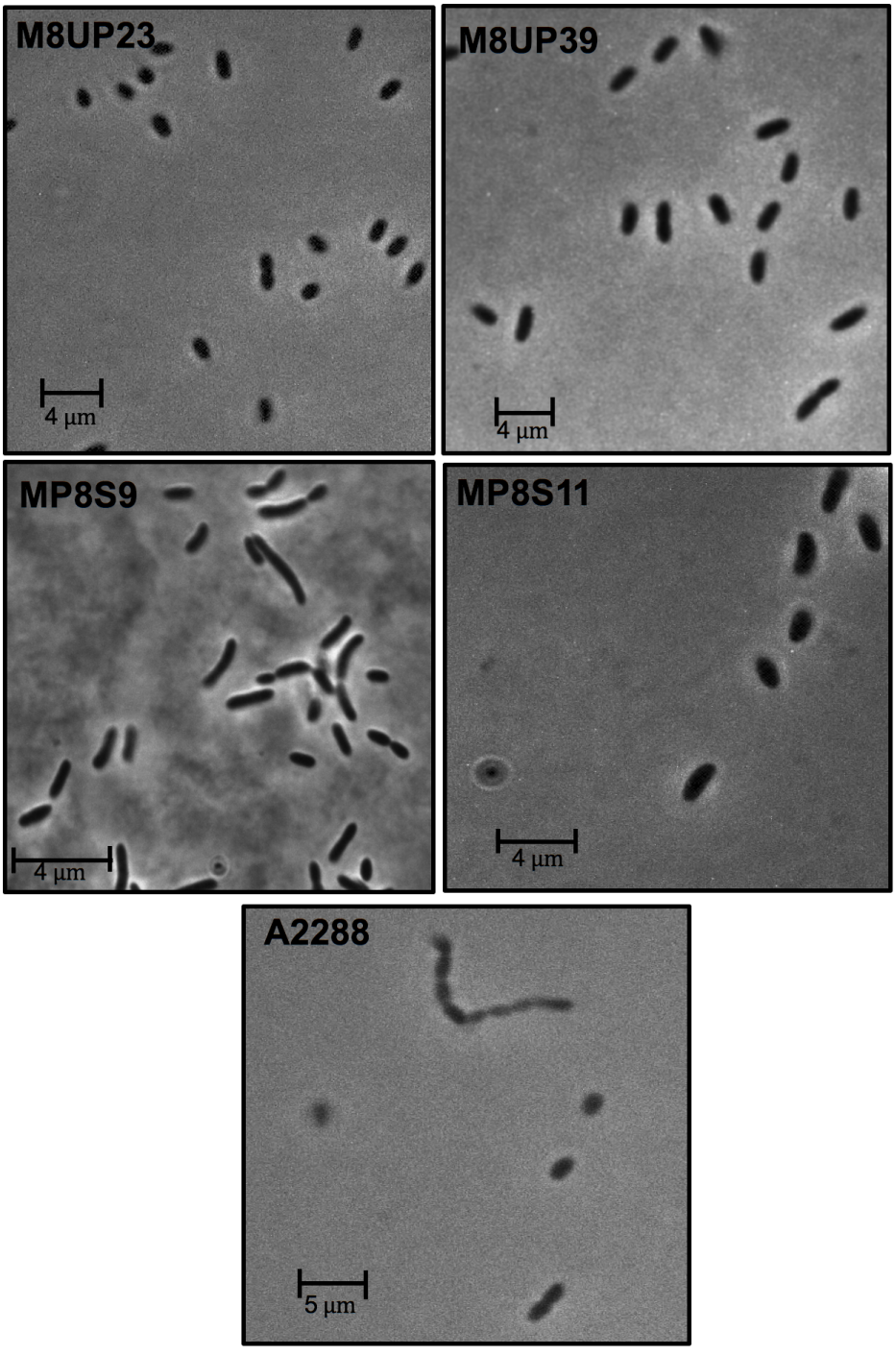

Figure 3.4: Phase contrast microscopy of new *Acidobacteria* strains grown on solid media and viewed after 72 hours.

Polysaccharide utilization and enzymatic capabilities

Using API Zym strips, isolates were tested for polysaccharide degradation and enzymatic capabilities by Dr. Minna Männistö. Isolates were able to use a wide array of sugars, and all but M8UP23 tested negative for the enzyme alpha-fucosidase (Table 3.4, data provided by Dr. Minna Männistö).

	M8UP23	M8UP39	A2288	MP8S11	MP8S7	MP8S9
Hydrolysis of polysaccharides						
CMC	-	+	+	+	+	-
Xylan	+	+	-	+	+	+
Pectin	+	+	+	+	+	+
Lichenin	-	+	+	+	+	-
Starch	-	+	+	-	-	+
Xanthan	+	-	+	+	-	+
Gum arabic	+	+	+	+	+	+
Chitin (NAG test)	+	+	+	+	+	+
Enzyme Activity						
esterase (C8)	-	+	+	+	+	+
trypsin	-	-	+	+	+	+
a-chymotrypsin	-	-	-	+	+	+
a-galactosidase	+	+	+	+	+	+
b-galactosidase	+	+	+	+	+	+
b-glucuronidase	+	+	+	+	+	+
a-glucosidase	+	+	+	+	+	+
b-glucosidase	+	+	+	+	+	+
N-acetyl-b-glucosaminidase	+	+	+	+	+	+
a-fucosidase	+	-	-	-	-	-

Table 3.3: New isolates of *Acidobacteria* were tested for the ability to use polysaccharides or the presences of certain enzymes using the using API Zym testing.

Genome Characteristics of Acidobacteria isolates

Genomes were uploaded and analyzed by QUAST to determine overall characteristics of the draft assemblies. All strains had 56-60 G+C% content, with a genome size of 5-7.2 Mb. Additional details are shown in Table 3.5.

Organism	Contigs	Bases (bp)	CDS	G+C Content %
MP8S11	273	6266013	5318	56.23
MP8S9	104	7296663	6061	60.52
MP8S7	80	6994016	5729	58.62
M8UP39	45	5582838	4779	57.42
M8UP23	121	5029249	4251	57.80
A2288	176	5625642	4808	56.69

Table 3.5: Genome characteristics of new *Acidobacteria* strains after assembly.

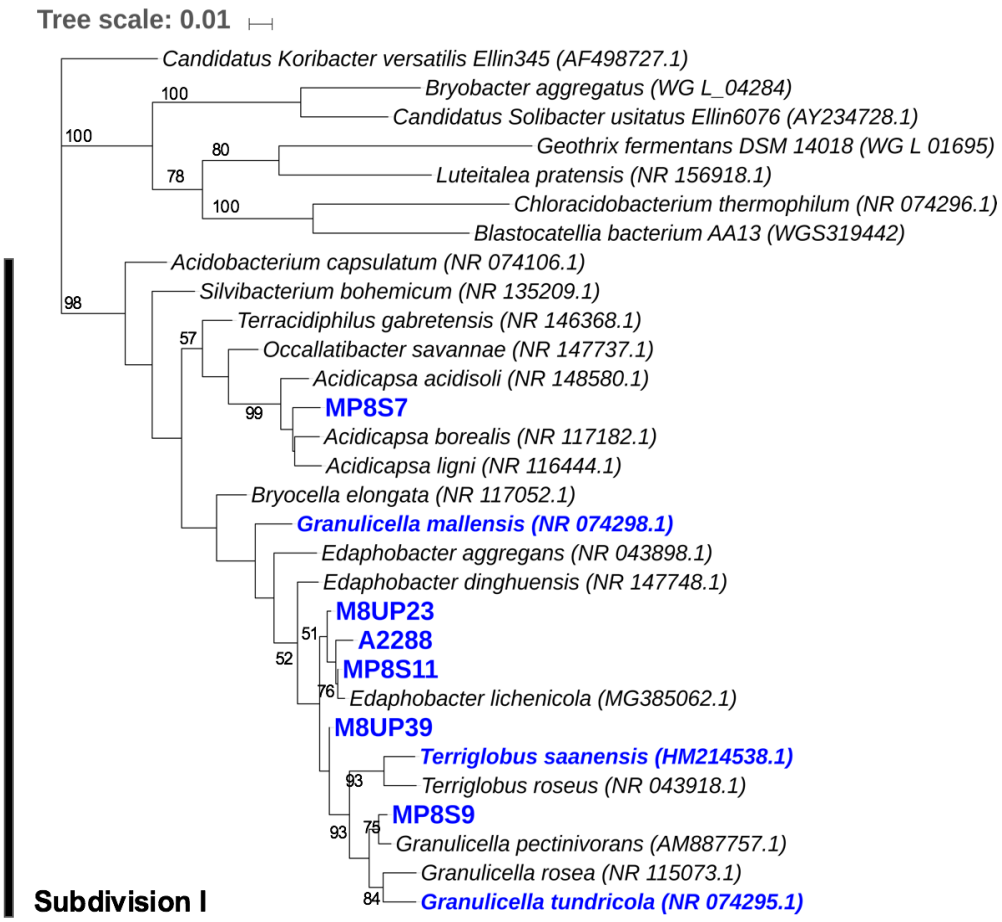

Figure 3.5: Phylogeny of 16S rRNA gene (1354 bases) of *Acidobacteria* was constructed by maximum-likelihood methodologies with 500 bootstrap replicates.

Phylogeny of Acidobacteria using the 16S rRNA gene

In Figure 3.5, the 16S rRNA gene of several established acidobacterial strains was compared with the undescribed strains of A2288, M8UP23, M8UP39, MP8S11, MP8S7, and MP8S9. Based on this analysis, all new strains fall into subdivision 1 of the *Acidobacteria*. Strains MP8S7 is most distantly related based on this phylogeny, while strains MP8S11, A2288, M8UP23, and *Edaphobacter lichenicola* cluster closely. Strains MP8S11, A2288, and M8UP23 are likely *Edaphobacter* spp.

Phylogeny of Acidobacteria using the core genome

16S rRNA gene phylogeny is routinely used at a cutoff of <97% similarity to aid in delineating a new species, but this definition is being postulated for a new update for <99% similarity to help describe a new species using a full length 16S rRNA gene sequence (Stackebrandt and Goebel 1994; Edgar 2018). Thereby, comparing other genetic elements of a strain (*e.g.* genes of interest) may also help determining whether a new isolate is a novel species, and contribute to overall species announcement.

In order to compare other features, genomes of select publically available *Acidobacteria* were downloaded, and analyzed by Roary v.3.1.1.2, in conjunction with new strains as pangenomes. Phylogeny of these strains was constructed using a “core” set of genes (i.e., genes that are in >50% of all organisms being compared). To visualize this phylogenetic analysis further, a presence/absence matrix of all genes in these *Acidobacteria* strains was illustrated next to the added phylogeny of “core” *Acidobacteria* genes in Figure 3.6. There were 382 core genes detected amongst the *Acidobacteria* new strains and the established whole genomes, out of a total of 39,555 genes as shown in Figure 3.6. These 382 genes established the core genome of these strains.

Both the core genome phylogeny, as well as the 16S rRNA gene phylogeny are in agreement that these new *Acidobacteria* isolates fall into division 1, with strains A2288, M8UP23, M8S11, and M8UP39 being most closely related (Figures 3.5, 3.6).

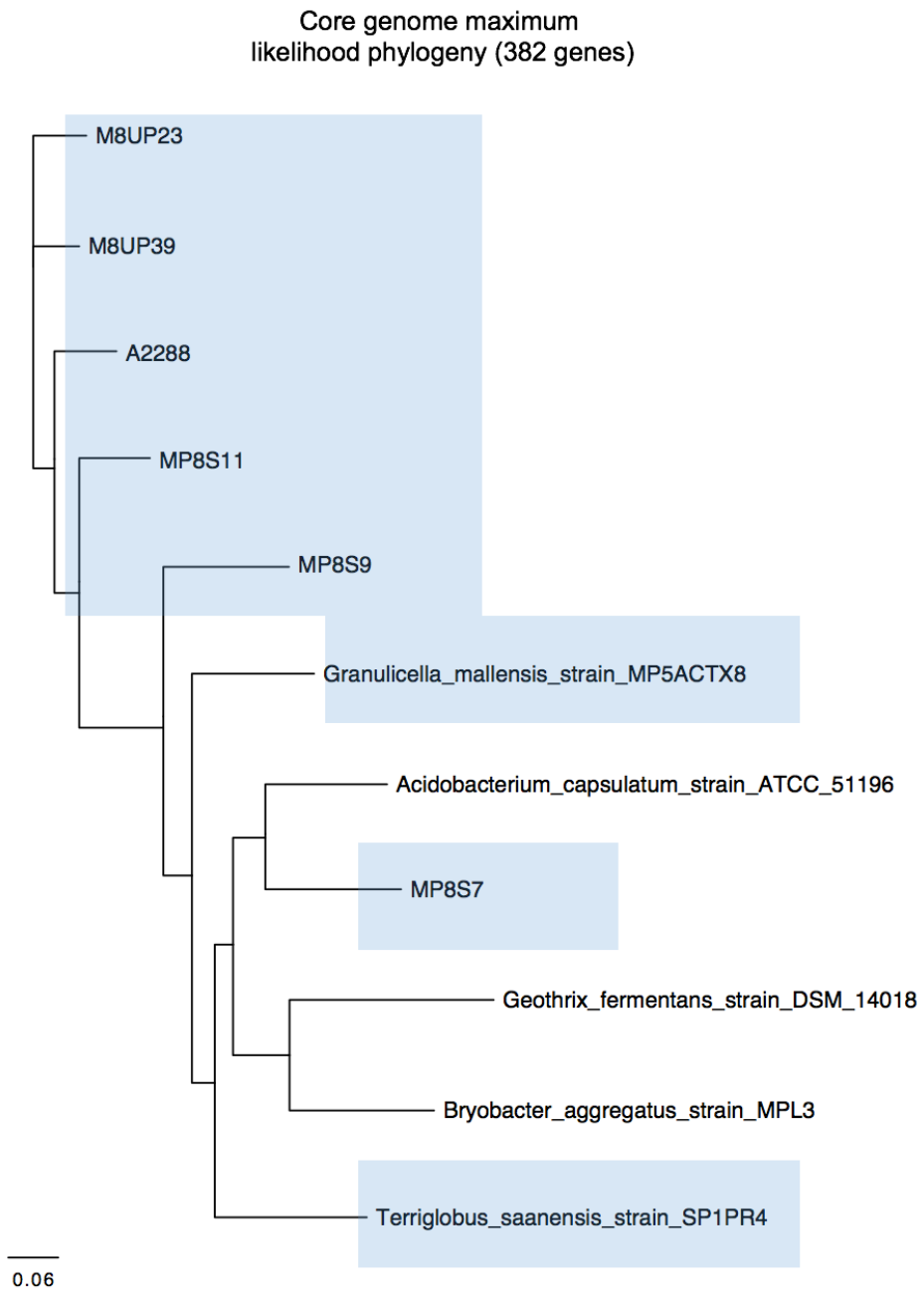

Figure 3.6: Maximum likelihood phylogeny of core genes (genes in at least 50% of the organisms listed). The core genome consisted of 382 of genes that were shared by all listed *Acidobacteria* members.

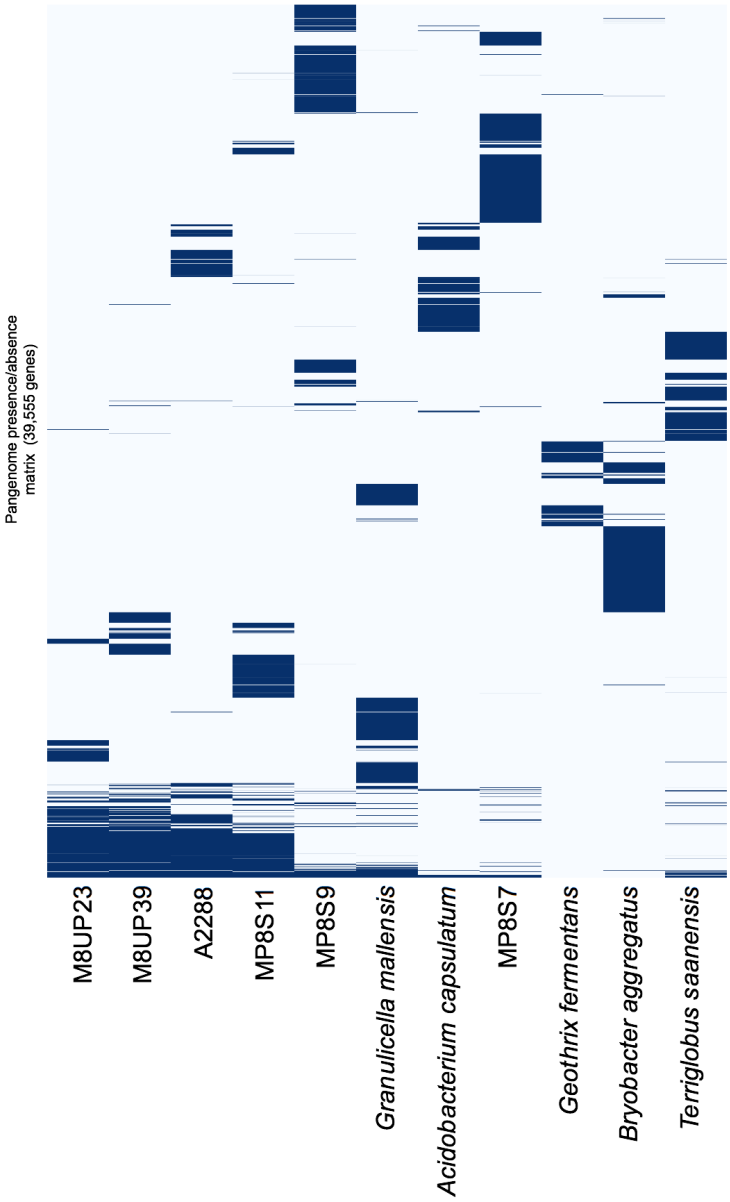

Figure 3.7: Core genes (genes in at least 50% of species) with comparison every single gene's presence/absence amongst species (single black line represents 1 gene).

Genetic Pathway of Hopanoid and Carotenoid Biosynthesis in Acidobacteria

The genetic pathway was assembled by scanning genomes for nucleotide identity >70% to known hopanoid and carotenoid biosynthesis genes. For reference, each of the hopanoid and carotenoid biosynthesis pathways have been catalogued in Table 3.6 (hopanoids) and Table 3.7 (carotenoids) with the location in bp for described species as listed in the NCBI-Genome database. For new *Acidobacteria* strains, the exact location could not be determined, though relevant matches to the genes were extracted and putative genetic pathways were assembled.

The gene *crtB* encoding for squalene-phytoene synthase (SPS) is sometimes either annotated with the label “phytoene-synthase” or “squalene-phytoene synthase”. As a result, both labels have been taken into account whenever *crtB*/SPS was detected. It is of interest that the overlap between the carotenoid and hopanoid pathway lies with this essential enzyme (Hemmi et al. 1994; Kannenberg et al. 1999; Zhang 2007). The function of *crtB*/SPS in the carotenoid biosynthesis pathway is to generate phytoene, which is the first step in the pathway towards the carotenoids lycopene, neurorosporene, zeta-carotene, and phytofluene biosynthesis. The function of the *crtB*/SPS in the hopanoid pathway is to generate squalene, which is a critical metabolite that gets cyclized into the basic hopanoid, diploptene.

Hopanoids

InterPro #	Enzyme Function (UniProtKB)	Enzyme name	Gene name	Substrate	Product	Genome location (bases) *G. mallensis*	*G. tundricola*	*T. saanensis*
IPR006449	GO:0051996	Squalene synthase, Squalene/phytoene synthase, farnesyl-diphosphate farnesyltransferase (FDFT)	*hpnC, crtB*	farnesyl-diphosphate; presqualene diphosphate	presqualene diphosphate; hydroxysqualene	1150595..1151644, 3202152..3203099	1894010…1894957	2230022..2230981, 2230978…2231934
IPR036188	GO:0016491	squalene-associated, FAD-dependent desaturase, FAD-dependent oxidoreductase, phytoene desaturase	*hpnE, crtI*	hydroxysqualene, phytoene	squalene	1150595..1151644	1895880..1897241, 1021483..1023039, 1016483..1017673	2231931..2233304 4408895..4,410547 4410652...4412154
IPR006400, IPR017826	GO:0016866	squalene-hopene/tetraprenyl-beta-curcumene cyclase	*hpnF*, SHC	Squalene	diplopterol or diploptene	15655426 ...1567456	1844610…1846631	2391213…2393294
IPR017833	GO:0003824, GO:0051536	hopanoid-biosynthesis associated radical SAM protein	*hpnH*	diploptene	adenosyl hopane	1567511...1568665	1846669..1847805	2389844..2390992
IPR017831	GO:0003824	hopanoid-associated phosphorylase	*hpnG*	adenosyl hopane	robosyl hopane	1570423…1571103	1849271..1849,996	2385720…2386409
IPR017835	GO:0008120, GO:0102769	hopanoid-biosynthesis associated glycosyl transferase protein	*hpnI*	Bacteriopanetetrol (BHT)	BHT N-acetylglucosamine	190180..191346	63467..64645	4853188..4854399
IPR017836	GO:0016787, GO:0046872	ChbG/HpnK family deacetylase	*hpnK*	N-acetylglucosaminyl BHT	Glucosaminyl BHT	1667728..1668594	1707841..1708770	2979451...2980296
IPR017834	GO:0003824, GO:0031419, GO:0051536, GO:0046872	hopanoid biosynthesis associated radical SAM protein	*hpnJ*	BHT Glucosamine	BHT cyclitol ether	3199434...3200912	1902815…1904305	2235364…2236842
IPR017832	GO:0016740	hopene-associated glycosyltransferase	*hpnB*	varies	varies	3252216..3253346	2041131..2042306	1208627..1209787
IPR017829	GO:0003824, GO:0050662	hopanoid-associated sugar epimerase	*hpnA*	varies	varies	1569410 …1570426	1848312..1849331	2386816..2387826
IPR018333	GO:0000250/ GO:0016871	oxidosqualene cyclase/ squalene-hopene cyclase	OSC	2,3-Oxidosqualene	Lanosterol or Cycloartenol	1150595...1151644	not found	not found
	+ strand	-strand						
		-strand						

Table 3.6: Enzymes involved in hopanoid biosynthetic reactions are listed with database reference numbers, substrates and products involved, and gene name/location in genome.

Carotenoid Biosynthesis

KO #	Enzyme Function (KEGG)	Enzyme name(s)	Gene name	Substrate	Product	Genome location (bases)		
						G. mallensis	*G. tundricola*	*T. saanensis*
K02291 K10208, K00801	2.5.1.32 2.5.1.96	15-cis-phytoene synthase, geranylgeranyl-diphosphate geranylgeranyltransferase, prephytoene-diphosphate synthase, phytoene synthetase	*crtB* FDFT, SQS, *hpnC*	geranylgeranyl diphosphate; prephytoene diphosphate, farnesyl diphosphate , NADH; NADPH, presqualene diphosphate	diphosphate, prephytoene diphosphate;15-cis-phytoene	3202152..3203099 1150595..1151644	1894954..1895883	2230978..2231934
K10211	2.4.1.-	4,4'-diaponeurosporenoate glycosyltransferase	*crtQ*	4,4'-Diaponeurosporenic acid	Glycosyl-4,4'-diaponeurosporenoate	not found	not found	not found
K10027	1.3.99.26 , 1.3.99.28 , 1.3.99.29, 1.3.99.31	phytoene desaturase	*crtI*	15-cis-phytoene; zeta-carotene; neurosporene	neurosporene; zeta-carotene; lycopene	not found	1021483..1023039	4408895..4410547, 4410652..4412154
K10210	1.14.99.44	diapolycopene oxygenase	*crtP*	4,4'-diapolycopene, O2	4,4'-diapolycopenedial, water	not found	not found	not found
K15746	1.14.15.24	beta-carotene 3-hydroxylase, beta-carotene 3,3'-monooxygenase	*crtZ*	beta-carotene; beta-cryptoxanthin, O2, H+	beta-cryptoxanthin; water, zeaxanthin,	not found	not found	not found
K09844	4.2.1.131	carotenoid 1,2-hydratase	*crtC*	1-hydroxy-1,2-dihydrolycopene; 1,1'-dihydroxy-1,1',2,2'-tetrahydrolycopene	lycopene, water; 1-hydroxy-1,2-dihydrolycopene	not found	not found	not found
K10212	2.3.1.-	glycosyl-4,4'-diaponeurosporenoate acyltransferase	*crtO*	Glycosyl-4,4'-diaponeurosporenoate	Staphyloxanthin	not found	not found	not found
	+ strand	-strand						
		-strand						

Table 3.7: Enzymes involved in carotenoid biosynthetic reactions are listed with database reference numbers, substrates and products involved, and gene name/location in genome.

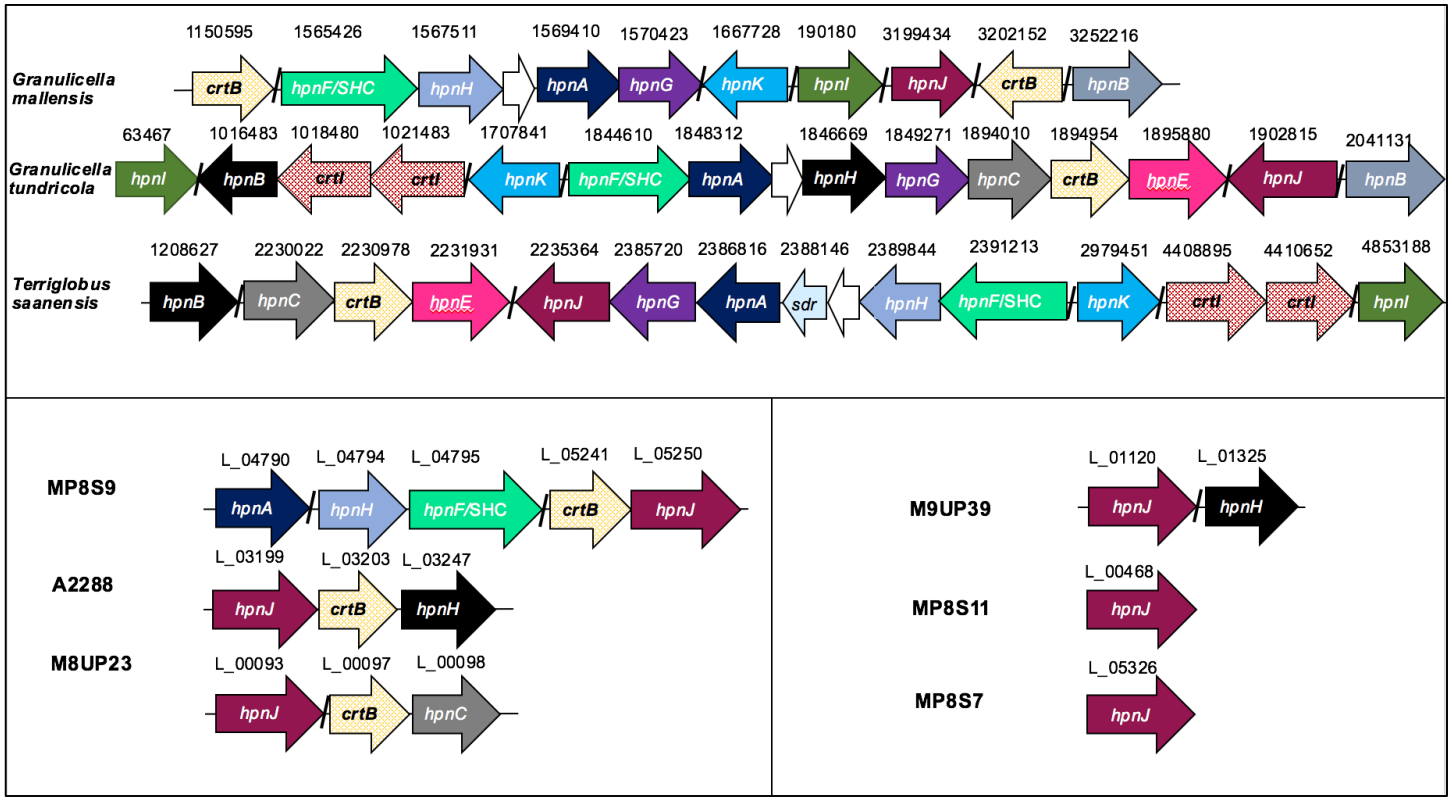

Figure 3.7: Hopanoid biosynthetic pathways detected by matching genes onto genomes (available on NCBI). Numbers inside gene arrows indicate size of the gene (in bp) and numbers above gene arrows indicate the position of the gene within the genome. Black colored gene indicates hopanoid biosynthetic genes, grey colored gene indicates carotenoid biosynthetic genes.

From the identification of genes present in these *Acidobacteria*, the potential ability to produce specific carotenoids and hopanoids can be determined. Based on the presence of genes, *G. mallensis*, *G. tundricola*, and *T. saanensis* have the potential of producing diploptene, adenosylhopane, ribosylhopane, bacteriohopanetetrol (BHT), BHT acetylglucosamine, BHT glucosamine, and BHT cyclitol ether. Genes in the same regional proximity have been boxed in these maps. Strain MP8S9 has the capability of producing diplopetene, adenosylhopane, ribosylhopane, and BHT. The presence of *hpnJ* implies that the ability to make BHT cyclitol ether is possible, however genes needed to connect the overall pathway were not detected in strain MP8S9. Additionally*, hpnJ* appears in all new *Acidobacteria* strains even though other essential genes were not identified, suggesting either an alternative or divergent pathway(s). Further, it appears that *hpnJ* appears to be the most conserved gene based on detection across all the strains in this study.

The key genes in the hopanoid biosynthesis pathway are those that make squalene and those that cyclize squalene. While the synthesis of squalene is catalyzed by squalene synthase (*hpnC*), this process may also be accomplished by squalene/phytoene synthase (SPS), or even the annotated “phytoene synthase (*crtB*)”. This is likely the case in many of these strains, as there appears to be the presence of *crtB* but not necessarily *hpnF* (Figures 3.7, 3.8). As a result, hopanoid biosynthesis pathways could be identified in the species of *G. mallensis*, *G. tundricola*, and *T. saanensis*, and MP8S9. It is possible that this biosynthetic pathway is also found in the new acidobacterial strains, but the

sequence diversity may be too great to detect missing hopanoid/carotenoid biosynthesis genes. Further, the protein squalene-synthase (encoded by *hpnC*) also synthesizes squalene, but is detected separately from the *crtB*/SPS in select strains, and may add functional redundancy. Thus, when generating phylogeny of *crtB*/SPS, separate phylogenies were constructed for each protein, per their annotated identity.

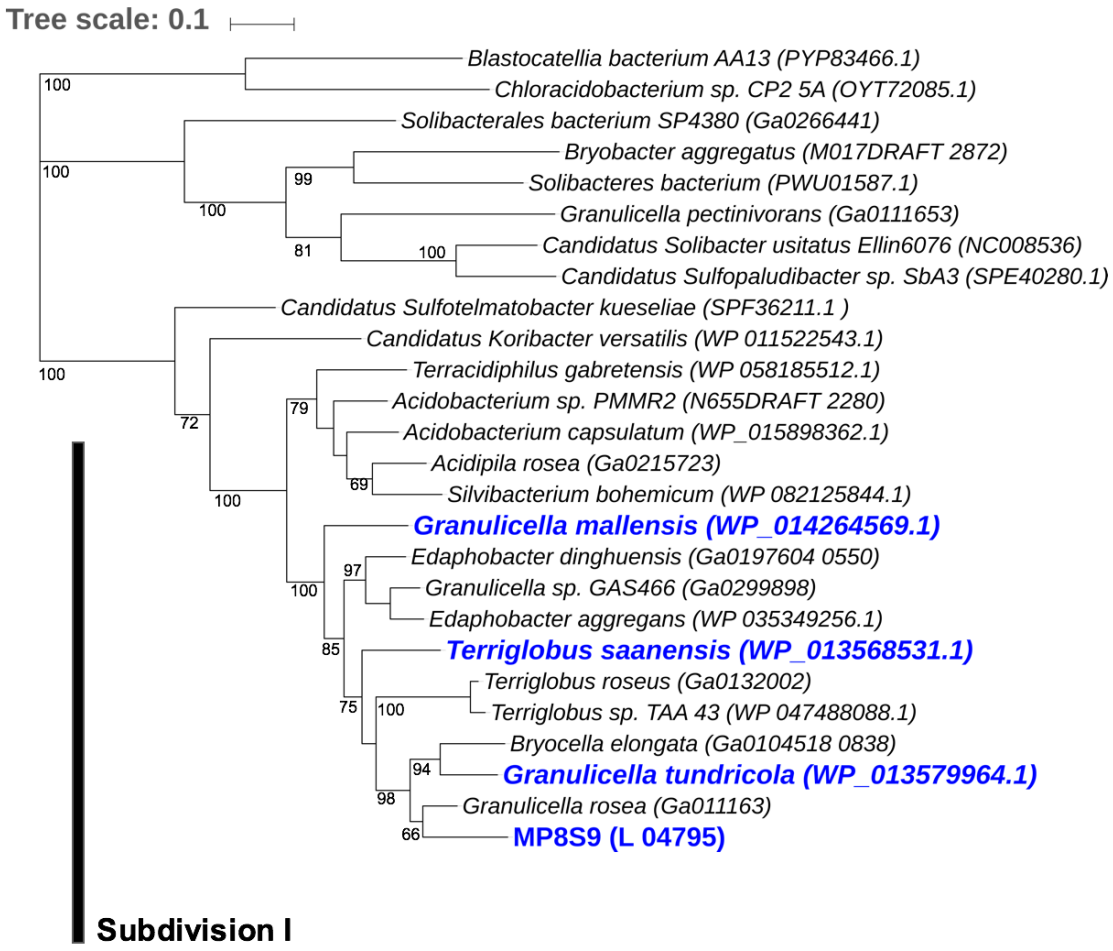

Figure 3.9: Maximum likelihood phylogeny using amino acids sequences of 721 positions of HpnF, and 500 bootstrap replicates. The distinct cluster of subdivision 1 *Acidobacteria* was highlighted with a bar.

Enzyme HpnF/SHC is critical in catalyzing the formation of the first and simplest hopanoid, diploptene. Hence this enzyme is of the utmost importance for any downstream hopanoid biosynthesis pathway. Based on the phylogeny of this critical enzyme, there appears to be clustering of HpnF/SHC encoding *Acidobacteria* similar to the 16S rRNA gene phylogeny, as shown in Figure 3.9.

Strain MP8S9 was the only new strain where the HpnF/SHC was detected using known sequences, and clusters similarly with the *Granulicella* genus members.

Genes in the production of carotenoids were also detected in the same genome region of the hopanoids. *crtB (*phytoene synthase) and *crtI* (phytoene desaturase) encode for the complete pathway for the synthesis of phytoene to the production of phytofluene, zeta-carotene, neurosporene, and finally, lycopene (Henke et al. 2017). The genes *crtB* and *crtI* were detected in *G. tundricola* and *T. saanensis*, but not in *G. mallensis* (*crtI* not detected). Perhaps the lack of *crtI* is consistent with the physical color description of *G. mallensis*, as colonies are white or light beige due to the lack of the lycopene pigment, while the phytoene carotenoid synthesized by *crtB* is colorless (Männistö et al. 2012). In contrast, *crtI* was identified in *G. tundricola* and *T. saanensis*, providing them with the potential to express the full pathway of lycopene biosynthesis. As expected, colonies of *G. tundricola* and *T. saanensis* are pink (Männistö et al. 2011, 2012).

crtB was the only carotenoid biosynthesis gene detected in strains A2288, MP8S9, M8UP23, suggesting that phytoene synthase may be a more essential enzyme for carotenoid biosynthesis. Based on the slight yellow colony pigmentation of remaining new strains where carotenoid genes were not detected, there is most likely a divergent or different carotenoid biosynthesis pathways present.

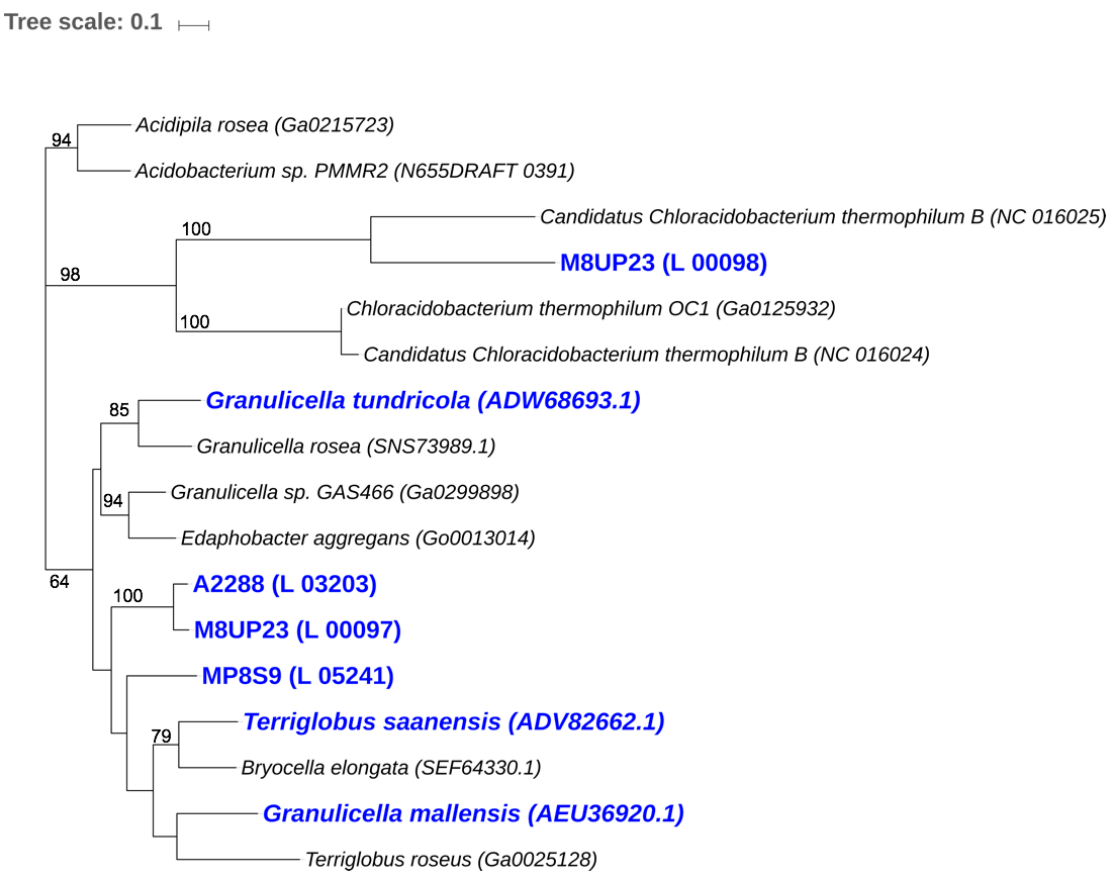

Figure 3.10: Phylogeny of CrtB (phytoene synthase) of *Acidobacteria*. Phylogeny was generated by maximum likelihood using amino acids sequences of 278 positions, and 500 bootstrap replicates.

The phylogeny of CrtB surprisingly does not follow the same trend as the HpnF/SHC or of the 16S rRNA gene tree as demonstrated by Figure 3.10. Here, strain M8UP23 clusters more closely with strains outside of subdivision 1 *Acidobacteria* unlike the 16S rRNA gene or the whole genome phylogeny. To continue with this analysis, proteins that are annotated as CrtB, but also encode for squalene/phytoene synthase (SPS) were also analyzed by creating another amino acid phylogeny of *Acidobacteria* strains in Figure 3.11.

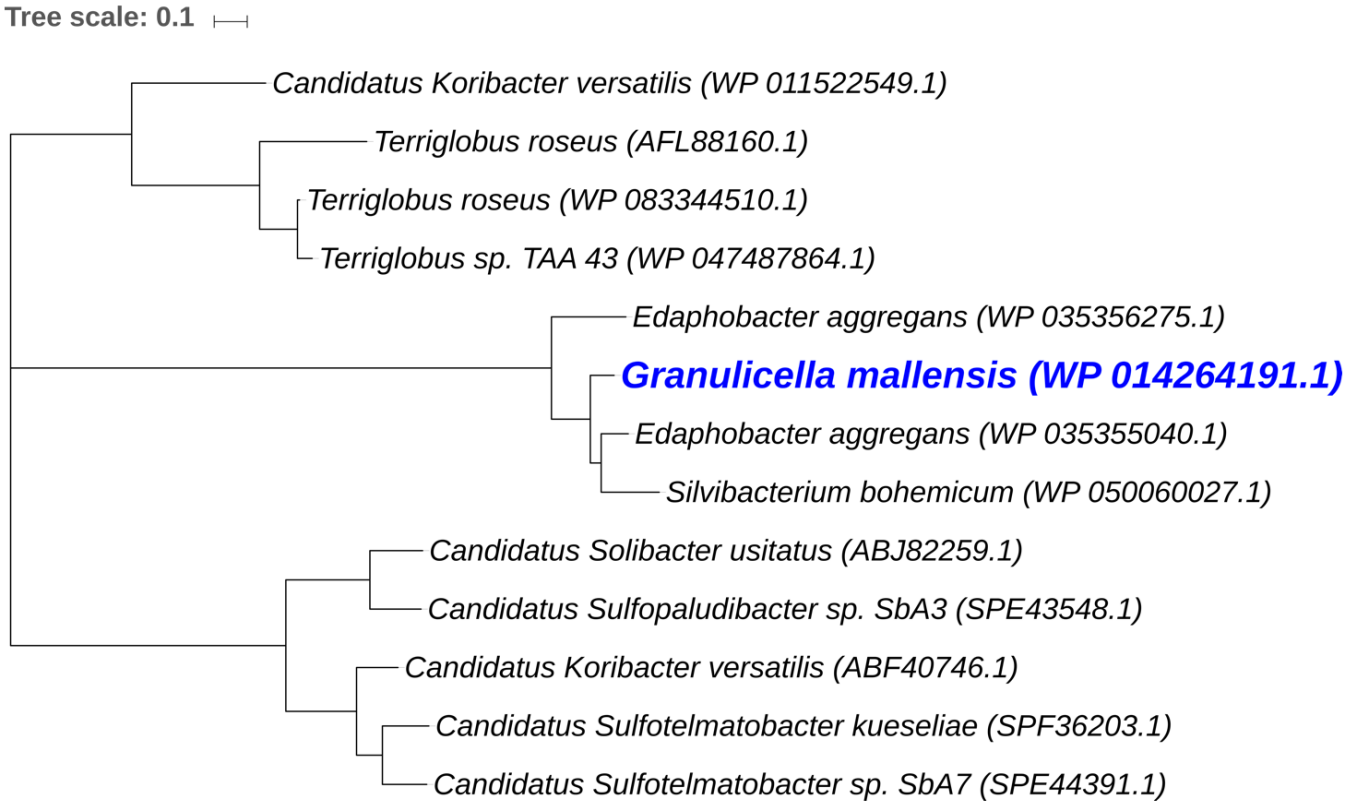

Figure 3.11: Phylogeny of SPS (phytoene synthase)/CrtB of *Acidobacteria*.Phylogeny was generated by maximum likelihood using amino acids sequences of 280 positions, and 500 bootstraps replicates.

Upon examination, it is apparent that only *G. mallensis* has the enzyme SPS amongst the select tundra *Acidobacteria* strain isolates (Figure 3.11). This also suggests that squalene biosynthesis for these other tundra *Acidobacteria* strains is accomplished by the squalene synthase (HpnC). However, for *G. mallensis*, SPS is a critical enzyme for the potential hopanoid/carotenoid biosynthesis.

Preliminary Data on Hopanoid Production in Acidobacteria strains and Future Work

The whole genome sequencing, and bioinformatic analysis of tundra soil isolates has provided the framework for future gene expression studies, by identifying key genes and synthetic pathways (see supplemental material for of 16S rRNA gene and hopanoid biosynthetic gene sequences of *Acidobacteria* tundra isolates). This future work will more precisely unravel the dynamics of hopanoid or carotenoid function in tundra soil *Acidobacteria* under changing conditions. In preliminary work (Zahorik 2016) diploptene, BHT glucosamine, and BHT cyclitol ether hopanoids were detected in *G. mallensis*, *G. tundricola*, and *T. saanensis*. Though additional replication of hopanoid measurements need to be carried out for future work, there appears to be a weak trend that the higher temperatures induce higher diploptene production by some *Acidobacteria* isolates. Results of this preliminary work are summarized in Table 3.8.

Species	°C	pH	Diploptene	BHT glucosamine	BHT cyclitol ether
G. mallensis	15	5	21.6	29.8	15.6
G. mallensis	15	5.5	11.3	42.7	2.7
T. saanensis	15	5	12.6	54.1	10.2
T. saanensis	15	6	6.1	42.9	15.8
T. saanensis	15	7	24.6	45.7	6.8
G. mallensis	25	5	44.7	31.3	8.6
T. saanensis	25	6	41.6	32.1	7.5

Table 3.8: Relative abundance of *Acidobacteria* hopanoids under varying temperature and pH conditions. This data comes from the G.H. Cook Scholar Senior Thesis of Amanda Zahorik (2016).

Similar analysis of acidobacterial carotenoid production could be performed in future work. Detection and quantification of the pigments phytoene, phytofluene, neurosporene, zeta-carotene, and lycopene could be carried out under varying environmental parameters (temperature, pH, salinity, radiation, etc.) to understand which carotenoids are are produced in response to particular stressors. Because the production of these have been detected to increase during thermal stress, both warmer and colder temperatures could be used to explore whether certain pigments, or pigment combinations are expressed under varying thermal conditions (Fong et al. 2001; Dieser et al. 2010; Mojib et al. 2013). This study design could answer, though also raise further questions into

which carotenoid is expressed during which thermal stress, and how this expression affects overall lipid membrane and cell survival.

Carotenoid and hopanoid synthesis in bacteria have intertwined pathways, and are understudied in combination. In *Methylobacterium extorquens,* when the hopanoid synthesis pathway was disrupted by the mutation of the HpnF/SHC protein, the bacterium overproduced carotenoids (Bradley et al. 2017). Furthermore, systems of both carotenoid/hopanoids biosynthesis of tundra bacteria are likely divergent from those of warmer regions. The acidobacterium *Chloracidobacterium thermophilium* was isolated from the hot springs of Yellow Stone National Park, and has the ability to make carotenoids and hopanoids (Bryant et al. 2007; Tank and Bryant 2015). Thus, it would also be interesting to contrast the inverse adaption strategies of the thermophilic phototrophic *C. thermophilum* with those of the Arctic tundra soils. While it is difficult to generalize what the effect of hopanoids/carotenoids would be on an organism when stressed, one can hypothesize that the response may result in modifications of these isoprenoids uniquely to each organism. The type/amount of carotenoid/hopanoid produced, environmental stresses, strain biology could be compared to explore the potential adaptations.

3.5 SUPPLEMENTAL INFORMATION

S.1 16S rRNA GENES OF NEW ACIDOBACTERIA STRAINS EXTRACTED FROM WHOLE GENOMES

>A2288_L_04284_16S_ribosomal_RNA

AGAGTTTGATCCTGGCTCAGAATCAACGCTGGCGGCGTGCCTAACACATGC
AAGTCGCACGAGAAAGGGGCTTCGGCTCTGAGTAAAGTGGCGCACGGGTG
AGTAACACGTGACTAATCTACCCTCGAGTGGGGAATAACTGAGAGAAATCTT
AGCTAATACCGCATAACACTTACGAGTCAAAGCAGTAATGCGCTTGGGGAG
GAGGTCGCGGCCGATTAGCTAGTTGGCGGGGTAATGGCCCACCAAGGCGA
TGATCGGTATCCGGCCTGAGAGGGCGCACGGACACACTGGAACTGAAACA
CGGTCCAGACTCCTACGGGAGGCAGCAGTGGGGAATTTTGCGCAATGGGG
GAAACCCTGACGCAGCAACGCCGCGTGGAGGATGAAATATCTTGGTATGTA
AACTCCTTTCGATGGGGAAGATTATGACGGTACCCATAGAAGAAGCCCCGG
CTAACTTCGTGCCAGCAGCCGCGGTAATACGAGGGGGGCAAGCGTTGTTC
GGATTTATTGGGCGTAAAGGGTGCGTAGGCGGTTTGATAAGTCTGATGTGA
AATCTATGGGCTCAACCCATAGTCTGCATTAGAAACTGTCGGGCTTGAGTAT
GGGAGAGGTGAGTGGAATTTCCGGTGTAGCGGTGAAATGCGTAGATATCG
GAAGGAACACCTGTGGCGAAAGCGGCTCACTGGACCATAACTGACGCTGAT
GCACGAAAGCTAGGGGAGCAAACAGGATTAGATACCCTGGTAGTCCTAGCC
CTAAACGATGATTGCTTGGTGTGGCAGGTACCCAATCCTGCCGTGCCGAAG
CTAACGCGATAAGCAATCCGCCTGGGGAGTACGGTCGCAAGGCTGAAACT
CAAAGGAATTGACGGGGGCCCGCACAAGCGGTGGAGCATGTGGTTTAATT
CGACGCAACGCGAAGAACCTTACCTGGGCTCGAAATGTAGTGGAATCCGG
CAGAAACGTCGGCGTCTAGCAATAGACCGCTATATAGGTGCTGCATGGCTG
TCGTCAGCTCGTGTCGTGAGATGTTGGGTTAAGTCCCGCAACGAGCGCAAC
CCTTATCTTCAGTTGCTACCATTTAGTTGAGCACTCTGACGAAACCGCCTCG
GATAACGGGGAGGAAGGTGGGGATGACGTCAAGTCCTCATGGCCTTTATGT
CCAGGGCTACACACGTGCTACAATGGCCGGTACAAACCGCTGCAAACCCG
CGAGGGGGAGCTAATCGGAAAAAGCCGGCCTCAGTTCGGATTGGAGTCTG
CAACTCGACTCCATGAAGCTGGAATCGCTAGTAATCGTGGATCAGCATGCC
ACGGTGAATACGTTCCCGGGCCTTGTACACACCGCCCGTCACATCACGAAA
GTGGGTTGCACTAGAAGTCGGTGCG-CTAAC-CGCAAGGGAGCAGCCGCCC

>M8UP39_L_02005_16S_ribosomal_RNA

AGAGTTTGATCCTGGCTCAGAATCAACGCTGGCGGCGTGCCTAACACATGC
AAGTCGCACGAGAAAGGGTAGCAATACCTGAGTAAAGTGGCGCACGGGTG
AGTAACACGTGACTAATCTACCCTCGAGTGGGGAATAACTGAGAGAAATCTT
AGCTAATACCGCATAACACTTACGAGTCAAAGCAGCAATGCGCTTGGGGAG
GAGGTCGCGGCCGATTAGCTAGTTGGCGGGGTAATGGCCCACCAAGGCGA
TGATCGGTATCCGGCCTGAGAGGGCGCACGGACACACTGGAACTGAAACA
CGGTCCAGACTCCTACGGGAGGCAGCAGTGGGGAATTTTGCGCAATGGGG

GAAACCCTGACGCAGCAACGCCGCGTGGAGGATGAAATATCTTGGTATGTA
AACTCCTTTCGATGGGGAAGATTATGACGGTACCCATAGAAGAAGCCCCGG
CTAACTTCGTGCCAGCAGCCGCGGTAATACGAGGGGGGCAAGCGTTGTTC
GGATTTATTGGGCGTAAAGGGTGCGTAGGCGGTTTGGCAAGTCTTGTGTGA
AATCTTCGGGCTCAACCCGAAGTCTGCACAAGAAACTGCCGGGCTTGAGTA
TGGGAGAGGTGAGTGGAATTTCCGGTGTAGCGGTGAAATGCGTAGATATCG
GAAGGAACACCTGTGGCGAAAGCGGCTCACTGGACCATAACTGACGCTGAT
GCACGAAAGCTAGGGGAGCAAACAGGATTAGATACCCTGGTAGTCCTAGCC
CTAAACGATGATTGCTTGGTGTGGCAGGTACCCAATCCTGCCGTGCCGAAG
CTAACGCGATAAGCAATCCGCCTGGGGAGTACGGTCGCAAGGCTGAAACT
CAAAGGAATTGACGGGGGCCCGCACAAGCGGTGGAGCATGTGGTTTAATT
CGACGCAACGCGAAGAACCTTACCTGGGCTCGAAATGTAGTGGAATCCGG
CAGAAACGTCGGCGTCTAGCAATAGACCGCTATATAGGTGCTGCATGGCTG
TCGTCAGCTCGTGTCGTGAGATGTTGGGTTAAGTCCCGCAACGAGCGCAAC
CCTTATCTTCAGTTGCTACCATTTAGTTGAGCACTCTGACGAAACCGCCTCG
GATAACGGGGAGGAAGGTGGGGATGACGTCAAGTCCTCATGGCCTTTATGT
CCAGGGCTACACACGTGCTACAATGGCCGGTACAAACCGCTGCAAACCCG
CGAGGGGGAGCTAATCGGAAAAAGCCGGCCTCAGTTCGGATTGGAGTCTG
CAACTCGACTCCATGAAGCTGGAATCGCTAGTAATCGTGGATCAGCATGCC
ACGGTGAATACGTTCCCGGGCCTTGTACACACCGCCCGTCACATCACGAAA
GTGGGTTGCACTAGAAGTCGGTGCGCTAACCGCAAGGGAGCAGCCGCCC

>MP8S11_L_02935_16S_ribosomal_RNA

AGAGTTTGATCCTGGCTCAGAATCAACGCTGGCGGCGTGCCTAACACATGC
AAGTCGCACGAGAAAGGGTAGCAATACCTGAGTAAAGTGGCGCACGGGTG
AGTAACACGTGACTAATCTACCCTCGAGTGGGGAATAACTGAGAGAAATCT
CAGCTAATACCGCATAACACTTACGAGTCAAAGCAGCAATGCGCTTGGGGA
GGAGGTCGCGGCCGATTAGCTAGTTGGCGGGGTAATGGCCCACCAAGGCG
ATGATCGGTATCCGGCCTGAGAGGGCGCACGGACACACTGGAACTGAAAC
ACGGTCCAGACTCCTACGGGAGGCAGCAGTGGGGAATTTTGCGCAATGGG
GGAAACCCTGACGCAGCAACGCCGCGTGGAGGATGAAATATCTTGGTATGT
AAACTCCTTTCGATGGGGAAGATTATGACGGTACCCATAGAAGAAGCCCCG
GCTAACTTCGTGCCAGCAGCCGCGGTAATACGAGGGGGGCAAGCGTTGTT
CGGATTTATTGGGCGTAAAGGGTGCGTAGGCGGTTTGATAAGTCTGATGTG
AAATCTATGGGCTCAACCCATAGTCTGCATTAGAAACTGTCGGGCTTGAGTA
TGGGAGAGGTGAGTGGAATTTCCGGTGTAGCGGTGAAATGCGTAGATATCG
GAAGGAACACCTGTGGCGAAAGCGGCTCACTGGACCATAACTGACGCTGAT
GCACGAAAGCTAGGGGAGCAAACAGGATTAGATACCCTGGTAGTCCTAGCC
CTAAACGATGATTGTTTGATGTGGCAGGTACCCAATCCTGCCGTGTCGAAG
CTAACGCGATAAACAATCCGCCTGGGGAGTACGGTCGCAAGGCTGAAACTC
AAAGGAATTGACGGGGGCCCGCACAAGCGGTGGAGCATGTGGTTTAATTC
GACGCAACGCGAAGAACCTTACCTGGGCTCGAAATGTAGTGGAATCCGGCA
GAAACGTCGGCGTCTAGCAATAGACCGCTATATAGGTGCTGCATGGCTGTC
GTCAGCTCGTGTCGTGAGATGTTGGGTTAAGTCCCGCAACGAGCGCAACCC
TTATCTTCAGTTGCTACCATTTAGTTGAGCACTCTGACGAAACCGCCTCGGA

TAACGGGGAGGAAGGTGGGGATGACGTCAAGTCCTCATGGCCTTTATGTCC
AGGGCTACACACGTGCTACAATGGCCGGTACAAACCGCTGCAAACCCGCG
AGGGGGAGCTAATCGGAAAAAGCCGGCCTCAGTTCGGATTGGAGTCTGCA
ACTCGACTCCATGAAGCTGGAATCGCTAGTAATCGTGGATCAGCATGCCAC
GGTGAATACGTTCCCGGGCCTTGTACACACCGCCCGTCACATCACGAAAGT
GGGTTGCACTAGAAGTCGGTGCG-CTAAC-CGCAAG-GGAGCAGCCGCCC

>MP8S7_L_00196_16S_ribosomal_RNA

AGAGTTTGATCCTGGCTCAGAATCAACGCTGGCGGCGTGCCTAACACATGC
AAGTCGAACGAGAAAGGGACTTCGGTCCTGAGTACAGTGGCGCACGGGTG
AGTAACACGTGACTAACCTACCCTGGAGTGGGGAATAACTGAGGGAAACCT
TAGCTAATACCGCATAACACCTACGGGTCAAAGGAGCAATTCGCTTCAGGA
GGGGGTCGCGGCCGATTAGTTAGTTGGCGGGGTAATGGCCCACCAAGACA
GTGATCGGTATCCGGCCTGAGAGGGCGCACGGACACACTGGAACTGAAAC
ACGGTCCAGACTCCTACGGGAGGCAGCAGTGGGGAATTTTGCGCAATGGG
GGAAACCCTGACGCAGCAACGCCGCGTGGAGGATGAAATCCCTTGGGATG
TAAACTCCTTTCGATCGGGACGATTATGACGGTACCGGAAGAAGAAGCCCC
GGCTAACTTCGTGCCAGCAGCCGCGGTAATACGAGGGGGGCAAGCGTTGT
TCGGAATTATTGGGCGTAAAGGGAGTGTAGGCGGTTTGGTAAGTTGTGTGT
GAAATCTTCGGGCTCAACCCGAAGTCTGCACACAAAACTGCCGGGCTTGAG
GGTGGGAGAGGTGAGTGGAATTTCCGGTGTAGCGGTGAAATGCGTAGATAT
CGGAAGGAACACCTGTGGCGAAAGCGGCTCACTGGACCATTTCTGACGCT
GAAACTCGAAAGCTAGGGGAGCAAACAGGATTAGATACCCTGGTAGTCCTA
GCCCTAAACGATGACTGTTTGGTGTGGCGGGTACCCAATCCCGCCGTGCC
GTAGCTAACGCGTTAAACAGTCCGCCTGGGGAGTACGGTCGCAAGGCTGA
AACTCAAAGGAATTGACGGGGGCCCGCACAAGCGGTGGAGCATGTGGTTT
AATTCGACGCAACGCGAAGAACCTTACCTGGGCTCGAAATGTACAGGAATC
CGGTGGAAACATCGGCGCCCAGCAATGGGCCTGTATATAGGTGCTGCATG
GCTGTCGTCAGCTCGTGTCGTGAGATGTTGGGTTAAGTCCCGCAACGAGCG
CAACCCTTACCTCCAGTTGCCATCATTTAGTTGGGCACTCTGGCGGAACCG
CCTCGGATAACGGGGAGGAAGGTGGGGATGACGTCAAGTCCTCATGGCCT
TTATGTCCAGGGCTACACACGTGCTACAATGGCCGGTACAAACCGTTGCAA
ACCCGCGAGGGGGAGCTAATCGGAAAAAGCCGGCCTCAGTTCGGATCGCA
GTCTGCAACTCGACTGCGTGAAGCTGGAATCGCTAGTAATCGCGGATCAGA
ATGCCGCGGTGAATACGTTCCCGGGCCTTGTACACACCGCCCGTCACATCA
CGAAAGTGGGTTGCACTAGAAGCCGGTGGGCTAACTCGCAAGAGAGGCAG
CCGTCC

>MP8S9_L_03184_16S_ribosomal_RNA

AGAGTTTGATCCTGGCTCAGAATCAACGCTGGCGGCGTGCCTAACACATGC
AAGTCGCACGAGAAAGGGCTTCGGCCTGAGTAAAGTGGCGCACGGGTGAG
TAACACGTGAATGATCTACCTCCGAGTGGGGAATAACTGAGAGAAATCTTAG
CTAATACCGCATAATACCCACGGGTCAAAGCAGCAATGCGCTTGGAGAGGA

GTTCGCGGCCGATTAGCTAGTTGGCGGGGTAATGGCCCACCAAGGCGATG
ATCGGTATCCGGCCTGAGAGGGCGCACGGACACACTGGAACTGAAACACG
GTCCAGACTCCTACGGGAGGCAGCAGTGGGGAATTTTGCGCAATGGGGGA
AACCCTGACGCAGCAACGCCGCGTGGAGGATGAAGTATCTTGGTACGTAAA
CTCCTTTCGATGGGGAAGATAATGACGGTACCCATAGAAGAAGCCCCGGCT
AACTTCGTGCCAGCAGCCGCGGTAATACGAGGGGGGCAAGCGTTGTTCGG
AATTATTGGGCGTAAAGGGTGCGTAGGCGGTTTGACAAGTCTTATGTGAAAT
CTTCGGGCTCAACCCGAAGTCTGCATGAGAAACTGTTGAGCTTGAGTATGG
GAGAGGTGAGTGGAATTTCCGGTGTAGCGGTGAAATGCGTAGATATCGGAA
GGAACACCTGTGGCGAAAGCGGCTCACTGGACCATAACTGACGCTGAGGC
ACGAAAGCTAGGGGAGCAAACAGGATTAGATACCCTGGTAGTCCTAGCCCT
AAACGATGATTGCTTGGTGTGGCCGGTACCCAATCCGGCCGTGCCGAAGCT
AACGCGATAAGCAATCCGCCTGGGGAGTACGGTCGCAAGGCTGAAACTCA
AAGGAATTGACGGGGGCCCGCACAAGCGGTGGAGCATGTGGTTTAATTCG
ACGCAACGCGAAGAACCTTACCTGGGCTCGAAATGTACATGAATCCGGCAG
AAACGTCGGCGTCTAGCAATAGACATGTATATAGGTGCTGCATGGCTGTCG
TCAGCTCGTGTCGTGAGATGTTGGGTTAAGTCCCGCAACGAGCGCAACCCT
TATCTTCAGTTGCTACCATTTAGTTGAGCACTCTGACGAAACCGCCTCGGAT
AACGGGGAGGAAGGTGGGGATGACGTCAAGTCCTCATGGCCTTTATGTCCA
GGGCTACACACGTGCTACAATGGCCGGTACAAACCGCTGCAACCCCGCGA
GGGTGAGCTAATCGGAAAAAGCCGGCCTCAGTTCGGATTGGAGTCTGCAAC
TCGACTCCATGAAGCTGGAATCGCTAGTAATCGTGGATCAGCATGCCACGG
TGAATACGTTCCCGGGCCTTGTACACACCGCCCGTCACATCACGAAAGTGG
GTTGCACTAGAAGTCGGTGCG-CTAAC-CGCAAG-GGAGCAGCCGCCC

S.2. CAROTENOID BIOSYNTHESIS SEQUENCES OF NEW ACIDOBACTERIA ISOLATES

Phytoene desaturase (CrtB)

>A2288_L_03203_All-trans-phytoene_synthase
VTNAEAYAVCAGIAQREAKNFYYSFRVLPEHKRNAMCAVYAFMRRADDISDDE
ALPVAQRRVVMGDWLEAWRAARRSGVSEDPVFVALNDTQRKFAIPDALLEDLV
RGTTMDLDIEGSQAGMVSVTETVADKTQTLQVYQDFEGLYRYCYLVASVVGLV
CIRIFGYTDPRAEDLAEKTGVAFQLTNILRDVSEDAERGRIYLPLQDLSAGRVEV
KQLLQVVRREAETKVVRSLLAQEAARALVYYAAAEELLPLIDKDSRAALWVLVTI
YRGLLERIMAKNYDVFSERVSVPTSRKLMILAQGMGMAVRNRMVS

>M8UP23_L_00097_All-trans-phytoene_synthase
VTTVEAYAVCAGIAQREAKNFYYSFRVLPEPKRNAMCAVYAFMRRADDISDEE
TMPVVERRVVMTEWLGAWREARRSGVSDDPVFVALNDTQKKFAIPDALLEDLV
RGTTMDLEESQADVVLVTDIVADKTQTLQVYEDFEGLYRYCYLVASVVGLVCIRI
FGYSDPRAEVLAEKTGVAFQLTNILRDVSEDAERGRIYLPMEDLTAGRVEVGQL
LQVVRREAETKVVRSLLAQEAARALVYYAAAEELLPLIDRDSRAALWVLVTIYRG
LLERIMAKNYDVFSERVSVPTSRKLLILAQGMGMAVRNRMVS

>M8UP23_L_00098_All-trans-phytoene_synthase
VNDTTAMQHALLGAPHEYLTPLERPTLAEARAWCRELATSHYENFHVATFFLP
AKVRPHFESIYAYCRVADDLGDEVEDHEVATRLLNSWGAMLEECYDAPERSM
HPVFVALRETIRECDPPRQLFLDLLHAFRMDQYKTEYESWEELLEYSHYSANPV
GRLVLWVCGYTDEARALMSDKVCTALQLANFWQDVVEDKERGRRYLPAESMV
RFGVDEGQIEGRVFTPEFRGMMQELVVRTRVMLLEGGEISQHVDKELKVVLDL
FRKGGEAILNGITRQDFDVLRGRPVVSKTRKAGLLIEALVGKLSAGMAS

>MP8S9_L_05241_All-trans-phytoene_synthase
VTVEAAYAACRVIAKREAKNFYYSFRVLPQAKSDAMCAVYAFMRKADDLSDDE
SLSLEARRAGMAEWLGAWRAARAGGATDDPVFLALGDAQRRFGISDGLLEDL
VRGTTLDLEERQDGVAPVAVKDETYQVYETFDGLYRYCYLVASVVGLVCIKVF
GYRDPAAEKLAEETGIAFQLTNILRDVKEDAERGRVYLPLDDMRTAGADVEQVV
VASEDGIVGRGVKFLMVREGDRAKAYYRSAEALMPMIDADSRAALWVMVTIYR
RLLEKIAAKGYPVTTRVSLSTVEKLSILVQGALMARRLKGAR

S. 3. HOPANOID BIOSYTHESIS SEQUENCES OF NEW ACIDOBACTERIA ISOLATES

Squalene-hopene cyclase (HpnF)

>MP8S9_L_04795
MESGSVNPQAKTQPARPRFGRMDLGLEYVAAGIERAKNWLLGQQHADGYWC
GELEADVMLEADYIFMHTLLGTGDPGRMKRAVNEILRHQNADGGWSLYPGGP
SNINYGVKAYFALKLMGWTADQPVLVKAREWVLANGGVVECNTFTKMYLCAM
GQYDYDAVPAVPPEIILFPDWFYFNIYEISAWSRAILVPLSIIYAKKPFKKLAAGQ
GIEELFVGGRAKADLRLKWDRKHIFSWRNVFLFADRVAHLAERVHIRPLRKKAL
KRAEQWMLDHFERSDGLGAIYPAMLNAIIALIVLGYSKDDPQVIRAMDEFEKLGI
DCPEGTTDYPTPTFRMQPCFSPVWDTAQVLSVLGEVGLAKDDPRLLKGADWL
LSKEIRYQGDWSHKAKIADASCWCFFHNNDHQPDVDDTCEVLLALKSVDHPHE
RHQHEVSQRAVAWIFAMQCKGGGWASFDKDNTKKLFESIPFADHNAMIDPPTA
DITGRALEMLAAYGYTQRDPRVAKAIEFVLKEQSIDGSWFGRWGVNYLYGTFL
VLRGLEAIGYWHHEPAVVSATEWIRMVQNPDGGWGETCGTYDDDMYKGVGP
STPSQTAWALLGLLAGGDSRSDSVAKGVRWLIERQHEDGSWDELMPGRNGE
SYYTGTGFPRVFYLGYHLYKQYFPLLALTTYKKAIEREQAEG

Hopanoid biosynthesis associated radical SAM protein (HpnJ)
>A2288_L_03199 HpnJ
MPLKTLFLNPPSFEKFDGGASSRWPATREIESYWYPVWLTYPAGMLEGSRLVD
APPHHIKWQEVVEILKDYEFLVLFTSTMGWDGDQKMAEVIKQTYSSIKISFVGPP
VTTSPDKALNECPAIDFICRREFDFSVVEYANGKPLNEILGVSYKDKATGKILHN
PDRAQVTPEQLDEMPWATEIYHRDLDVTKYNVPFLLHPYVALYSTRGCPAQCT
FCLWPQTLSGHAWRKRSTDDVAAEMKQAKELFPHVKEFFFDDDTFNIQKARTI

ELCEKLKPLGLTWSCTSRVTTDYDTLKAMKEAGCRLLIVGYESGDPQILKNIKKG
ATVQRALDFTRDCHKLGLVIHGDFILGLPGETRESIRNTIDFAKQLDCETIQVSIA
HAFPGTEFFDYAKDNGFITNEAMNDDGGHQMAHIEYPGLPVEYVMEMVHKFY
DEYYFRPKAAFRVVWQAIVNRDVPRLYTEAKSFMELRSKRNKAVRAVKEANAA
KAQESVSMNA

>M8UP39_L_01120 protein HpnJ
MPLKTLFLNPPSFEKFDGGASSRWPATREIESYWYPVWLTYPAGMLEGSRLLD
APPHHIKWQEVVEILKDYEFLVLFTSTMGWDGDQKMAEVIKQTYPSIKISFVGPP
VTTSPDKALNECPAIDFICRREFDFSVVEYANGKPLNEILGISYKDKATGKILHNP
DRPQVTPEELDEMPWATEIYHRDLDVTKYNVPFLLHPYVALYSTRGCPAQCTF
CLWPQTLSGHAWRKRSTDDVAAEMKQAKELFPHVKEFFFDDDTFNIQKVRTIE
LCEKLKPLGLTWSCTSRVTTDYDTLKAMKEAGCRLLIVGYESGDPQILKNIKKGA
TVQRALDFQRDCHKLGLVVHGDFILGLPGETRESIRNTIDFAKQLDCETIQVSIA
HAFPGTEFFDYAKDNGFITNEAMSDDGGHQMAHIEYPGLPVEYVMEMVHKFY
DEYYFRPKAAFRVVWQAIVNRDVPRLYTEAKSFMELRSKRNKAVRAVKEANAA
KAQESVSMNA

>MP8S9_L_05250 protein HpnJ
MKPLKTLFLNPPSFENFDGGASSRWPATREIESYWYPVWLAYPAGMLEGSKLL
DAPPHHVSAQETIEIAKDYEFLVLFTSTVGWHGDHGLAEAIKRGNPSIKIAFVGP
PVTTDPDRALNECPVIDFVCRREFDFSVVEYANGKPLPEILGISYKDATGTIQHN
PDRPQVEDLDAMPWVTDIYARDMDVTKYNVPFLLHPYVSLYSTRGCPAQCTFC
LWPQTLSGHAWRKRSTDDVAAEMAHAKKLFPHVKEFFFDDDTFNIQKARTIEL
CAKLKPLGLTWSCTSRVTTDRDTLKAMKEAGCRLLIVGFESGDPQILKNIKKGA
TVERARDFVKDCHDLGLIIHADFILGLPGETKESIRNTIEFAKQLDCETIQVSVAH
AFPGTEFYDYAAKNGFITNDVMADTGGHQMAHIEYPGVPAEYVMEMVHRFYD
EYYFRPKAAFRVVWKAIVNRDVPRLYVEARSFMKLRAQRNKASRAKKEENALK
AQESVSMNA

>M8UP23_L_00093 protein HpnJ
MPLKTLFLNPPSFEKFDGGASSRWPATREIESYWYPVWLTYPAGMLEGSRLLD
APPHHIKWQEVVEILKDYEFLVLFTSTMGWDGDQKMAEVIKQTYPNIKISFVGPP
VTTSPDKALTECPAIDFICRREFDFSVVEYANGKPLNEILGVSYKDKATGKILHNP
DRPQVTPEELDEMPWATEIYHRDLDVTKYSVPFLLHPYVSLYSTRGCPAQCTF
CLWPQTLSGHAWRKRSTDDVAAEMKQAKELFPHVKEFFFDDDTFNIQKARTVE
LCEKLKPLGLTWSCTSRVTTDYDTLKAMKEAGCRLLIVGYESGDPQILKNIKKGA
TVQRALDFQRDCHKLGLVVHGDFILGLPGETRESIRNTIDFAKQLDCETIQVSIA
HAFPGTEFFDYAKENGFITNEAMSDEGGHQMAHIEYPGLPVEYVMEMVHKFYD
EYYFRPKAAFRVVWQAIVNRDVPRLYTEAKSFMSLRSKRNKAVRAVKEANAAK
AQESVSMNA

>MP8S11_L_00468 protein HpnJ
MPLKTLFLNPPSFEKFDGGASSRWPATREIESYWYPVWLTYPAGMLEGSRLVD
APPHHISWQEVVEILKDYEFLVLFTSTMGWDGDQKMAEVIKQTYPNIKISFVGPP

VTTSPEKALNECPAIDFICRREFDFSVVEYANGKPLNEILGVSYKDKATGQILHN
PDRAQVTPEQLDEMPWATEIYHRDLDVTKYNVPFLLHPYVALYSTRGCPAQCT
FCLWPQTLSGHAWRKRSTDDVAAEMKQAKELFPHVKEFFFDDDTFNIQKARTI
ELCEKLKPLGLTWSCTSRVTTDFDTLKAMKEAGCRLLIVGYESGDPQILKNIKKG
ATVERARDFTRDCHKLGLVIHGDFILGLPGETRESIRNTIEFAKQIDCETIQVSIAH
AFPGTEFFDYAKTNGFITNEAMSDDGGHQMAHIEYPGLPVEYVMEMVHKFYDE
YYFRPKAAFRVVWQAIVNRDVPRLYTEAKSFMELRSKRNKAVRAVKEANAAKA
QESVSMNA

>MP8S7_L_05326 protein HpnJ
MSTTLPTKTAPLKTLFLNPPSFENFDGGASSRWPATREIESYWYPVWLAYPAG
LLEGSRLLDAPPHHVTAAETIEICKEYEFLVLFTSTVGWEGDQRLAEAIKAANPAI
KIAFVGPPVTTSPDKALNECLALDFICRREFDYSIVEYAQGKPLSEILGISYRANS
ATGYKIIHNPDRPQIEDLDAMPWATKIYKRDMDVTRYNVPFLLHPYIALYSTRGC
PAQCTFCLWPQTLSGHAWRKRSTDDVAAELKWAKENFPEVKEFFFDDDTFNI
QRARTIELCEKLKPLNITWSCTSRVTTEYDTLKAMKEAGCRLLIVGFESGDPQIL
KNIKKGATVEKARQFAKDCNDLGLVIHGDFILGLPGETKESIQNTINFAKSLDVET
IQVSIAHAYPGTEFFDYAEKNGFITNEDAMSDAGGHQMAHIEYPGLPKEYVLEM
VHKFYDAYYFRPKAAFRVIWKAIVNRDVPRLYVEAKAFLKLRKERMNMVKDAKK
LQGKADPVGAGA

Hopanoid adenosyl-hopene transferase (HpnH)
>A2288_L_03247 HpnH
MAVPVSQAWTVATYVLKQKLMGRKKYPLVLMLEPLFRCNLACAGCGKIQYPAH
ILKAELSPEECFRAVEECGTPMVAIPGGEPLLHPQMPEIVAGLVARKKYVYMCT
NALLLKEKLHLFKPSKYLSFSVHVDGQREHHDFSVCREGGYDIAMEGVRVAVE
AGFRVTTNTTLFDGADPNSVRAHFDELMVAGVESMMVSPGYTYDKAPDQKHF
LGRARSKKLFRSILSNRKKTWRFNASPIFMEFLMGKKDLTCTPWGMPTFSIFG
WQKPCYLLQDGYADSFKELMETVQWSNYGTESGNPQCANCMVHSGYEASGV
NYTFSSLKGLLQTAKGIFFSKYEDEGAMKLLNEWKPTSHGPLVQIGSPVAKSAT
ELQEVSGD

>M8UP39_L_01325 HpnH
MAVPVSQAWTVATYVLKQKMMGRKKYPLVLMLEPLFRCNLACAGCGKIQYPA
HILKAELSPEECFKAVEECGTPMVAIPGGEPLLHPQMPEIVAGLVARKKYVYMC
TNALLLKEKLHLFKPSKYLSFSVHVDGQREHHDFSVCREGGYDIAMEGVRVAV
EAGFRVTTNTTLFDGADPNSVRAHFDELMVAGVESMMVSPGYTYDKAPDQKH
FLGRARSKKLFRSILSNRKKTWRFNASPIFMEFLMGKKDLTCTPWGMPTFSIFG
WQKPCYLLQDGYADSFKELMETVEWSNYGTESGNPQCANCMVHSGYEASGV
NYTFSSLKGLLQTAKGIFFSKYEDEGAMKLLNEWKPASYGPLVQIGAPVTNSAS
ELQEVSGD

Hopanoid Phytoene/Squalene Synthase HpnC/CrtB
>M8UP23_L_00098
MQHALLGAPHEYLTPLERPTLAEARAWCRELATSHYENFHVATFFLPAKVRPH
FESIYAYCRVADDLGDEVEDHEVATRLLNSWGAMLEECYDAPERSMHPVFVAL
RETIRECDPPRQLFLDLLHAFRMDQYKTEYESWEELLEYSHYSANPVGRLVLW
VCGYTDEARALMSDKVCTALQLANFWQDVVEDKERGRRYLPAESMVRFGVDE
GQIEGRVFTPEFRGMMQELVVRTRVMLLEGGEISQHVDKELKVVLDLFRKGGE
AILNGITRQDFDVLRGRPVVSKTRKAGLLIEALVGKLSAGMAS

Chapter 4: THE COMPLETE GENOME SEQUENCE OF ARCTIC TUNDRA SOIL BACTERIUM *MUCILAGINIBACTER MALLENSIS*

ABSTRACT

The complete genome sequence of the Arctic tundra soil bacterium *Mucilaginibacter mallensis* MP1X4 is reported here from a single colony isolate. This psychrotolerant member of the *Bacteroidetes* is amongst the understudied family *Sphingobacteriaceae*. Genome analysis reveals a breadth of polysaccharide utilization loci (PUL) that are involved in degradation of complex glycans, making the species well adapted for organic carbon rich environments as the Arctic tundra heath soils. The genome sequence of *M. mallensis strain* MP1X4 is 6.01 MB, comprised of 1 contig. The G+C content is 41.28% with 5,079 total genes and 5,025 protein coding genes. There are two 5S, 16S and 23S rRNA genes and 45 tRNA genes. Here we also provide insights into carbon metabolism of *M*. *mallensis*, with an emphasis on carbohydrate-active enzymes.

4. 1 INTRODUCTION

As the Latin prefix “muci” indicates mucus, the genus *Mucilaginibacter* was fittingly described in 2007 for the slimy heterotrophic, aerobic, Gram-negative bacteria isolated from a Siberian peat bog (Pankratov et al. 2007). This genus is within the family *Sphingobacteriaceae*, and currently comprises 55 described species. Not much is known about the ecological roles or impacts of members of the genus *Mucilaginibacter*, though its species have been found in

aquatic, terrestrial, warm, cold, and industrial environments (Madhaiyan et al. 2010, Hwang et al 2013, Chen et al. 2014; Joung et al. 2015; Lee et al. 2015; Kim et al. 2016; Zhao et al. 2016; Zheng et al. 2016). Another observation amongst isolated species, is that members of *Mucilaginibacter* are found in carbon-rich environments (e.g. tundra/rhizosphere soils, plant matter, wetlands, lichens) and that they produce copious amount of extracellular polysaccharides (Pankratov et al. 2007; Han et al. 2012; Jiang et al. 2011; Paiva et al. 2014, Zheng et al. 2016). Thus, they are likely well-adapted to process complex polysaccharides, which is also consistent with many other members of the phylum *Bacteroidetes* (Salyers et al. 1977; Martens et al. 2009; Flint et al. 2012; Foley et al. 2016; Grondin et al. 2017).

This characteristic of complex carbohydrate digestion in many members of the *Bacteroidetes* is due to them having Polysaccharide Utilization Loci (PULs), identified based on the existence of the Starch Utilization System operon, *Sus* (Foley et al. 2016). The *Sus* operon encodes for proteins that bind and degrade starch/glycans at the cell surface prior to transport of oligosaccharides through the Gram-negative outer-membrane for conversion to monomers in the periplasm (Foley et al. 2016). Because members of the *Mucilaginibacter* have been frequently isolated from carbon-rich environments, they are hypothesized to play a vital role in carbon usage and cycling in carbon-rich soils such as the tundra (Männistö et al. 2010; Sanyal et al. 2018). Further, members of *Bacteroidetes* in these tundra soils were found to be resilient to freeze-thaw cycles (Männistö et al. 2009).

Several cold-adapted bacteria belonging to the genus *Mucilaginibacter* were isolated from the Arctic-Alpine tundra soils of the Malla nature preserve in Kilpisjärvi, Finland (Männistö et al. 2010). *Mucilaginibacter mallensis* strain MP1X4 is a copious producer of extracellular polymeric substances, thus making its complex carbon metabolism intriguing, and appears to be adapted for the temperature challenges of the frigid carbon-rich Arctic tundra soils (Männistö et al. 2010). In our analysis of its complete genome, we highlight the carbon processing capabilities of this bacterium.

4.2 ORGANISM INFORMATION

Classification and features

Mucilaginibacter mallensis MP1X4 is a Gram-negative bacterium and member of the family *Sphingobacteriaceae*, in the phylum *Bacteroidetes*. *M. mallensis* forms pale yellow mucoid colonies on R2A agar, growing at pH 4.5-7 and at a temperature range of -3-33˚C (Männistö et al. 2010). The cells are non-motile rods 1-2 µm in length, after being grown for 30 hours on ½ R2A plates of pH 5.5 at room temperature (Figure 4.1). The original announcement and species description *of Mucilaginibacter mallensis* MP1X4 was provided by Männistö et al. (2010), where details of its isolation from Arctic tundra soils in Kilpisjärvi, Finland are available. This species, along with *M frigotolerans*, was isolated from Finnish Lapland soil (Männistö and Häggblom 2006; Männistö et al. 2010). From the same region, *M. lappiensis* was isolated from a lichen (Männistö et al. 2010).

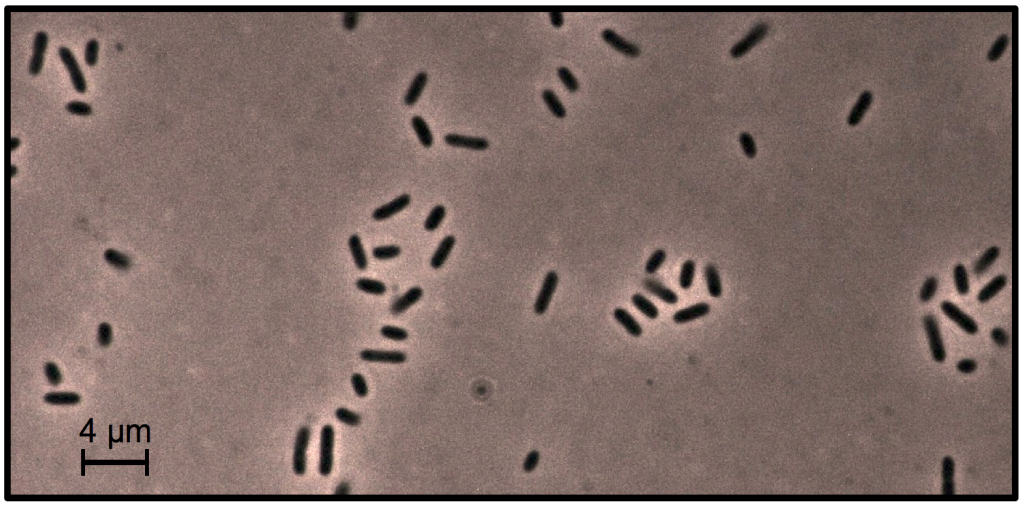

Figure 4.1: Microscopy of *Mucilaginibacter mallensis* MP1X4.

Most *Mucilaginibacter* species have been isolated from a variety of soils, or from plant/woody materials as illustrated in Figure 4.2. However, a few members of the genus *Mucilaginibacter* have been found in relatively unusual sources, such as air-conditioners (Kim et al. 2016), and dye wastewater (Hwang et al. 2014). Phylogeny of the 16S rRNA gene of all *Mucilaginibacter* species described in the genus is illustrated in Figure 4.3. This phylogenetic tree was constructed using a maximum likelihood phylogeny with 500 bootstraps using using 1338 positions through the program MEGA v. 7.0.14. Each of the 59 (excluding outgroups) described species is colored to indicate the source that each species was isolated from, and represents the same color in the phylogenetic tree in Figure 4.2 and in Figure 4.3. Members of the order *Sphingobacteriales* were used as a collective outgroup. The closest relative of *M. mallensis* is *M. gynuensis*, which was isolated from rotten wood in South Korea (Khan et al. 2013). Other closely

related species include *M. pedocola* (isolated from heavy-metal contaminated paddy field), and *M. pyschrotolerans* (from Tibetan peatlands) (Tang et al. 2016; Deng et al. 2017). Within clusters, there is some pattern of grouping depending on the source of isolation, for example the group of *M. jinhuensis*, *M. polytrichastri*, *M. daejeonensis*, and *M. galli*, which were from plant matter (Figure 4.3).

M. mallensis is likely to possess complex plant polysaccharide processing adaptations since it has been isolated from carbon-rich soil. This is also likely consistent with the current characterization of the *Mucilaginibacter* genus. This study explored the complex plant polysaccharide processing adaptations of *Mucilaginibacter mallensis* with comparison to other relatives in the genus. Additional taxonomic information of *M. mallensis* can be found in Table 4.1, using Minimum Information of a Genome Sequences (MIGS) classification, evidence codes Traceable Author Statement (TAS), Non-traceable Author Statement (NAS), per the Gene Ontology project (Gene Ontology Consortium 2000).

MIGS ID	Property	Term	Evidence codea
	Classification	Domain *Bacteria*	TAS [Woese et. al 1991]
		Phylum *Bacteriodetes*	TAS [Krieg 2010]
		Class *Sphingobacteria*	TAS [Kämpfer 2012]
		Order *Sphingobacteriales*	TAS [Kämpfer 2015]
		Family *Sphingobacteriaceae*	TAS [Yabuuchi et. al. 1983]
		Genus *Mucilaginibater*	TAS [Pankratov et al. 2007]
		Species *Mucilaginibacter mallensis*	TAS [Männistö et al 2010]
		Type strain: MP1X4	TAS [Männistö et al 2010]
	Gram stain	Negative	TAS [Männistö et al 2010]
	Cell shape	Rod	TAS [Männistö et al 2010]
	Motility	Non-motile	TAS Männistö et al 2010]
	Sporulation	Non	TAS [Männistö et al 2010]
	Temperature range	minus 3 °C–33 °C	TAS [Männistö et al 2010]
	Optimum Temperature	25 °C	TAS [Männistö et al 2010]
	pH range; optimum	4.5–7.0	TAS [Männistö et al 2010]
	Carbon source	Glucose	TAS [Männistö et al 2010]
MIGS-6	Habitat	Soil	TAS [Männistö et al 2010]
MIGS-6,3	Salinity	Not reported	
MIGS-22	Oxygen requirement	aerobe	TAS [Männistö et al 2010]
MIGS-15	Biotic relationship	Tundra soil isolate	NAS
MIGS-14	Pathogenicity	Nonpathogenic	NAS
MIGS-4	Geographic location	Finland	TAS [Männistö et al 2010]
MIGS-5	Sample collection		TAS [Männistö et al 2010]
MIGS-4,1	Latitude	69˚ 019' N	TAS [Männistö et al 2010]
MIGS-4,2	Longitude	20˚ 50' E	TAS [Männistö et al 2010]
MIGS-4,4	Altitude	700 meters above sea-level	TAS [Männistö et al 2010]

Table 4.1: Minimum Information of a Genome Sequences (MIGS) classification, evidence codes Traceable Author Statement (TAS), Non-traceable Author Statement (NAS).

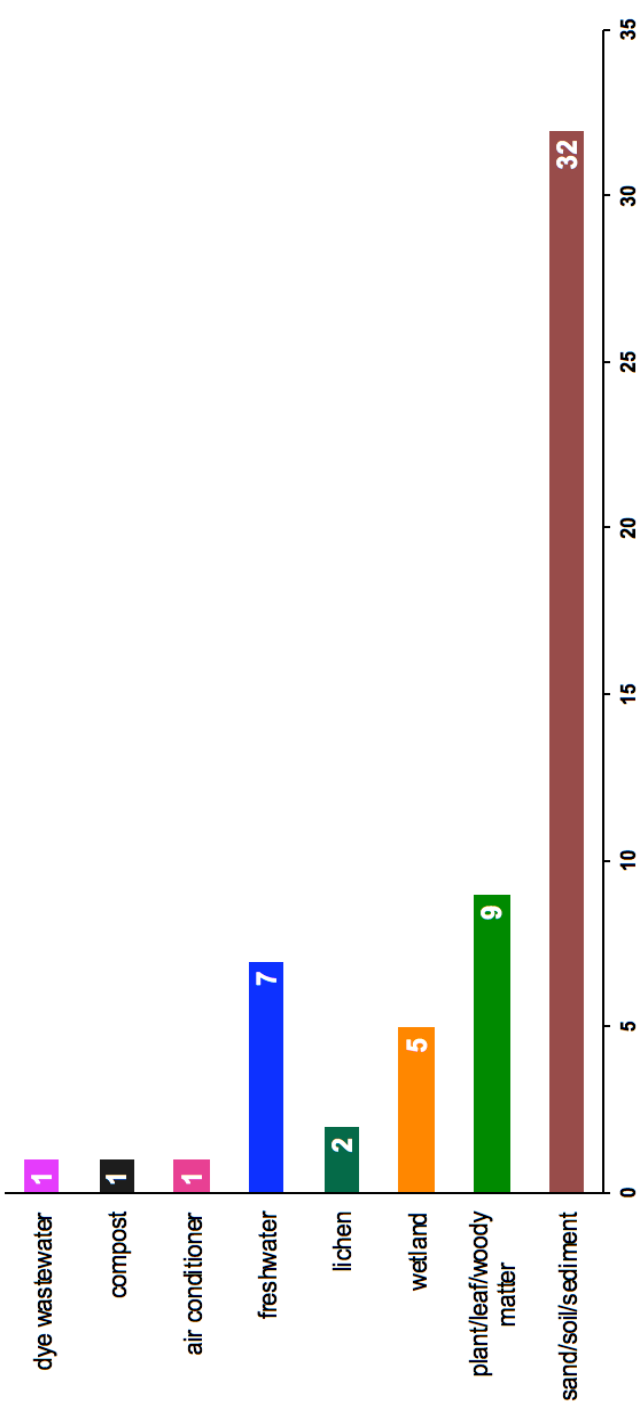

Figure 4.2: Sources of isolation for all currently described species in the genus *Mucilaginibacter*.

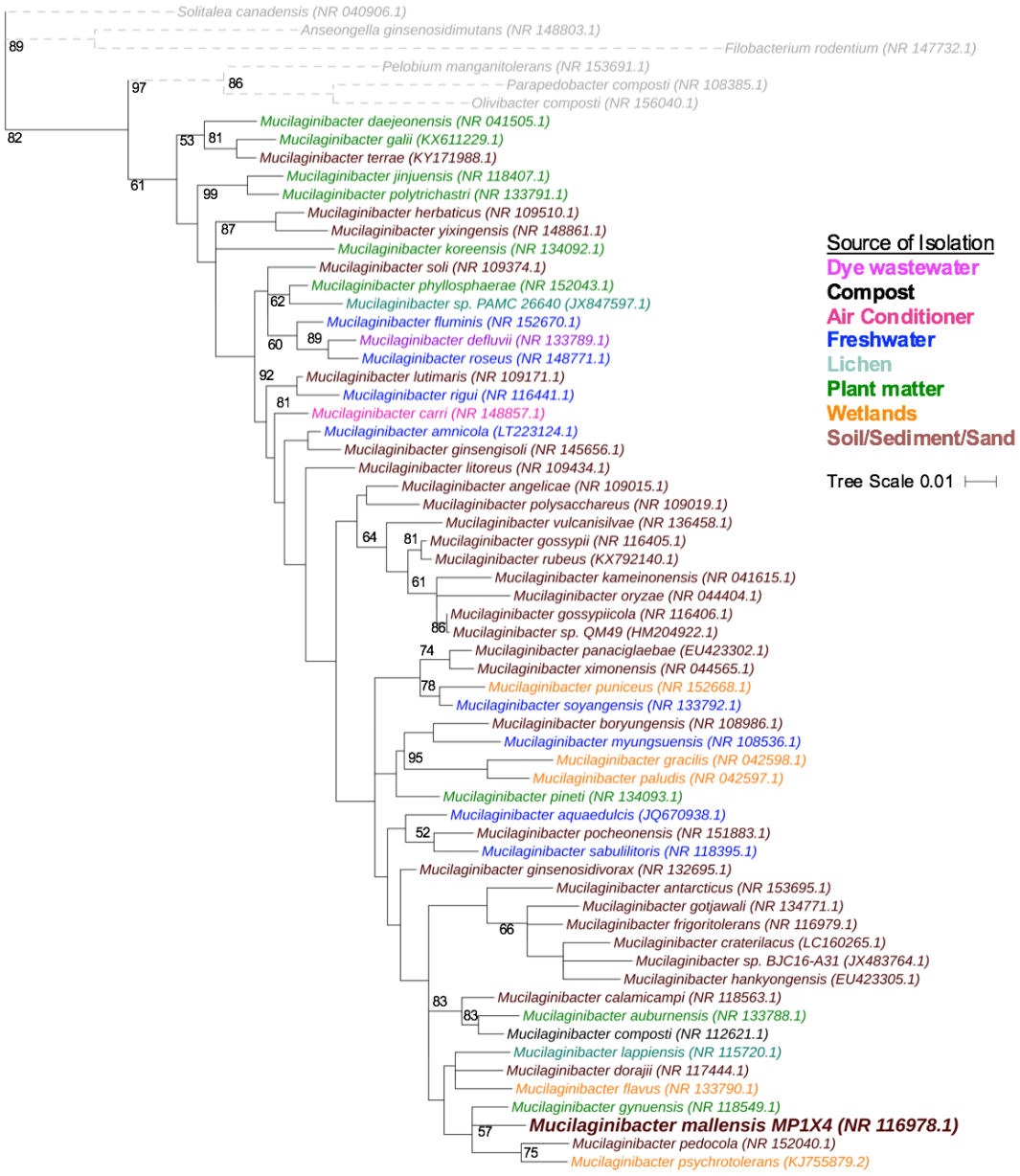

Figure 4.3: 16S rRNA gene phylogeny of all described *Mucilaginibacter* spp. Phylogeny was constructed using a maximum likelihood methodology, with 500 bootstraps using 1338 positions. Bootstrap values of >50 are displayed. Each of the 64 described species is colored to indicate the source that it was isolated from. Members of the order *Sphingobacteriales* were used as a collective outgroup in faded grey.

4.3 GENOME SEQUENCING

Genome project history

This project was selected for the exploration of “Thermal adaptation and carbon metabolism in permafrost isolates” by the JGI-DOE based on its isolation from a carbon-rich Arctic tundra soil. This genome represents the first draft and complete sequence of *M. mallensis* strain MP1X4. The genome was sequenced with PacBio RS/PacBio RS II methodology with 100% scaffold coverage, and 114X sequencing coverage with a final contig of 1 as described in Table 4.3.1. The genome data has been submitted to GenBank under ID NZ_LT629740.1 and is also publicly available through JGI GOLD ID Gp0123649. More details of the project history can be found in Table 4.3.1 with its association with MIGS. Annotations of this genome was carried through the IMG annotation platform and can be accessed through IMG online.

MIGS ID	Property	Term
MIGS 31	Finishing quality	Improved-High-Quality Draft
MIGS-28	Libraries used	PacBio Low Input 10kb; PacBio >10kb w/ AMPure Bead Size Selection, Tubes PacBio RS
MIGS 29	Sequencing platforms	PacBio RS II
MIGS 31.2	Fold coverage	114x
MIGS 30	Assemblers	Hierarchical Genome Assembly Process v. 2.3.0
MIGS 32	Gene calling method	IMG Annotation Pipeline v.4.10.2
	GenBank ID	NZ_LT629740.1
	GenBank Date of Release	29-Jul-17
	GOLD ID	Gp0123649
	BIOPROJECT	PRJNA224116
	Project relevance	Thermal adaption and carbon metabolism in permafrost isolates

Table 4.2: Project information regarding the sequencing of *Mucilaginibacter mallensis* Minimum Information of a Genome Sequences (MIGS). Information for public access via GenBank or through JGI's GOLD database is listed for each category.

Growth conditions and genomic DNA preparation

To generate sufficient biomass for DNA sequencing, *M. mallensis* was grown for 30 hours on ½ strength R2A (Difco) plates adjusted to pH 5.5 at room temperature. Biomass was scraped off the solid medium and used for DNA extraction. DNA extraction was carried out using a modified CTAB-Phenol Chloroform protocol (Griffiths et al. 2000; Männistö et al. 2010). To summarize, *M. mallensis* biomass was mixed with equal volumes of 5% CTAB and phenol:chloroform:isoamyl alcohol (25:24:1) with two 3-mm glass beads. Bead-beating of this mixture was carried out on a bench-top vortex for 2 minutes, after which the biomass was pelleted by centrifugation. Following centrifugation, an equal part chloroform:isoamyl alcohol (24:1) was added to the removed top phase, and mixed. Following another round of centrifugation, the upper phase was transferred to a new microfuge tube with 2X volume of 30% w/v of polyethylene 8000. This mixture was allowed to stand for 45 min at 4°C, and then centrifuged for 15 min at 4°C. Next, the supernatant was removed, and the DNA was precipitated with 70-100% ethanol washes. The DNA pellet was dried and resuspended in DNAse-free water. Quality control was performed to meet JGI's standard for DNA submission with both gel electrophoresis and spectrophotometric measurements.

Genome sequencing and assembly

High quality DNA was sent to the Joint Genome Institute (JGI) for sequencing using PacBio RS/PacBio RS II. After fragmentation, DNA templates

of >10kb were filtered with AMPure beads and then sequenced. Details of this pipeline are available in Table 4.2. The genome was assembled using Hierarchical Genome Process v. 2.3.0 by the JGI pipeline using *de novo* assembly with a Celera Assembler with a single library type following PacBio sequencing (Chin et al. 2013). Visualization of the annotated genome was carried out using CGView (Stothard and Wishart 2004). with GC skew, GC content, and ORFs depicted, and is illustrated in Figure 4.4.

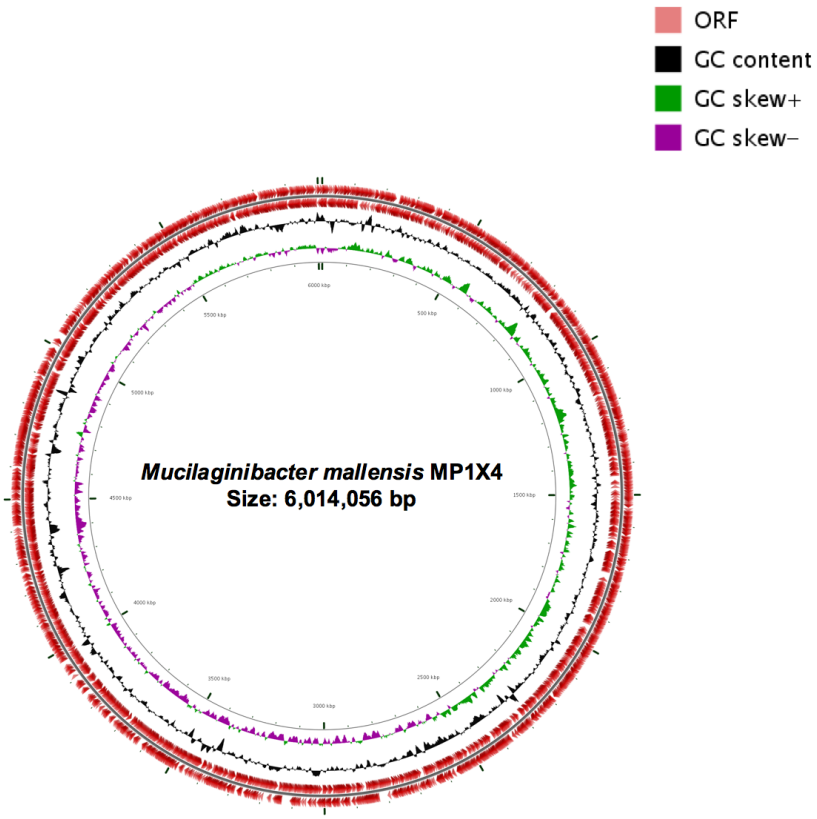

Figure 4.4: Complete genome of *Mucilaginibacter mallensis* MP1X4 with features colored using CGView. Red triangles indicate ORFs and are drawn in direction of the strand.

Genome annotation

This genome was annotated and is publically available online at JGI under project ID 1090154. The genome was annotated using the IMG Annotation Pipeline v.4.10.2 by JGI, and the standard operating procedure (Huntemann et al. 2015). Briefly, preprocessing eliminated any sequences <150 nucleotides and sequences were structurally annotated using CRT, PILER-CR, tRNAscan-SE, BLAST, HMMER 3.0, and Prodigal v2.50 ab initio gene prediction (Huntemann et al. 2015, Bland et. al 2007, Edgar 2007, Lowe and Eddy 1997, Eddy 1997, and Hyatt et al. 2010). Functional annotation was carried out using the Conserved Domain Database (Huntemann et al. 2015, Marchler-Bauer et al. 2010). Protein coding sequences were matched with COG PSSMs via RPS-BLAST with an e-value cut-off of 1e-2 and 70% consensus sequence length.

4.4 GENOMIC INSIGHTS

General genome properties

Using the Integrated Microbial Genomes & Microbiomes pipeline, the genome was assembled, and annotated (Huntemann et al. 2015). Exhaustive genome details can be accessed in Table 4.2 and 4.3. Using 100% of the DNA scaffold, this genome was assembled into 1 contig yielding 6,013,956 bases with a G+C content of 41.28%. There were 5,079 total genes detected, with 5,025 protein coding genes. Out of these protein coding genes, 3,699 genes had a function predicted (Table 4.3). Further characterization of these genes using the COG database is presented in Table 4.4.

Mucilaginibacter mallensis	Number	% of Total
DNA, total number of bases	**6013956**	**100.00%**
DNA coding number of bases	5343576	88.85%
DNA G+C number of bases	2482725	41.28% 1
DNA scaffolds	**1**	**100.00%**
Genes total number	**5079**	**100.00%**
Protein coding genes	5025	98.94%
Pseudo Genes	50	0.98%2
RNA genes	54	1.06%
rRNA genes	6	0.12%
5S rRNA	2	0.04%
16S rRNA	2	0.04%
23S rRNA	2	0.04%
tRNA genes	45	0.89%
Other RNA genes	3	0.06%
Protein coding genes with function prediction	3699	72.83%
without function prediction	1326	26.11%
Protein coding genes with enzymes	1060	20.87%
w/o enzymes but with candidate KO based enzymes	29	0.57%
Protein coding genes connected to KEGG pathways3	1021	20.10%
not connected to KEGG pathways	4004	78.83%
Protein coding genes connected to KEGG Orthology (KO)	1814	35.72%
not connected to KEGG Orthology (KO)	3211	63.22%
Protein coding genes connected to MetaCyc pathways	943	18.57%
not connected to MetaCyc pathways	4082	80.37%
Protein coding genes with COGs3	2750	54.14%
with KOGs3	870	17.13%
with Pfam3	3898	76.75%
with TIGRfam3	1189	23.41%
with InterPro	2549	50.19%
with IMG Terms	617	12.15%
with IMG Pathways	221	4.35%
with IMG Parts List	265	5.22%
in internal clusters	1569	30.89%
in Chromosomal Cassette	4999	98.42%
Chromosomal Cassettes	483	-
Biosynthetic Clusters	20	-
Genes in Biosynthetic Clusters	314	6.18%
Fused Protein coding genes	251	4.94%
Protein coding genes coding signal peptides	854	16.81%
Protein coding genes coding transmembrane proteins	1343	26.44%
COG clusters	**1383**	**50.29%**
KOG clusters	**514**	**18.69%**
Pfam clusters	**2051**	**52.62%**
TIGRfam clusters	**857**	**72.08%**

Table 4.3: Genome information about *Mucilaginibacter mallensis*. Information gathered through JGI's IMG pipeline.

There were 2,750 protein coding genes that matched the COG database, representing 54% of the genome. Of these COG functional genes, 19.5% had unknown function, and 11.2% have only general function predicted (Table 4.4), serving as a reminder about how little is characterized about gene function amongst environmental isolates, and the need for generating more meaningful annotations. 5% of COGs with 247 genes detected comprised of carbohydrate transport and metabolism.

Code	Value	%age	Description
J	330	6.71	Translation, ribosomal structure and biogenesis
A	7	0.14	RNA processing and modification
K	198	4.02	Replication, recombination and repair
L	181	3.68	Replication, recombination and repair
B	6	0.12	Chromatin structure and dynamics
D	62	1.26	Cell cycle control, cell division, chromosome partitioning
V	115	2.34	Defense mechanisms
T	182	3.70	Signal transduction mechanisms
M	216	4.39	Cell wall/membrane/envelope biogenesis
N	87	1.77	Cell motility
U	100	2.03	Intracellular trafficking, secretion, and vesicular transport
O	191	3.88	Posttranslational modification, protein turnover, chaperones
C	274	5.57	Energy production and conversion
G	247	5.02	Carbohydrate transport and metabolism
E	274	5.57	Amino acid transport and metabolism
F	118	2.40	Nucleotide transport and metabolism
H	215	4.37	Coenzyme transport and metabolism
I	123	2.50	Lipid transport and metabolism
P	232	4.71	Inorganic ion transport and metabolism
Q	97	1.97	Secondary metabolites biosynthesis, transport and catabolism
R	551	11.20	General function prediction only
S	960	19.51	Function unknown
-	155	3.15	Not in COGs

Table 4.4: The COG functional genes and the relative abundance in the total number of genes in *M. mallensis.*

Carbon processing in Mucilaginibacter

As *Mucilaginibacter* members have been found in many carbon-rich environments, gaining insights from their genomes can help current

understanding of their metabolic carbon-processing capabilities. Thus, it is interesting to understand how *M. mallensis* is potentially able to take part in carbon turnover processes in its carbon-rich Arctic tundra soil habitat, and be able to investigate their presence in community surveys (Männistö et al. 2010; Loya and Grogan 2014). To expand on our understanding of carbon processing in *M. mallensis*, carbohydrate-active enzymes (CAZYmes) and polysaccharide utilization loci (PUL) were investigated and compared with available *Mucilaginibacter* members in the CAZy/PUL database (Lombard et al. 2014, Terrapon et al. 2014, 2018). Genes from *M. mallensis* were matched in the CAZyme database (Lombard et al. 2014) to the sequences and 3D structures of all known carbohydrate processing enzymes that can modify, degrade, or build oligo- and/or polysaccharides. The PUL Database of *Bacteroidetes* (PULDB) is a collection of physically linked genes that break down a particular glycan together with the presence of a *susC* or *susD* starch utilization gene, and are predominant in the phylum *Bacteroidetes* (Terrapon et al. 2014, 2018). PULs have been frequently studied in the gut microbiome of ruminants, humans, and other plant consumers, and can similarly be used to understand carbon processing in soils. (Terrapon et al. 2014, Grondin et al. 2018, Mathieu et al. 2018).

The PUL database has been especially curated for PUL predictions from 956 members of the *Bacteroidetes* phylum, and was used for the *M. mallensis* genome analysis using experimentally characterized sequences, as well as predictions based on Sus operon features (Terrapon et al. 2014, 2018). The genome of *M. mallensis*, along with available genomes of other members for the

genus, *Mucilaginibacter* sp. strain BJC16-A31, *M. gotajawali,* and *Mucilaginibacter* sp. strain PAMC 26640 were analyzed and compared for PUL, as shown in Table 4.5. Compared to these relatives, *M. mallensis* has the highest amount of predicted PUL, 59 in total (Table 4.5). Other clusters of similar genes without the *susCD* genes, called CAZy clusters, were also counted and compared across the same *Mucilaginibacter* members, revealing that *M. mallensis* had the highest CAZyme clusters, 7 in total (Table 4.5). This suggests that *M. mallensis* is especially adapted for carbohydrate processing.

Features	*M. BJC16-A31*	*M. gotajawali*	*M. mallensis*	*M. PAMC 26640*
PUL	3	24	59	34
CAZyme clusters	3	6	7	3

Table 4.5: Carbohydrate Active Enzymes of *Mucilaginibacter mallensis* and related species detected using the CAZy database.

To discern the particular type of CAZymes that are represented in the PUL and CAZy clusters, the enzyme classes were broken into glycoside hydrolases, glycosyl transferases, polysaccharide lyases, carbohydrate-esterases, and carbohydrate binding molecules (Lombard et al. 2014). Classes of these CAZymes were then tallied and analyzed across *M. mallensis* and the same relatives. Unsurprisingly, *M. mallensis* had the most number of glycoside hydrolases (Henrissat and Davies 1997), polysaccharide lyases (Lombard et al. 2010), and carbohydrate-binding modules (Boraston et al. 2004) compared to other curated *Mucilaginibacter* members (Figure 4.5). Overlaps in possessing

certain Cazymes were in categories of glycoside hydrolases, glycoside transferases, carbohydrate esterases, and carbohydrate binding module families.

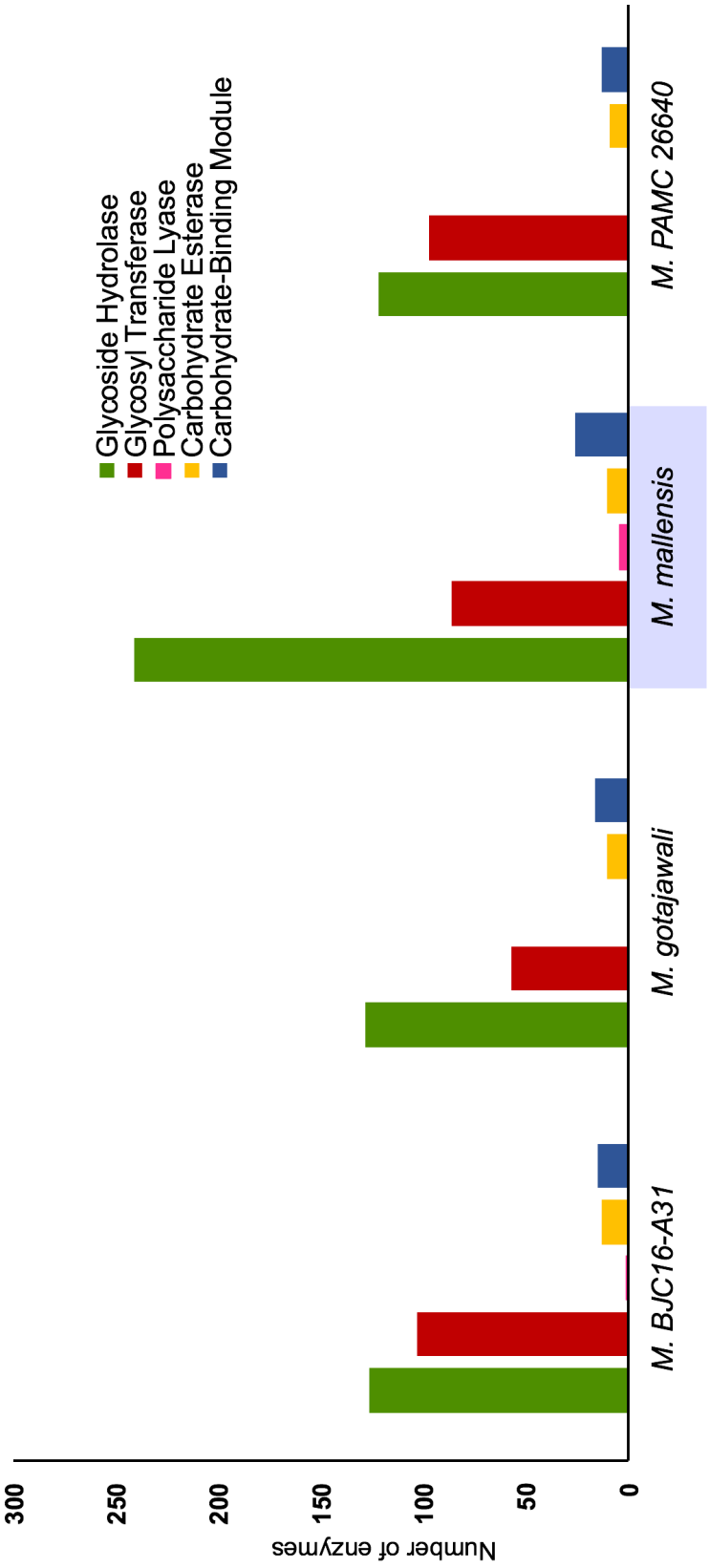

Figure 4.5: CAZy Enzyme Families of *Mucilaginibacter mallensis* and relatives. Number of enzymes indicate number of genes associated with polysaccharide metabolism in each CAZy category.

4.5 CONCLUSIONS

The genome of the Arctic tundra soil bacterium *Mucilaginibacter mallensis* was successfully sequenced, assembled, and annotated using PacBio technology and JGI's IMG pipeline. Of interest was discerning the PUL/CAZy profile of *M. mallensis*, and it was discovered to have the most predicted PULs, glycosidal hydrolases, polysaccharide lyases, and carbohydrate-binding modules among available *Mucilaginibacter* genomes in the PUL/CAZy database. This gene profile suggests that *M. mallensis* is well suited for carbon-rich tundra soils, and further expression analyses could be carried to test the specificity and differential responses of these pathways to variety of conditions.

Chapter 5. DISCUSSION

5.1 OVERALL DISSERTATION GOALS

Tundra microbiology is a relatively new area of research, where current findings are becoming more consequential as the planet undergoes climate change. The aims of this dissertation were to investigate tundra bacterial biology using ecological and genomic approaches. The goals were to determine which bacteria are metabolically active at subzero temperatures, and learn about tundra bacterial features by analyzing genomes from the same Arctic tundra site. These goals were explored using both tundra soil and isolates of *Mucilaginibacter* spp. and *Acidobacteria* members from Kilpisjärvi, Finland.

5.2 KEY AIMS AND FINDINGS

Specific Aim 1: To determine which bacteria are active at subzero temperatures.

Here, stable isotope probing (SIP) was used with tundra soil incubations at subzero temperatures. Briefly, ^{12}C- and ^{13}C-labelled cellobiose was amended to soil incubations at 0, -4, and -16˚C, and DNA from incubations with bacterial activity was sequenced. Bacterial families that were active at subzero temperatures were very different in composition than the initial bacterial resident community. Further, temperature was found to affect bacterial community composition within subzero temperature ranges. The subzero active bacteria were largely members of families *Melioribacteraeae*, *Verrucomicrobiaceae*, *Burkholderiaceae*, *Acetobacteraceae*, *Armatimonadaceae*, and *Planctomycetaceae*. Some of the subzero-active families represented only a

minor part of the initial bacterial community, such as the *Ignavibacteria*, and the Candidatus Saccharibacteria. Overall, relative abundance of members of the *Verrucomicrobia* remained relatively consistent, as they were detected in the initial community, and were also metabolically active during subzero temperatures. Phylogeny of the *Ignavibacteria* OTUs detected in this study revealed a new subzero-active clade, contrary to previous descriptions of its members as thermophiles. The phylogeny of Candidatus Saccharibacteria showed that OTUs from this study grouped closer with those from soil environments than animal environments. Subzero active *Verrucomicrobia* appeared to be uniformly distributed throughout the phylum, unlike the clustering of *Ignavibacteria* and Candidatus Saccharibacteria. This study demonstrated that subzero temperatures impact active bacterial community composition, and adds to previously described physiological potential and habitats of *Ignavibacteria*, Candidatus Saccharibacteria, and *Verrucomicrobia*.

Specific Aim 2: Analyze isoprenoid biosynthetic pathways in the genomes of the ubiquitous tundra soil Acidobacteria.

With an emphasis on the isoprenoids membrane structures such as hopanoids and carotenoids, genome analysis of previously described *Acidobacteria (Granulicella mallensis*, *Granulicella tundricola*, *Terriglobus saanensis*), and genome annotation/analysis of potentially novel species (new strains A2288, M8UP23, M8UP39, MP8S11, MP8S7, and MP8S9) from Kilpisjärvi, Finland was conducted. These membrane structures are understudied

in bacteria, and are thought to help organisms survive stress by maintaining membrane fluidity.

Genes that encode for production of hopanoids diploptene (*hpnF*/*shc*), adenosylhopane (*hpnH*), ribosylhopane (*hpnG*), bacteriohopanetetrol (BHT) (*hpnA*), BHT acetylglucosamine (*hpnI*), BHT glucosamine (*hpnK*), and BHT cyclitol ether (*hpnJ*) were identified in the genomes of *G. mallensis*, *G. tundricola*, and *T. saanensis*. In the new *Acidobacteria* strains, only strain MP8S9 was detected to have the capability of producing diplopetene(*hpnF*/*shc*), adenosylhopane (*hpnH*), ribosylhopane (*hpnG*), and BHT(*hpnA*). These findings also remind that not all *Acidobacteria* spp. have the same hopanoid properties, and might thereby respond to environmental stress differently.

The genomes of *T. saanensis* and *G. tundricola*, genes encoding for the production of carotenoids of phytoene (*crtB*), phytofluene (*crtI*), zeta-carotene (*crtI*), neurosporene (*crtI*), and lycopene (*crtI*) were identified. A gene encoding for the production of phytoene was identified in *G. mallensis*, which could explain the unpigmented appearance of *G. mallensis* colonies. The same was true for the new *Acidobacteria* strains A2288, MP8S9, M8UP23 with only genes for phytoene (*crtB*) biosynthesis detected.

The combined membrane variations of isoprenoid properties, combined with other adaptions to life are expected to impact each species dynamics in these tundra soils. Other general features of the new *Acidobacteria* strains such as morphologies, enzymatic activities, gene/enzyme phylogenies, genome size, and G+C% content have also been determined. From these data, it can be

ascertained that these isolates are unique strains, but further testing needs to be conducted to assess if they are new species of *Acidobacteria*. The most likely candidate for new species are strains MP8S9 and MP8S7, with 98% similarity of the 16S rRNA gene to their closest relatives. Strains M8UP23, A2288, and MP8S11 are likely *Edaphobacter* spp. Another intriguing discovery is that the phylogeny of the HpnF/SHC follows the same branching pattern as the 16S rRNA gene tree, making the HpnF/SHC another marker in analyzing *Acidobacteria* strain relationships.

Specific Aim 3: Genome analysis of the tundra soil bacterium, Mucilaginibacter mallensis MP1X4, with an emphasis on carbohydrate processing.

Members of the *Mucilaginibacter* have been found in carbon-rich environments, globally. The DNA of this tundra soil isolate was extracted in the laboratory, and had its genome fully sequenced, assembled, and annotated by the Joint Genome Institute (JGI). Using a combination of databases/platforms such as JGI and Carbohydrate-Active enZYmes (CAZy), analysis of the the *M. mallensis* genome was carried out, and compared with available genomes of *Mucilaginibacter* spp. in the CAZy database. *M. mallensis* had the highest polysaccharide utilization loci (PULs) and CAZyme clusters compared to *Mucilaginibacter* sp. strain PAMC 26640, *M. gotajawali,* and *Mucilaginibacter* sp. strain BJC16-A3. Within the CAZyme clusters, *M. mallensis* had the highest amounts of glycoside hydrolases, glycosyl transferases, carbohydrate-binding modules and polysaccharide lyases. This finding suggests that *M. mallensis* is

well suited for the breakdown of glycans. General genome characteristics of *M. mallensis* were also determined in this study. Overall, *M. mallensis* is 6.01 MB, with 41.28 G+C% content, with 5079 total genes (5025 protein coding genes).

5.3 CONCLUSIONS

After investigating each aim, it is humbling to admit that this dissertation only makes a small dent in vast unknowns of tundra soil microbiology. Overall, this work demonstrates that subzero temperature impacts bacterial community compositions and activity in frozen tundra soils, that isolates from the same tundra soil have the ability complex systems to breakdown glycans (PULs and CAZymes), and some species have variations in adaptations of isoprenoid biosynthesis to help survive or even thrive in this environment. This work lays the foundation of future experiments to further characterize these detected genomic capabilities.

REFERENCES

Ahn J-H, Kim B-C, Joa J-H, Kim S-J, Song J, Kwon S-W, et al. Mucilaginibacter ginsengisoli sp. nov. isolated from a ginseng-cultivated soil. *International Journal of Systematic and Evolutionary Microbiology* 2015; **65**: 3933–3937.

Ai C, Liang G, Sun J, Wang X, He P, Zhou W, et al. Reduced dependence of rhizosphere microbiome on plant-derived carbon in 32-year long-term inorganic and organic fertilized soils. *Soil Biology and Biochemistry* 2015; **80**: 70–78.

Alcaíno J, Baeza M, Cifuentes V. Carotenoid Distribution in Nature. *Carotenoids in Nature: Biosynthesis, Regulation and Function*. 2016. Springer International Publishing, 3–33.

An D-S, Yin C-R, Lee S-T, Cho C-H. Mucilaginibacter daejeonensis sp. nov., isolated from dried rice straw. *International Journal of Systematic and Evolutionary Microbiology* 2009; **59**: 1122–5.

Angel R, Panhölzl C, Gabriel R, Herbold C, Wanek W, Richter A, et al. Application of stable-isotope labelling techniques for the detection of active diazotrophs. *Environmental Microbiology* 2017; **20**: 44–61.

Annous BA, Becker LA, Bayles DO, Labeda DP, Wilkinson BJ. Critical role of anteiso-C15:0 fatty acid in the growth of *Listeria monocytogenes* at low temperatures. *Applied and Environmental Microbiology* 1997; **63**: 3887-3894.

Anwar M, Khan TH, Prebble J, Zagalsky PF. Membrane-bound carotenoid in *Micrococcus luteus* protects naphthoquinone from photodynamic action. *Nature* 1977; **270**: 538–540.

Arthur H, Watson K. Thermal adaptation in yeast: growth temperatures, membrane lipid, and cytochrome composition of psychrophilic, mesophilic, and thermophilic yeasts. *Journal of Bacteriology* 1976; **128**: 56–68.

Ayala-del-Río HL, Chain PS, Grzymski JJ, Ponder MA, Ivanova N, Bergholz PW, et al. The genome sequence of *Psychrobacter arcticus* 273-4, a Psychroactive Siberian permafrost bacterium, reveals mechanisms for adaptation to low-temperature growth. *Appl Environ Microbiol* 2010; **76**.2304-12.

Baek K, Ok Jeon C. *Mucilaginibacter vulcanisilvae* sp. nov., isolated from a volcanic forest. *International Journal of Systematic and Evolutionary Microbiology* 2015; **65**: 2036–2041.

Baik KS, Park SC, Kim EM, Lim CH, Seong CN. Mucilaginibacter rigui sp. nov., isolated from wetland freshwater, and emended description of the genus Mucilaginibacter. *International Journal of Systematic and Evolutionary Microbiology* 2009; **60**: 134–139.

Bakermans C, Tsapin AI, Souza-Egipsy V, Gilichinsky DA, Nealson KH. Reproduction and metabolism at − 10°C of bacteria isolated from Siberian permafrost. *Environmental Microbiology* 2003; **5**: 321–326.

Barghoorn ES, Schopf JW. Years Old from the Precambrian of South Africa. *Science* 1966; **152**: 758–763.

Barria C, Malecki M, Arraiano CM. Bacterial adaptation to cold. *Microbiology* 2013; **159**: 2437–2443.

Beckering CL, Steil L, Weber MHW, Vo U. Genomewide Transcriptional Analysis of the Cold Shock Response in Bacillus subtilis. *Journal of Bacteriology* 2002; **184**: 6395–6402.

Begum Z, Srinivas TNR, Manasa P, Sailaja B, Sunil B, Prasad S, et al. Winogradskyella psychrotolerans sp. nov., a marine bacterium of the family Flavobacteriaceae isolated from Arctic sediment. *International Journal of Systematic and Evolutionary Microbiology* 2013; **63**: 1646–1652.

Belin BJ, Busset N, Giraud E, Molinaro A, Silipo A. Hopanoid lipids : from membranes to plant – bacteria interactions. *Nature Publishing Group* 2018; **16**: 304–315.

Belshe EF, Schuur EAG, Bolker BM. Tundra ecosystems observed to be CO_2 sources due to differential amplification of the carbon cycle. *Ecology Letters* 2013; **16**: 1307–1315.

Bergmann GT, Bates ST, Eilers KG, Lauber CL, Caporaso JG, Walters WA, et al. The under-recognized dominance of *Verrucomicrobia* in soil bacterial communities. *Soil Biology & Biochemistry* 2011; **43**: 1450–1455.

Biasi C, Jokinen S, Marushchak ME, Hämäläinen K, Trubnikova T, Oinonen M, et al. Microbial Respiration in Arctic Upland and Peat Soils as a Source of Atmospheric Carbon Dioxide. *Ecosystems* 2014; **17**: 112–126.

Bore EK, Apostel C, Halicki S, Kuzyakov Y, Dippold MA. Microbial Metabolism in Soil at Subzero Temperatures: Adaptation Mechanisms Revealed by Position-Specific ^{13}C Labeling. *Frontiers in Microbiology* 2017; **8**: 946.

Boraston AB, Bolam DN, Gilbert HJ, Davies GJ. Carbohydrate-binding modules: fine-tuning polysaccharide recognition. *The Biochemical journal* 2004; **382**: 769–781.

Bradley AS, Swanson PK, Muller EEL, Marx CJ, Caroll SM, Pearson A. Hopanoid-free Methylobacterium extorquens DM4 overproduces carotenoids and has widespread growth impairment. *PLoS ONE* 2017; 1–18.

Bryant DA, Costas AMG, Maresca JA, Chew AGM, Klatt CG, Bateson MM, et al. Candidatus Chloracidobacterium thermophilum: An Aerobic Phototrophic Acidobacterium. *Science* 2007; **317**: 523 LP-526.

Bullock MS, Nelson SD, Kemper WD. Soil Cohesion as Affected by Freezing, Water Content, Time and Tillage. *Soil Science Society of America Journal* 1988; **52**: 770–776.

Chattopadhyay MK, Jagannadham MV, Vairamani M, Shivaji S. Carotenoid pigments of an antarctic psychrotrophic bacterium *Micrococcus roseus*: Temperature dependent biosynthesis, structure, and interaction with synthetic membranes. *Biochemical and Biophysical Research Communications* 1997; **239**: 85–90.

Chen W-M, Chen Y-L, Sheu S-Y. Mucilaginibacter roseus sp. nov., isolated from a freshwater river. *International Journal of Systematic and Evolutionary Microbiology* 2015; **66**; 1112–1118

Chen XY, Zhao R, Tian Y, Kong BH, Li XD, Chen ZL, et al. Mucilaginibacter polytrichastri sp. nov., isolated from a moss (Polytrichastrum formosum), and emended description of the genus Mucilaginibacter. *International Journal of Systematic and Evolutionary Microbiology* 2014; **64**: 1395–1400.

Cheng L, Zhang N, Yuan M, Xiao J, Qin Y, Deng Y, et al. Warming enhances old organic carbon decomposition through altering functional microbial communities. *Nature Publishing Group* 2017; **11**: 1825–1835.

Chin C-S, Alexander DH, Marks P, Klammer AA, Drake J, Heiner C, et al. Nonhybrid, finished microbial genome assemblies from long-read SMRT sequencing data. *Nature Methods* 2013; **10**: 563.

Christensen S, Tiedje JM. Brief and vigorous N2O production by soil at spring thaw. *Journal of Soil Science* 1990; **41**: 1–4.

Chu H, Fierer N, Lauber CL, Caporaso JG, Knight R, Grogan P. Soil bacterial diversity in the Arctic is not fundamentally different from that found in other biomes. *Environmental Microbiology* 2010; **12**: 2998–3006.

Clein JS, Schimel JP. Microbial activity of tundra and taiga soils at sub-zero temperatures. *Soil Biology and Biochemistry* 1995; **27**: 1231–1234.

Correa-Llantén DN, Amenábar MJ, Blamey JM. Antioxidant capacity of novel pigments from an Antarctic bacterium. *Journal of Microbiology* 2012; **50**: 374–379.

Crits-Christoph A, Diamond S, Butterfield CN, Thomas BC, Banfield JF. Novel soil bacteria possess diverse genes for secondary metabolite biosynthesis. *Nature* 2018; **558**: 440–444.

Cui C-H, Choi T-E, Yu H, Jin F, Lee S-T, Kim S-C, et al. Mucilaginibacter composti sp. nov., with ginsenoside converting activity, isolated from compost. *The Journal of Microbiology* 2011; **49**: 393–398.

Cui C-H, Liu Q-M, Kim J-K, Sung B-H, Kim S-G, Kim S-C, et al. Identification and Characterization of a Mucilaginibacter sp. Strain QM49 β-Glucosidase and Its Use in the Production of the Pharmaceutically Active Minor Ginsenosides (S)-Rh1 and (S)-Rg2. *Applied and Environmental Microbiology* 2013; **79**: 5788–5798.

Dai Y, Yan Z, Zhang S, Liu X, Jia L, Gao L, et al. The composition, localization and function of low-temperature-adapted microbial communities involved in methanogenic degradations of cellulose and chitin from Qinghai–Tibetan Plateau wetland soils. *Journal of Applied Microbiology* 2016; **121**: 163–176.

Dall'Agnol HPMB, Baraúna RA, de Sá PHCG, Ramos RTJ, Nóbrega F, Nunes CIP, et al. Omics profiles used to evaluate the gene expression of *Exiguobacterium antarcticum* B7 during cold adaptation. *BMC Genomics* 2014; **15**: 986.

Damsté JSS, Rijpstra WIC, Dedysh SN, Foesel BU, Villanueva L. Pheno- and Genotyping of Hopanoid Production in *Acidobacteria*. *Frontiers in Microbiology* 2017; **8**: 968–968.

De Maayer P, Anderson D, Cary C, Cowan DA. Some like it cold: understanding the survival strategies of psychrophiles. *EMBO reports* 2014.**5**: 508-517

Dieser M, Greenwood M, Foreman CM, , et al. Carotenoid Pigmentation in Antarctic Heterotrophic Bacteria as a Strategy to Withstand Environmental Stresses Carotenoid Pigmentation in Antarctic Heterotrophic Bacteria as a Strategy to Withstand Environmental Stresses. *Arctic, Antarctic, and Alpine Research* 2010; **42**: 396–405.

Drotz SH, Sparrman T, Nilsson MB, Schleucher J, Öquist MG. Both catabolic and anabolic heterotrophic microbial activity proceed in frozen soils. *Proceedings of the National Academy of Sciences of the United States of America* 2010; **107**: 21046–21051.

Dumont MG, Murrell JC. Stable Isotope Probing — Linking Microbial Identity to Function. *Nature Reviews Microbiology* 2005; **3**: 499.

Edgar RC. Updating the 97% identity threshold for 16S ribosomal RNA OTUs. *Bioinformatics* 2018; **34**: 2371–2375.

Edwards AC, Cresser MS. Freezing and Its Effect on Chemical and Biological Properties of Soil. In: Stewart BA (ed). *Advances in Soil Science*. 1992. Springer New York, New York, NY, pp 59–79.

Eichorst SA, Kuske CR. Identification of Cellulose-Responsive Bacterial and Fungal Communities in Geographically and Edaphically Different Soils by Using Stable Isotope Probing. *Applied and Environmental Microbiology* 2012; **78**: 2316–2327.

Eichorst SA, Trojan D, Roux S, Herbold C, Rattei T, Woebken D. Genomic insights into the Acidobacteria reveal strategies for their success in terrestrial environments. *Environmental Microbiology* 2018; **20**: 1041–1063.

El Khawand M, Crombie AT, Johnston A, Vavlline DV, McAuliffe JC, Latone JA, et al. Isolation of isoprene degrading bacteria from soils, development of isoA gene probes and identification of the active isoprene-degrading soil community using DNA-stable isotope probing. *Environmental Microbiology* 2016; **18**: 2743–2753.

Fahnestock JT, Jones MH, Welker JM. Wintertime CO2 efflux from Arctic soils: Implications for annual carbon budgets. *Global Biogeochemical Cycles* 1999; **13**: 775–779.

Felsenstein J. Confidence Limits on Phylogenies: An Approach Using the Bootstrap. *Evolution* 1985; **39**: 783–791.

Fierer N, Leff JW, Adams BJ, Nielsen UN, Bates ST, Lauber CL, et al. Cross-biome metagenomic analyses of soil microbial communities and their functional attributes. *Proceedings of the National Academy of Sciences* 2012; **109**: 21390–21395.

Fischer WW, Summons RE, Pearson A. Targeted genomic detection of biosynthetic pathways: anaerobic production of hopanoid biomarkers by a common sedimentary microbe. *Geobiology* 2005; **3**: 33–40.

Flanagan PW, Veum AK. Relationships between respiration, weight loss, temperature and moisture in organic residues on tundra. *Soil Organisms and Decomposition in Tundra* 1974; 249–277.

Flint HJ, Scott KP, Duncan SH, Louis P, Forano E. Microbial degradation of complex carbohydrates in the gut. *Gut Microbes* 2012; **3**: 289–306.

Foley MH, Cockburn DW, Koropatkin NM. The Sus operon : a model system for starch uptake by the human gut Bacteroidetes. *Cellular and Molecular Life Sciences* 2016; **73**: 2603–2617.

Fong NJ, Burgess ML, Barrow KD, Glenn DR. Carotenoid accumulation in the psychrotrophic bacterium *Arthrobacter agilis* in response to thermal and salt stress. *Applied microbiology and biotechnology* 2001; **56**: 750–756.

Ganzert L, Bajerski F, Wagner D. Bacterial community composition and diversity of five different permafrost-affected soils of Northeast Greenland. *FEMS Microbiology Ecology* 2014; **89**: 426–441.

Gavazov K, Ingrisch J, Hasibeder R, Mills RTE, Buttler A, Gleixner G, et al. Winter ecology of a subalpine grassland: Effects of snow removal on soil respiration, microbial structure and function. *The Science of the Total Environment* 2017; **590**–**591**: 316–324.

Georlette D, Jónsson ZO, Van Petegem F, Chessa J-P, Van Beeumen J, Hübscher U, et al. A DNA ligase from the psychrophile *Pseudoalteromonas haloplanktis* gives insights into the adaptation of proteins to low temperatures. *European Journal of Biochemistry* 2003; **267**: 3502–3512.

Gibbons SM, Gilbert JA. Microbial diversity — exploration of natural ecosystems and microbiomes. *Curr Opin Genet Dev* 2016; 66–72.

Gittel A, Bárta J, Kohoutová I, Mikutta R, Owens S, Gilbert J, et al. Distinct microbial communities associated with buried soils in the Siberian tundra. *The ISME Journal* 2014; **8**: 841–853.

Gittel A, Bárta J, Kohoutová I, Schnecker J, Wild B, Čapek P, et al. Site- and horizon-specific patterns of microbial community structure and enzyme activities in permafrost-affected soils of Greenland. *Frontiers in Microbiology* 2014; **5**: 541.

Gkarmiri K, Mahmood S, Ekblad A, Alström S, Högberg N, Finlay R. Identifying the Active Microbiome Associated with Roots and Rhizosphere Soil of Oilseed Rape. *Applied and Environmental Microbiology* 2017; **83**.1-14.

Goodwin TW. Biogeochemistry of Carotenoids. In: Goodwin TW (ed). *The Biochemistry of the Carotenoids: Volume I Plants*. 1980. Springer Netherlands, Dordrecht, pp 346–349.

Goordial J, Davila A, Lacelle D, Pollard W, Marinova MM, Greer CW, et al. Nearing the cold-arid limits of microbial life in permafrost of an upper dry valley, Antarctica. *ISME J* 2016; **10**: 1613–1624.

Graham DE, Wallenstein MD, Vishnivetskaya TA, Waldrop MP, Phelps TJ, Pfiffner SM, et al. Microbes in thawing permafrost: the unknown variable in the climate change equation. *ISME J* 2012; **6**: 709–712.

Graham EB, Knelman JE, Schindlbacher A, Siciliano S, Breulmann M, Yannarell A, et al. Microbes as Engines of Ecosystem Function: When Does Community Structure Enhance Predictions of Ecosystem Processes? *Frontiers in Microbiology* 2016; **7**: 214–214.

Gurevich A, Saveliev V, Vyahhi N, Tesler G. QUAST: quality assessment tool for genome assemblies. *Bioinformatics* 2013; **29**: 1072–1075.

Haichar F el Z, Roncato M-A, Achouak W. Stable isotope probing of bacterial community structure and gene expression in the rhizosphere of *Arabidopsis thaliana*. *FEMS microbiology ecology* 2012; **81**: 291–302.

Han S-I, Lee H-J, Lee H-R, Kim K-K, Whang K-S. Mucilaginibacter polysacchareus sp. nov., an exopolysaccharide-producing bacterial species isolated from the rhizoplane of the herb Angelica sinensis. *International Journal of Systematic and Evolutionary Microbiology* 2012; **62**: 632–7.

Han S-R, Kim K-H, Ahn D-H, Park H, Oh T-J. Complete genome sequence of carotenoid-producing *Microbacterium* sp. strain PAMC28756 isolated from an Antarctic lichen. *Journal of Biotechnology* 2016; **226**: 18–19.

Hausmann B, Pelikan C, Herbold CW, Köstlbacher S, Albertsen M, Eichorst SA, et al. Peatland *Acidobacteria* with a dissimilatory sulfur metabolism. *The ISME Journal* 2018; **12**: 1729–1742.

Henrissat B, Davies G. Structural and sequence-based classification of glycoside hydrolases. *Current opinion in structural biology* 1997; **7**: 637–644.

Hertzberg S, Borch G, Liaaen-Jensen S. Bacterial carotenoids. L. Absolute configuration of zeaxanthin dirhamnoside. *Archives of microbiology* 1976; **110**: 95–99.

Hisashi Hemmi SO Kuniaki Nagaoka, and Tokuzo Nishino. Identification of Genes Affecting Lycopene Formation in *Escherichia coli* Transformed with

Carotenoid Biosynthetic Genes : Candidates Early Genes in Isoprenoid Biosynthesis. *Journal of Biochemistry* 1998; **1096**: 1088–1096.

Högberg MN, Högberg P. Extramatrical ectomycorrhizal mycelium contributes one-third of microbial biomass and produces, together with associated roots, half the dissolved organic carbon in a forest soil. *New Phytologist* 2002; **154**: 791–795.

Hultman J, Waldrop MP, Mackelprang R, David MM, McFarland J, Blazewicz SJ, et al. Multi-omics of permafrost, active layer and thermokarst bog soil microbiomes. *Nature* 2015; **521**: 208–212.

Hunter S, Apweiler R, Attwood TK, Bairoch A, Bateman A, Binns D, et al. InterPro: the integrative protein signature database. *Nucleic Acids Research* 2009; **37**: D211–D215.

Huntemann M, Ivanova NN, Mavromatis K, Tripp HJ, Paez-espino D, Palaniappan K, et al. The Standard Operating Procedure of the DOE-JGI Microbial Genome Annotation Pipeline (MGAP v.4). *IMG Microbial Genome Annotation Pipeline SOP* 2015.

Hwang YM, Baik KS, Seong CN. Mucilaginibacter defluvii sp. nov., isolated from a dye wastewater treatment facility. *International Journal of Systematic and Evolutionary Microbiology* 2013; **64**: 565–571.

Hyatt D, Chen G, Locascio PF, Land ML, Larimer FW, Hauser LJ. Prodigal: prokaryotic gene recognition and translation initiation site identification. *BMC Bioinformatics* 2010; **11**:119.

Jagannadham MV, Chattopadhyay MK, Subbalakshmi C, Vairamani M, Narayanan K, Rao CM, et al. Carotenoids of an Antarctic psychrotolerant bacterium, *Sphingobacterium antarcticus*, and a mesophilic bacterium, *Sphingobacterium multivorum*. *Archives of Microbiology* 2000; **173**: 418–424.

Jansson JK, Tas N. The microbial ecology of permafrost. *Nat Rev Micro* 2014; **12**: 414–425.

Jeon Y, Lee S-S, Chung BS, Kim JM, Bae J-W, Park SK, et al. Mucilaginibacter oryzae sp. nov., isolated from soil of a rice paddy. *International journal of systematic and evolutionary microbiology* 2009; **59**: 1451–4.

Jiang F, Dai J, Wang Y, Xue X, Xu M, Guo Y. *Mucilaginibacter soli* sp . nov ., isolated from Arctic tundra soil. *International Journal of Systematic and Evolutionary Microbiology* 2012; **0**: 1630–1635.

Johnston ER, Rodriguez-R LM, Luo C, Yuan MM, Wu L, He Z, et al. Metagenomics Reveals Pervasive Bacterial Populations and Reduced Community Diversity across the Alaska Tundra Ecosystem. *Frontiers in Microbiology* 2016; **7**: 579–579.

Jones RT, Robeson MS, Lauber CL, Hamady M, Knight R, Fierer N. A comprehensive survey of soil acidobacterial diversity using pyrosequencing and clone library analyses. *The ISME journal* 2009; **3**: 442–453.

Joung Y, Joh K. Mucilaginibacter myungsuensis sp. nov., isolated from a mesotrophic artificial lake. *International Journal of Systematic and Evolutionary Microbiology* 2010; **61**: 1506–1510.

Joung Y, Kim H, Kang H, Lee B-I, Ahn T-S, Joh K. Mucilaginibacter soyangensis sp. nov., isolated from a lake. *International Journal of Systematic and Evolutionary Microbiology* 2013; **64**: 413–419.

Joung Y, Kang H, Lee B-I, Kim H, Joh K, Kim K-J. Mucilaginibacter aquaedulcis sp. nov., isolated from fresh water. *International Journal of Systematic and Evolutionary Microbiology* 2015; **65**: 698–703.

Joung Y, Kim H, Lee B-I, Kang H, Kim T-S, Kim SB, et al. Mucilaginibacter flavus sp. nov., isolated from wetland. *International journal of systematic and evolutionary microbiology* 2014; **64**: 1304–9.

Juottonen H, Eiler A, Biasi C, Tuittila E-S, Yrjälä K, Fritze H. Distinct Anaerobic Bacterial Consumers of Cellobiose-Derived Carbon in Boreal Fens with Different CO_2/CH_4 Production Ratios. *Applied and Environmental Microbiology* 2017; **83**.2533-2516.

Kämpfer P, Busse H-J, McInroy JA, Glaeser SP. *Mucilaginibacter auburnensis* sp. nov., isolated from a plant stem. *International Journal of Systematic and Evolutionary Microbiology* 2014; **64**: 1736–42.

Kandror O, DeLeon A, Goldberg AL. Trehalose synthesis is induced upon exposure of *Escherichia coli* to cold and is essential for viability at low temperatures. *Proceedings of the National Academy of Sciences of the United States of America* 2002; **99**: 9727–9732.

Kang C-H, Jung Y-T, Yoon J-H. Mucilaginibacter sabulilitoris sp. nov., isolated from marine sand in a firth. *International journal of systematic and evolutionary microbiology* 2013; **63**: 2865–71.

Kannenberg EL, Poralla K. Hopanoid Biosynthesis and Function in Bacteria. *Naturwissenschaften* 1999; **86**: 168–176.

Khan H, Chung EJ, Jeon CO, Chung YR. *Mucilaginibacter gynuensis* sp. nov., isolated from rotten wood. *International Journal of Systematic and Evolutionary Microbiology* 2013; **63**: 3225–3231.

Kielak AM, Barreto CC, Kowalchuk GA, van Veen JA, Kuramae EE. The Ecology of *Acidobacteria*: Moving beyond Genes and Genomes. *Frontiers in Microbiology* 2016; **7**:744.

Kielak AM, Cipriano MAP, Kuramae EE. *Acidobacteria* strains from subdivision 1 act as plant growth-promoting bacteria. *Archives of Microbiology* 2016; **198**: 987–993.

Kim B-C, Poo H, Lee KH, Kim MN, Kwon O-Y, Shin K-S. Mucilaginibacter angelicae sp. nov., isolated from the rhizosphere of Angelica polymorpha Maxim. *International Journal of Systematic and Evolutionary Microbiology* 2011; **62**: 55–60.

Kim D-U, Lee H, Kim H, Kim S-G, Park SY, Ka J-O. Mucilaginibacter carri sp. nov., isolated from a car air conditioning system. *International Journal of Systematic and Evolutionary Microbiology* 2016; **66**: 1754–1759.

Kim HM, Jung JY, Yergeau E, Hwang CY, Hinzman L, Nam S, et al. Bacterial community structure and soil properties of a subarctic tundra soil in Council, Alaska. *FEMS Microbiology Ecology* 2014; **89**: 465–475.

Kim J-K, Choi T-E, Liu Q-M, Park H-Y, Yi T-H, Yoon M-H, et al. Mucilaginibacter ginsenosidivorax sp. nov., with ginsenoside converting activity isolated from sediment. *Journal of Microbiology* 2013; **51**: 394–399.

Kim M, Pak S, Rim S, Ren L, Jiang F, Chang X, et al. *Luteolibacter arcticus* sp. nov., isolated from high Arctic tundra soil, and emended description of the genus *Luteolibacter*. *International Journal of Systematic and Evolutionary Microbiology* 2015; **65**: 1922–1928.

Kirti K, Amita S, Priti S, Kumar AM, Jyoti S. Colorful World of Microbes: Carotenoids and Their Applications. *Advances in Biology* 2014; **2014**:13.

Kishimoto N, Kosako Y, Tano T. *Acidobacterium capsulatum* gen. nov., sp. nov.: An acidophilic chemoorganotrophic bacterium containing menaquinone from acidic mineral environment. *Current Microbiology* 1991; **22**: 1–7.

Kong Y, Zhu C, Ruan Y, Luo G, Wang M, Ling N, et al. Are the microbial communities involved in glucose assimilation in paddy soils treated with different fertilization regimes for three years similar? *Journal of Soils and Sediments* 2018; **18**: 2476–2490.

Koyama A, Wallenstein MD, Simpson RT, Moore JC, Stein LY. Soil bacterial community composition altered by increased nutrient availability in Arctic tundra soils. *Frontiers in Microbiology* 2014; **5**: 1–16.

Králová S. Role of fatty acids in cold adaptation of Antarctic psychrophilic. *Systematic and Applied Microbiology* 2017; **40**: 329–333.

Kramer S, Dibbern D, Moll J, Huenninghaus M, Koller R, Krueger D, et al. Resource Partitioning between Bacteria, Fungi, and Protists in the Detritusphere of an Agricultural Soil. *Frontiers in Microbiology* 2016; **7**: 1524.

Krinsky NI. Non-Photosynthetic Functions of Carotenoids. *Philosophical Transactions of the Royal Society of London Series B, Biological Sciences* 1978; **284**: 581–590.

Kumar M, Brader G, Sessitsch A, Mäki A, van Elsas JD, Nissinen R. Plants Assemble Species Specific Bacterial Communities from Common Core Taxa in Three Arctic-Alpine Climate Zones. *Frontiers in Microbiology* 2017; **8**.12.

Kumar S, Stecher G, Tamura K. MEGA7: Molecular Evolutionary Genetics Analysis Version 7.0 for Bigger Datasets. *Molecular Biology and Evolution* 2016; **33**: 1870–1874.

Lange BM, Rujan T, Martin W, Croteau R. Isoprenoid biosynthesis: The evolution of two ancient and distinct pathways across genomes. *Proc Natl Acad Sci USA* 2000; **97**: 13172–13177.

Larsen KS, Jonasson S, Michelsen A. Repeated freeze–thaw cycles and their effects on biological processes in two arctic ecosystem types. *Applied Soil Ecology* 2002; **21**: 187–195.

Lee H-R, Han S-I, Rhee K-H, Whang K-S. Mucilaginibacter herbaticus sp. nov., isolated from the rhizosphere of the medicinal plant Angelica sinensis. *International Journal of Systematic and Evolutionary Microbiology* 2013; **63**: 2787–93.

Lee KC, Kim KK, Eom MK, Kim J-S, Kim D-S, Ko S-H, et al. Mucilaginibacter gotjawali sp. nov., isolated from soil of a lava forest. *International Journal of Systematic and Evolutionary Microbiology* 2015; **65**: 952–958.

Lee YM, Jung Y-J, Hong SG, Chun J, Hahm D, Park SH. Bacterial community of sediments from the Australian-Antarctic ridge. *Polar Biology* 2014; **37**: 587–593.

Lee Y, Kim S-Y, Jung J, Kim E, Cho K, Schinner F, et al. Cultured bacterial diversity and human impact on alpine glacier cryoconite. *The Journal of Microbiology* 2011; **49**: 355–362.

Letunic I, Bork P. Interactive tree of life (iTOL) v3: an online tool for the display and annotation of phylogenetic and other trees. *Nucleic Acids Research* 2016; **44**: 242–245.

Lino T, Mori K, Uchino Y, Nakagawa T. *Ignavibacterium album* gen . nov ., sp . nov ., a moderately thermophilic anaerobic bacterium isolated from microbial mats at a terrestrial hot spring and proposal of *Ignavibacteria* classis nov ., for a novel lineage at the periphery of green sulfur bacter. *International Journal of Systematic and Evolutionary Microbiology* 2010; **60**: 1376–1382.

Liu S, Chen X, He H, Zhang X, Xie B. Structure and ecological roles of a novel exopolysaccharide from the Arctic sea ice bacterium *Pseudoalteromonas* sp. SM20310. *Appl Environ Microbiol* 2012; **79**: 224–230.

Lloyd J, Taylor JA. On the Temperature Dependence of Soil Respiration. *Functional Ecology* 1994; **8**: 315–323.

Lombard V, Bernard T, Rancurel C, Brumer H, Coutinho PM, Henrissat B. A hierarchical classification of polysaccharide lyases for glycogenomics. *Biochemical Journal* 2010; **432**: 437 LP – 444.

Loya, Wendy M. and Grogan P. Carbon conundrum on the tundra. *Nature* 2004; **431**: 406–408.

Lupascu M, Czimczik CI, Welker MC, Ziolkowski LA, Cooper EJ, Welker JM. Winter Ecosystem Respiration and Sources of CO_2 from the High Arctic Tundra of Svalbard: Response to a Deeper Snow Experiment. *Journal of Geophysical Research: Biogeosciences* 2018; **123**. 2627-2642

Luo X, Zhang L, Dai J, Liu M, Zhang K, An H, et al. Mucilaginibacter ximonensis sp. nov., isolated from Tibetan soil. *International Journal of Systematic and Evolutionary Microbiology* 2009; **59**: 1447–1450.

Madhaiyan M, Poonguzhali S, Lee J-S, Senthilkumar M, Lee KC, Sundaram S. *Mucilaginibacter gossypii* sp. nov. and *Mucilaginibacter gossypiicola* sp. nov., plant-growth-promoting bacteria isolated from cotton rhizosphere soils. *International journal of systematic and evolutionary microbiology* 2010; **60**: 2451–2457.

Männistö MK, Häggblom MM. Characterization of psychrotolerant heterotrophic bacteria from Finnish Lapland. *Syst Appl Microbiol* 2006; **29**: 229–243.

Männistö MK, Tiirola M, Häggblom MM. Bacterial communities in Arctic fjelds of Finnish Lapland are stable but highly pH-dependent. *FEMS Microbiology Ecology* 2007; **59**: 452–465.

Männistö MK, Tiirola M, Häggblom MM. Effect of Freeze-Thaw Cycles on Bacterial Communities of Arctic Tundra Soil. *Microbial Ecology* 2009; **58**: 621–631.

Männistö MK, Tiirola M, Häggblom MM. Effect of freeze-thaw cycles on bacterial communities of arctic tundra soil. *Microbial ecology* 2009; **58**: 621–631.

Männistö MK, Tiirola M, McConnell J, Häggblom MM. *Mucilaginibacter frigoritolerans* sp. nov., *Mucilaginibacter lappiensis* sp. nov. and *Mucilaginibacter mallensis* sp. nov., isolated from soil and lichen samples. *International Journal of Systematic and Evolutionary Microbiology* 2010; **60**: 2849–2856.

Männistö MK, Rawat S, Starovoytov V, Häggblom MM. *Terriglobus saanensis* sp. nov., an acidobacterium isolated from tundra soil. *International Journal of Systematic and Evolutionary Microbiology* 2011; **61**: 1823–1828.

Männistö MK, Rawat S, Starovoytov V, Häggblom MM. *Granulicella arctica* sp. nov., *Granulicella mallensis* sp. nov., *Granulicella tundricola* sp. nov. and *Granulicella sapmiensis* sp. nov., novel acidobacteria from tundra soil. *International Journal of Systematic and Evolutionary Microbiology* 2012; **62**: 2097–2106.

Männistö MK, Kurhela E, Tiirola M, Häggblom MM. Acidobacteria dominate the active bacterial communities of Arctic tundra with widely divergent winter-time snow accumulation and soil temperatures. *FEMS Microbiology Ecology* 2013; **84**: 47–59.

Markowitz VM, Chen I-. MA, Palaniappan K, Chu K, Szeto E, Grechkin Y, et al. IMG: the integrated microbial genomes database and comparative analysis system. *Nucl Acids Res* 2012; **40**: 115-22.

Martens EC, Koropatkin NM, Smith TJ, Gordon JI. Complex Glycan Catabolism by the Human Gut Microbiota : The Bacteroidetes Sus-like Paradigm. *Journal of Biological Chemistry* 2009; **284**: 24673–24677.

Martineau C, Whyte LG, Greer CW. Stable Isotope Probing Analysis of the Diversity and Activity of Methanotrophic Bacteria in Soils from the Canadian High Arctic. *Applied and Environmental Microbiology* 2010; **76**: 5773-5784.

McCalley CK, Woodcroft BJ, Hodgkins SB, Wehr RA, Kim E-H, Mondav R, et al. Methane dynamics regulated by microbial community response to permafrost thaw. *Nature* 2014; **514**: 478–481.

McMahon SK, Wallenstein MD, Schimel JP. Microbial growth in Arctic tundra soil at −2°C. *Environmental Microbiology Reports* 2009; **1**: 162.

Meléndez-Martínez AJ, Mapelli-brahm P, Benítez-gonzález A, Stinco CM. A comprehensive review on the colorless carotenoids phytoene and phytofluene. *Arch Biochem Biophys* 2015; **572**: 188–200.

Michaelson GJ, Ping CL. Soil Organic carbon and CO_2 respiration at Subzero Temperature in Soils of Arctic Alaska. *Journal of Geophysical Research: Atmospheres* 2003; **108**: 28627-29106.

Mikan CJ, Schimel JP, Doyle AP. Temperature controls of microbial respiration in arctic tundra soils above and below freezing. *Soil Biology and Biochemistry* 2002; **34**: 1785–1795.

Mojib N, Farhoomand A, Andersen DT, Bej AK. UV and cold tolerance of a pigment-producing Antarctic Janthinobacterium sp. Ant5-2. *Extremophiles* 2013; **17**: 367–378.

Monson RK, Lipson DL, Burns SP, Turnipseed AA, Delany AC, Williams MW, et al. Winter forest soil respiration controlled by climate and microbial community composition. *Nature* 2006; **439**: 711–714.

Morawe M, Hoeke H, Wissenbach DK, Lentendu G, Wubet T, Kröber E, et al. Acidotolerant Bacteria and Fungi as a Sink of Methanol-Derived Carbon in a Deciduous Forest Soil. *Frontiers in Microbiology* 2017; **8**: 1361.

Murfin KE, Dillman AR, Foster JM, Bulgheresi S, Slatko BE, Sternberg PW, et al. Nematode-Bacterium Symbioses - Cooperation and Conflict Revealed in the 'Omics' Age. *The Biological Bulletin* 2012; **223**: 85–102.

Mykytczuk NCS, Foote SJ, Omelon CR, Southam G, Greer CW, Whyte LG. Bacterial growth at -15°C; molecular insights from the permafrost bacterium *Planococcus halocryophilus* Or1. *The ISME Journal* 2013; **7**: 1211–1226.

Mykytczuk NCS, Lawrence JR, Omelon CR, Southam G, Whyte LG. Microscopic characterization of the bacterial cell envelope of *Planococcus halocryophilus* Or1 during subzero growth at −15°C. *Polar Biology* 2016; **39**: 701–712.

Natali SM, Schuur EAG, Trucco C, Hicks Pries CE, Crummer KG, Baron Lopez AF. Effects of experimental warming of air, soil and permafrost on carbon balance in Alaskan tundra. *Global Change Biology* 2011; **17**: 1394–1407.

Natali SM, Schuur EAG, Mauritz M, Schade JD, Celis G, Crummer KG, et al. Permafrost Thaw and Soil Moisture Driving CO_2 and CH_4 Release from Upland Tundra. *Journal of Geophysical Research: Biogeosciences* 2015; **120**: 525–537.

Navarrete AA, Soares T, Rossetto R, van Veen JA, Tsai SM, Kuramae EE. Verrucomicrobial community structure and abundance as indicators for changes in chemical factors linked to soil fertility. *Antonie van Leeuwenhoek* 2015; **108**: 741–752.

Nealson KH, Conrad PG. Life: past, present and future. *Philosophical Transactions of the Royal Society B: Biological Sciences* 1999; **354**: 1923–1939.

Neufeld JD, Mohn WW. Unexpectedly High Bacterial Diversity in Arctic Tundra Relative to Boreal Forest Soils, Revealed by Serial Analysis of Ribosomal Sequence Tags. *Applied and Environmental Microbiology* 2005; **71**: 5710–5718.

Nikrad MP, Kerkhof LJ, Häggblom MM. The subzero microbiome: microbial activity in frozen and thawing soils. *FEMS Microbiology Ecology* 2016; **92**. fiw081

Nobrega S, Grogan P. Deeper Snow Enhances Winter Respiration from Both Plant-associated and Bulk Soil Carbon Pools in Birch Hummock Tundra. *Ecosystems* 2007; **10**: 419–431.

Nupur LNU, Vats A, Dhanda SK, Raghava GPS, Pinnaka AK. ProCarDB : a database of bacterial carotenoids. *BMC Microbiology* 2016; **16**: 1–8.

Oechel WC, Hastings SJ, Vourlrtis G, Jenkins M, Riechers G, Grulke N. Recent change of Arctic tundra ecosystems from a net carbon dioxide sink to a source. *Nature* 1993; **361**: 520–523.

Öquist MG, Sparrman T, Klemedtsson L, Drotz SH, Grip H, Schleucher J, et al. Water availability controls microbial temperature responses in frozen soil CO_2 production. *Global Change Biology* 2009; **15**: 2715–2722.

Ourisson G, Rohmer M, Albrecht P. Hopanoid Palaeochemistry and Biochemistry of a Group of Natural Products. *International Symposium on Chemistry of Natural Products* 1979; **51**: 709–729.

Page AJ, Cummins CA, Hunt M, Wong VK, Reuter S, Holden MTG, et al. Roary: rapid large-scale prokaryote pan genome analysis. *Bioinformatics* 2015; **31**: 3691–3693.

Pan J, Solbiati JO, Ramamoorthy G, Hillerich BS, Seidel RD, Cronan JE, et al. Biosynthesis of Squalene from Farnesyl Diphosphate in Bacteria: Three Steps Catalyzed by Three Enzymes. 2015; 1–6.

Panikov NS, Dedysh SN. Cold season CH_4 and CO_2 emission from boreal peat bogs (West Siberia): Winter fluxes and thaw activation dynamics. *Global Biogeochemical Cycles* 2000; **14**: 1071–1080.

Panikov NS, Flanagan PW, Oechel WC, Mastepanov MA, Christensen TR. Microbial activity in soils frozen to below −39°C. *Soil Biology and Biochemistry* 2006; **38**: 785–794.

Pankratov TA. *Acidobacteria* in microbial communities of the bog and tundra lichens. *Microbiology* 2012; **81**: 51–58.

Pankratov TA, Ivanova AO, Dedysh SN, Liesack W. Bacterial populations and environmental factors controlling cellulose degradation in an acidic Sphagnum peat. *Environmental Microbiology* 2011; **13**: 1800–1814.

Pérez V, Hengst M, Kurte L, Dorador C, Jeffrey WH, Wattiez R, et al. Bacterial Survival under Extreme UV Radiation: A Comparative Proteomics Study of *Rhodobacter* sp., Isolated from High Altitude Wetlands in Chile. *Frontiers in Microbiology* 2017; **8**: 1173–1173.

Phadtare S, Alsina J, Inouye M. Cold-shock response and cold-shock proteins. *Current Opinion in Microbiology* 1999; **2**: 175–180.

Piette F, D'Amico S, Struvay C, Mazzucchelli G, Renaut J, Tutino ML, et al. Proteomics of life at low temperatures: trigger factor is the primary chaperone in the Antarctic bacterium *Pseudoalteromonas haloplanktis* TAC125. *Molecular microbiology* 2010; **76**: 120–132.

Pinnell LJ, Dunford E, Ronan P, Hausner M, Neufeld JD. Recovering glycoside hydrolase genes from active tundra cellulolytic bacteria. *Canadian journal of microbiology* 2014; **60**: 469–476.

Podosokorskaya OA, Kadnikov VV, Gavrilov SN, Mardanov AV, Merkel AY, Karnachuk OV, et al. Characterization of *Melioribacter roseus* gen. nov., sp. nov., a novel facultatively anaerobic thermophilic cellulolytic bacterium from the class *Ignavibacteria*, and a proposal of a novel bacterial phylum *Ignavibacteriae*. *Environmental Microbiology* 2013; **15**: 1759–1771.

Qiu Q, Noll M, Abraham W-R, Lu Y, Conrad R. Applying stable isotope probing of phospholipid fatty acids and rRNA in a Chinese rice field to study activity and composition of the methanotrophic bacterial communities in situ. *The ISME Journal* 2008; **2**: 602.

Radajewski S, Ineson P, Parekh NR, Murrell JC. Stable-isotope probing as a tool in microbial ecology. *Nature* 2000; **403**: 646–646.

Rawat SR, Männistö MK, Bromberg Y, Häggblom MM. Comparative genomic and physiological analysis provides insights into the role of *Acidobacteria* in organic carbon utilization in Arctic tundra soils. *FEMS Microbiology Ecology* 2012; **82**: 341–355.

Rawat SR, Männistö MK, Starovoytov V, Goodwin L, Nolan M, Hauser L, et al. Complete genome sequence of *Granulicella tundricola* type strain MP5ACTX9(T), an *Acidobacteria* from tundra soil. *Standards in Genomic Sciences* 2014; **9**: 449–461.

Rawat SR, Männistö MK, Starovoytov V, Goodwin L, Nolan M, Hauser LJ, et al. Complete genome sequence of *Granulicella mallensis* type strain MP5ACTX8(T), an acidobacterium from tundra soil. *Standards in Genomic Sciences* 2013; **9**: 71–82.

Reina-Bueno M, Argandoña M, Salvador M, Rodríguez-Moya J, Iglesias-Guerra F, Csonka LN, et al. Role of Trehalose in Salinity and Temperature Tolerance in the Model Halophilic Bacterium Chromohalobacter salexigens. *PLOS ONE* 2012; **7**: e33587.

Rettedal EA, Brözel VS. Characterizing the diversity of active bacteria in soil by comprehensive stable isotope probing of DNA and RNA with $H_2{}^{18}O$. *Microbiology Open* 2015; **4**: 208–219.

Reyes C, Dellwig O, Dähnke K, Gehre M, Noriega-Ortega BE, Böttcher ME, et al. Bacterial communities potentially involved in iron-cycling in Baltic Sea and North Sea sediments revealed by pyrosequencing. *FEMS Microbiology Ecology* 2016; **92**: fiw054.

Rinnan R, Michelsen A, Bååth E, Jonasson S. Fifteen years of climate change manipulations alter soil microbial communities in a subarctic heath ecosystem. *Global Change Biology* 2007; **13**: 28–39.

Rohmer M, Bouvier-Nave P, Ourisson G. Distribution of Hopanoid Triterpenes in Prokaryotes. *Journal of General Microbiology* 1984; 1137–1150. **187**. 1137-1150.

Rousk J, Baath E, Brookes PC, Lauber CL, Lozupone C, Caporaso JG, et al. Soil bacterial and fungal communities across a pH gradient in an arable soil. *The ISME journal* 2010; **4**: 1340–1351.

Sáenz JP, Grosser D, Bradley AS, Lagny TJ, Lavrynenko O, Broda M, et al. Hopanoids as functional analogues of cholesterol in bacterial membranes. *Proceedings of the National Academy of Sciences of the United States of America* 2015; **112**: 11971.

Sait M, Davis KER, Janssen PH. Effect of pH on isolation and distribution of members of subdivision 1 of the phylum *Acidobacteria* occurring in soil. *Applied and environmental Microbiology* 2006; **72**: 1852–1857.

Sanyal A, Antony R, Samui G, Thamban M. Microbial communities and their potential for degradation of dissolved organic carbon in cryoconite hole environments of Himalaya and Antarctica. *Microbiological Research* 2018; **208**: 32–42.

Schaefer K, Jafarov E. A parameterization of respiration in frozen soils based on substrate availability. *Biogeosciences* 2016; **13**: 1991–2001.

Schimel JP, Mikan C. Changing microbial substrate use in Arctic tundra soils through a freeze-thaw cycle. *Soil Biology and Biochemistry* 2005; **37**: 1411–1418.

Schimel J, Schaeffer S. Microbial control over carbon cycling in soil. *Frontiers in Microbiology* 2012; **3**: 348.

Schimel JP, Bilbrough C, Welker JM. Increased snow depth affects microbial activity and nitrogen mineralization in two Arctic tundra communities. *Soil Biology and Biochemistry* 2004; **36**: 217–227.

Schimel JP, Clein JS. Microbial response to freeze-thaw cycles in tundra and taiga soils. *Soil Biology and Biochemistry* 1996; **28**: 1061–1066.

Schmerk CL, Welander PV, Hamad MA, Bain KL, Bernards MA, Summons RE, et al. Elucidation of the *Burkholderia cenocepacia* hopanoid biosynthesis pathway uncovers functions for conserved proteins in hopanoid-producing bacteria. *Environmental Microbiology* 2015; **17**: 735–750.

Schuur EAG, McGuire AD, Schadel C, Grosse G, Harden JW, Hayes DJ, et al. Climate change and the permafrost carbon feedback. *Nature* 2015; **520**: 171–179.

Schwartz E, Buelow HN, Gooseff MN, Barrett JE, Jordan G, Takacs-vesbach CD, et al. Characterization of Growing Bacterial Populations in McMurdo Dry Valley Soils through Stable Isotope Probing with ^{18}O-water. *FEMS Microbiol Ecol* 2015; **89**: 415–425.

Seddon JM, Ajani UA, Sperduto RD, Hiller R, Blair N, Burton TC, Farber MD, Graggoudas, Haller J, Miller DT et al. Dietary carotenoids, vitamins a, c, and e, and advanced age-related macular degeneration. *JAMA* 1994; **272**: 1413–1420.

Seemann T. Prokka: rapid prokaryotic genome annotation. *Bioinformatics (Oxford, England)* 2014; **30**: 2068–2069.

Sharma S, Szele Z, Schilling R, Munch JC, Schloter M. Influence of Freeze-Thaw Stress on the Structure and Function of Microbial Communities and Denitrifying

Populations in Soil. *Applied and Environmental Microbiology* 2006; **72**: 2148-2154.

Shi Y, Xiang X, Shen C, Chu H, Neufeld JD, Walker VK, et al. Vegetation-associated impacts on arctic tundra bacterial and microeukaryotic communities. *Applied and environmental Microbiology* 2015; **81**: 492–501.

Singer E, Wagner M, Woyke T. Capturing the genetic makeup of the active microbiome in situ. *ISME J* 2017; **11**: 1949–1963.

Singh P, Hanada Y, Singh SM, Tsuda S. Antifreeze protein activity in Arctic cryoconite bacteria. *FEMS Microbiology Letters* 2014; **351**: 14–22.

Sistla SA, Moore JC, Simpson RT, Gough L, Shaver GR, Schimel JP. Long-term warming restructures Arctic tundra without changing net soil carbon storage. *Nature* 2013; **497**: 615–618.

Sjögersten S, Turner BL, Mahieu N, Condrom L, Wookey PA. Soil organic matter biochemistry and potential susceptibility to climatic change across the forest-tundra ecotone in the Fennoscandian mountains. *Global Change Biology* 2003; **9**: 759–772.

Stackebrandt E, Goebel BM. Taxonomic Note: A Place for DNA-DNA Reassociation and 16S rRNA Sequence Analysis in the Present Species Definition in Bacteriology. *International Journal of Systematic and Evolutionary Microbiology* 1994; **44**: 846–849.

Stackhouse B, Lau MCY, Vishnivetskaya T, Burton N, Wang R, Southworth A, et al. Atmospheric CH4 oxidation by Arctic permafrost and mineral cryosols as a function of water saturation and temperature. *Geobiology* 2017; **15**: 94–111.

Stark S, Männistö MK, Ganzert L, Tiirola M, Häggblom MM. Grazing intensity in subarctic tundra affects the temperature adaptation of soil microbial communities. *Soil Biology and Biochemistry* 2015; **84**: 147–157.

Starr EP, Shi S, Blazewicz SJ, Probst AJ, Herman DJ, Firestone MK, et al. Stable isotope informed genome-resolved metagenomics reveals that Saccharibacteria utilize microbially-processed plant-derived carbon. *Microbiome* 2018; **6**:122.

Stothard P, Wishart DS. Circular genome visualization and exploration using CGView. *Bioinformatics* 2018; **21**: 537–539.

Sturm M, Schimel J, Michaelson G, Welker JM, Oberbauer SF, Glen E, et al. Winter Biological Processes Could Help Convert Arctic Tundra to Shrubland. *BioScience* 2005; **55**: 17–26.

Summons RE, Jahnke LL, Hope JM, Logan GA. 2-Methylhopanoids as biomarkers for cyanobacterial oxygenic photosynthesis. *Nature* 1999; **400**: 554–557.

Tarnocai C, Canadell JG, Schuur EAG, Kuhry P, Mazhitova G, Zimov S. Soil organic carbon pools in the northern circumpolar permafrost region. *Global Biogeochemical Cycles* 2009; **23** :GB203.

Taş N, Prestat E, Wang S, Wu Y, Ulrich C, Kneafsey T, et al. Landscape topography structures the soil microbiome in arctic polygonal tundra. *Nat Commun* 2018; **9**:777.

Tatusov RL, Galperin MY, Natale DA, Koonin EV. The COG database : a tool for genome-scale analysis of protein functions and evolution. *Nucleic Acids Research* 2000; **28**: 33–36.

Terrapon N, Lombard V, Lap P, Al-masaudi S, Gilbert HJ, Henrissat B. PULDB : the expanded database of Polysaccharide Utilization Loci. *Nucleic Acids Research* 2018; **46**: 677–683.

Thirkell D, Strang RHC. Analysis and Comparison of the Carotenoids of Sarcinu flava and S. lutea*. Microbiology* 1967; **49**:53–57.

Tuorto SJ, Darias P, McGuinness LR, Panikov N, Zhang T, Häggblom MM, et al. Bacterial genome replication at subzero temperatures in permafrost. *ISME Journal* 2014; **8**: 139–149.

Tveit A, Schwacke R, Svenning MM, Urich T. Organic carbon transformations in high-Arctic peat soils: key functions and microorganisms. *The ISME Journal* 2012; **7**: 299.

Vandekerckhove TT, Willems A, Gillis M, Coomans A. Occurrence of novel verrucomicrobial species, endosymbiotic and associated with parthenogenesis in *Xiphinema americanum*-group species (*Nematoda*, *Longidoridae*). *International Journal of Systematic and Evolutionary Microbiology* 2000; **50**: 2197–2205.

Verastegui Y, JC K Engel, D Kolczynski, S Mortimer, J Lavigne, J Montalibet, T Romantsov, M Hall, J McConkey, DR Rose, JJ Tomashek, BR Scott, TC Charles, JD Neufeld. Multisubstrate Isotope Labeling and Metagenomic Analysis of Active Soil Bacterial Communities. *mBio* 2014; **5**: 1–12.

Voigt C, Lamprecht RE, Marushchak ME, Lind SE, Novakovskiy A, Aurela M, et al. Warming of subarctic tundra increases emissions of all three important greenhouse gases – carbon dioxide, methane, and nitrous oxide. *Global Change Biology* 2016; **23**: 3121–3138.

Voigt C, Marushchak ME, Lamprecht RE, Jackowicz-Korczyński M, Lindgren A, Mastepanov M, et al. Increased nitrous oxide emissions from Arctic peatlands after permafrost thaw. *Proceedings of the National Academy of Sciences of the United States of America* 2017; **114**: 6238–6243.

Wagner D, Kobabe S, Pfeiffer E-M, Hubberten H-W. Microbial controls on methane fluxes from a polygonal tundra of the Lena Delta, Siberia. *Permafrost and Periglacial Processes* 2003; **14**: 173–185.

Welander PV, Hunter RC, Zhang L, Sessions AL, Summons RE, Newman DK. Hopanoids Play a Role in Membrane Integrity and pH Homeostasis in *Rhodopseudomonas palustris* TIE-1. *Journal of Bacteriology* 2009; **191**: 6145 LP-6156.

Yang S, Wen X, Zhao L, Shi Y, Jin H. Crude Oil Treatment Leads to Shift of Bacterial Communities in Soils from the Deep Active Layer and Upper Permafrost along the China-Russia Crude Oil Pipeline Route. *PLOS ONE* 2014; **9**: e96552–96552.

Yergeau E, Kowalchuk GA. Responses of Antarctic soil microbial communities and associated functions to temperature and freeze-thaw cycle frequency. *Environmental Microbiology* 2008; **10**: 2223–2235.

Yergeau E, Hogues H, Whyte LG, Greer CW. The functional potential of high Arctic permafrost revealed by metagenomic sequencing, qPCR and microarray analyses. *ISME J* 2010; **4**: 1206–1214.

Yi Y, Kimball JS, Rawlins MA, Moghaddam M, Euskirchen ES. The role of snow cover affecting boreal-arctic soil freeze–thaw and carbon dynamics. *Biogeosciences* 2015; **12**: 5811–5829.

Yoon J-H, Kang S-J, Park S, Oh T-K. Mucilaginibacter litoreus sp. nov., isolated from marine sand. *International Journal of Systematic and Evolutionary Microbiology* 2012; **62**: 2822–7.

Young AJ. The photoprotective role of carotenoids in higher plants. *Physiologia Plantarum* 1991; **83**: 702–708.

Zahorik A. Changes in Membrane Lipid Composition of Arctic *Acidobacteria* in Response to pH and Temperature Stress. *Rutgers University George H Cook Senior Thesis* 2016;1-47.

Zhang L, Yang Q, Luo X, Fang C, Zhang Q, Tang Y. Knockout of crtB or crtI gene blocks the carotenoid biosynthetic pathway in *Deinococcus radiodurans* R1

and influences its resistance to oxidative DNA-damaging agents due to change of free radicals scavenging ability. *Archives of Microbiology* 2007; **188**: 411–419.

Zhang T. Influence of the seasonal snow cover on the ground thermal regime: An overview. *Reviews of Geophysics* 2005; **4**:43.

Zona D, Gioli B, Commane R, Lindaas J, Wofsy SC, Miller CE, et al. Cold season emissions dominate the Arctic tundra methane budget. *Proceedings of the National Academy of Sciences* 2016; **113**: 40–45.